www.sciencemag.org/cgi/content/full/science.1253799/DC1

Supplementary Materials for

Use of human embryonic stem cells to model pediatric gliomas with H3.3K27M histone mutation

Kosuke Funato, Tamara Major, Peter W. Lewis, C. David Allis, Viviane Tabar*

*Corresponding author. E-mail: tabarv@mskcc.org

Published 20 November 2014 on *Science* Express
DOI: 10.1126/science.1253799

This PDF file includes

Supplementary Materials for

Use of Human Embryonic Stem Cells to Model Pediatric Gliomas with H3.3K27M Histone Mutation

Kosuke Funato[1], Tamara Major[1], Peter W. Lewis[2], C. David Allis[3], Viviane Tabar[1]

correspondence to: tabarv@mskcc.org

This PDF file includes:

Materials and Methods
Figs. S1 to S16
Tables S1 to S6

Materials and Methods

Cell culture

hESCs (WA-09; passages 35-45) were maintained at undifferentiated state on irradiated mouse embryonic fibroblasts (MEFs, Globalstem Inc) in medium consisting of DMEM/F12 (Invitrogen) supplemented with 20% Knockout Serum Replacement (KSR, Invitrogen), 10 ng/ml basic fibroblast growth factor (bFGF, R&D Systems), 1 mM L-glutamine (Invitrogen), 100 μM non essential amino acids and 0.1 mM β-mercaptoethanol (Sigma-Aldrich). The cells were fed daily and passaged weekly using 6 U/ml dispase. Human primary astrocytes (Sciencell) were maintained in Astrocyte Medium (Sciencell). MRC-5 lung fibroblasts (ATCC, CCL-171) were maintained in DMEM medium supplemented with 10% fetal bovine serum (FBS). Human patient-derived DIPG cells (DIPG-VI, kindly provided by Michelle Monje, Stanford University) were maintained in Neurobasal media (Invitrogen) supplemented with B27 without Vitamin A (Invitrogen), EGF (20ng/ml), bFGF (20 ng/ml, R&D Systems), PDGF-AA and -BB (20 ng/ml, Peprotech) and heparin (10 ng/ml).

Neural induction and neural subtype specification

For neural induction, a modified version of the dual-SMAD inhibition was used (*7*). Undifferentiated hES-cells were disaggregated using Accutase (Innovative Cell Technology) and plated on Matrigel (BD)-coated dishes at a density of 40,000 cells/cm^2 in MEF-conditioned ESC medium supplemented with 10 ng/ml of bFGF and ROCK inhibitor (Y-27632). When the cells reached the confluent state (2-3 days after plating), they were exposed for 9 days to LDN193189 (200 nM, Stemgent) and SB431542 (10 mM, Tocris) in KSR medium containing DMEM, 15% knockout serum replacement, 2 mM L-glutamine and 10 μM β-mercaptoethanol. KSR medium was gradually replaced with N2 medium (25%, 50%, 75%) starting on day 4 of differentiation as described previously. On day 12, cells were dissociated using Accutase and replated in high density conditions (300,000 cells per cm^2) on dishes pre-coated with polyornithine (PO; 15 μg/ml), laminin (Lam; 1 μg/ml) and fibronectin (FN; 2 μg/ml) in N2 medium supplemented with BDNF (brain-derived neurotrophic factor, 20 ng/ml, R&D), ascorbic

acid (0.2 mM, Sigma), Purmorphamine (1 mM, Stemgent) and FGF8 (100 mg/ml, R&D). They were patterned at P1 stage for two weeks and thereafter passaged by mechanical picking of the CNS clusters and re-plated on PO/Lam/FN coated dishes. Neural precursor cells (NPCs) were maintained in N2 medium supplemented with EGF (20 ng/ml), bFGF (20 ng/ml, R&D Systems) and B-27 supplement without vitamin A (1:50, Invitrogen). Medium was changed every 2 days while the cultures were passaged every two weeks. For the differentiation to astrocytes, NPCs (day 65-135) were exposed to N2 medium containing 5% FBS for an additional 14 days. For the differentiation to neurons, NPCs were cultured in N2 medium supplemented with BDNF (20 ng/ml) and ascorbic acid (AA, 0.2 mM) for 14 days. For the differentiation to oligodendrocytes, NPCs were cultured in N2 media supplemented with cAMP, triiodothyronine (T3), BDNF (20 ng/ml) and ascorbic acid (AA, 0.2 mM) for 21 days.

Immunostaining

Cells were fixed by incubation in 4% paraformaldehyde for 15 minutes and incubated in blocking buffer (10% fetal bovine serum or goat serum; 0.1% BSA; 0.3% Triton-X100 in PBS) for 1 hour. Cells were stained with primary (or conjugated) antibodies in blocking buffer at 4°C overnight, washed and stained with secondary antibodies in PBS supplemented with 0.1% BSA for 30 minutes at room temperature, in the dark. Nestin (MAB5326; 1:400), SOX2 (AB5603; 1:200), TRA-1-81 (MAB4381; 1:100), Olig2 (AB9610; 1:100), O4 (MAB345; 1:50) and MBP (MAB386; 1:1000) antibodies were obtained from Milliopore, H3K27me3 (clone C36B11; 1:1500) and phospho-Histone H2A.X (Ser139; clone 20E3; 1:400) from Cell signaling, Tuj1 (PRB-435P; 1:500) from Covance, GFAP (1:5000) and Ki67 (clone MIB-1; 1:200) from Dako, Nanog (H-155; 1:200) from Santa Cruz, p75 (clone ME20.4; 1:50) from Advanced Targeting Systems. Nuclei were stained by DAPI (Invitrogen). Mice were perfused with 4% paraformaldehyde solution. The brains were extracted and fixed by incubation in 4% paraformaldehyde at 4°C overnight. Following cryopreservation by incubation in 15% and 30% sucrose solutions, brains were frozen into OCT compound and cut by cryostat into 10 mm sections. For immunohistochemistry, sections were air-dried, washed by PBS and incubated in blocking buffer (10% fetal bovine serum or goat serum, 0.1% BSA and 0.3% Triton-X100 in PBS) for 1 hour. Cells were stained with primary antibodies in

blocking buffer at 4°C overnight, washed and stained with secondary antibodies in PBS supplemented with 0.1% BSA for 30 minutes at room temperature, in the dark, followed by nuclear staining by DAPI. Human specific GFAP antibody (STEM123; 1:1000) was obtained from StemCells Inc, HA-tag (clone 3F10; 1:200) from Roche, Ki67 (ab15580; 1:200) from Abcam, and human nuclear antigen (MAB1281; 1:200) from Millipore. Whole brain images are composed by stitching ~20 scan images. TUNEL assay was performed using TUNEL apoptosis detection kit from Millipore following manufacturer's instruction. Hematoxylin and Eosin (H&E) staining was performed according to standard procedures.

Gamma-radiation of cells

Cells were plated onto 48-well plates and irradiated at the dose of 5 Gy (3.45 Gy/minute) using X-RAD 225C Biological X-ray irradiator (Precision X-ray, Inc). Following incubation for the indicated time period, cells were fixed and immunostained for Ki67 and g-H2A.X (phosphorylated at Ser139). The number of Ki67-positive cells and g-H2A.X foci per cell was counted manually or using ImageJ software.

Sub-G1 assay

Cells were trypsinized, collected in PBS and fixed in cold 70% ethanol. Followed by RNase A (Ambion) treatment, cells were stained with propidium iodide (50 μg/ml, Invitrogen) in PBS and subjected to FACS analysis according to standard procedures.

Migration and invasion assay

Cell migration was assessed by the Boyden chamber assay. Briefly, the bottom chamber was coated with Lam/FN at 37°C overnight and air-dried. 3,000 cells were plated on the top chamber and allowed to migrate for 4 hours. Following PBS wash, cells that migrated to the bottom chamber were fixed, stained with DAPI and counted by fluorescence microscopy. For invasion assay, spheres of RFP-labeled transduced NPCs (~1.5 mm in diameter) were embedded in Matrigel (BD). Following 12 days of incubation, invasion of cells into Matrigel was analyzed by measuring the distance travelled from the sphere edge. P-values were calculated by Chi-square test.

Low density culture

3,000 cells were evenly plated onto 24 well plates precoated with PO/Lam/FN and cultured in N2 medium supplemented with EGF (20 ng/ml), bFGF (20 ng/ml, R&D

Systems) and B-27 supplement without vitamin A (1:50, Invitrogen) for 4 weeks. Medium was changed every 2-3 days. Crystal violet staining was performed according to standard procedures.

In vitro limiting dilution assay

Sphere-forming capacity was assessed by limiting dilution assay. 10~100 cells were plated into 96-well low-attachment plates. Following 12 days of incubation, spheres with more than 5 cells were counted. P-values were calculated using Extreme Limiting Dilution Analysis (ELDA) software(*22*).

Animal surgery and transplantation

All animal experiments were done in accordance with protocols approved by our Institutional Animal Care and Use Committee and following NIH guidelines for animal welfare. 100,000 or 500,000 cells were injected intracranially into NOD-SCID mice (6-day-old pups, 3 mm posterior to lambda-suture and 3 mm deep). Hypothermia was used for anesthesia. Animals were monitored for 3-6 months with neurological assessments and MRI imaging. For evaluating *in vivo* growth of menin-knockdown cells, Luciferase-labeled P5K cells were transduced with control or sh-MEN1-expressing lentivirus. Following 6 days of incubation, cells were dissociated by Accutase and intracranially injected into immunocompromised mice as described above.

In vivo imaging

Animals were anesthetized with isoflurane gas and injected with D-luciferin (Invitrogen; Pierce), followed by bioluminescent imaging by the IVIS imaging system (PerkinElmer) with a 5-minute exposure time (described in detail in (*23*). For MRI imaging, the mice were anesthetized using 1.5–2 % isoflurane in a 70% N_2O + 30% O_2 mixture. Imaging was performed on a Bruker Biospec 4.7-Tesla (200 MHz) 40 cm horizontal bore magnet. The system is equipped with a 300 mT/m gradient system. Examinations were conducted using a 32-mm quadrature birdcage resonator for excitation and detection.

Drug screening

We performed a chemical screen using a limited small molecule library of compounds that target epigenetic regulators (80 compounds; Cayman Chemicals) along with DNA damage reagents (Camptothecin and Doxorubicin, Santa Cruz) and RTK inhibitors (Sunitinib and Imatinib, Selleck) as controls. GFP-labeled normal NPCs and RFP-labeled

P5K cells were mixed and seeded onto 96-well plates pre-coated with PO/Lam/FN. 24 hours after plating, cells were then treated with each compound at 8 different concentrations (2-fold serial dilution, typically from 10 mM to 78.125 nM) in duplicate wells for 6 days. Following PBS wash, GFP and RFP fluorescence was quantified by a multi-wavelength automated plate reader (Tecan Infinite M1000 Pro). For calculating IC_{50} values, data were normalized by the values of vehicle-treated cells and fitted to Hill equation using the least squares method.

Microarray analysis

Total RNA was extracted with Trizol reagent (Invitrogen). The RNA was then processed by the MSKCC Genomic core facility and hybridized with Affymetrix U133 Plus2.0 arrays. Gene expression analysis was carried out within the GenePattern website (http://www.broadinstitute.org/cancer/software/genepattern/). Briefly, background correction and quantile normalization was done with the Robust Multi-array Average (RMA) algorithm(*24*). Probes that passed the variation filter were subjected to PCA and hierarchical clustering with average linkage and Pearson correlation distance. For identifying differentially expressed genes between conditions, probes were ranked by signal-to-noise ratio and statistical significance was determined by permutation test (Supplementary table 1 and 2). Microarray data of DIPG patients' samples was obtained from GSE34824/GSE36245 and early-stage NPCs was from GSE9921. Microarray data generated in this manuscript was deposited in GEO (GSE55541).

ChIP-seq

Native ChIP was performed as previously described(*25*). Briefly, ~10 million cells were washed, resuspended in digestion buffer (50 mM Tris-HCl, pH 7.6; 1 mM CaCl2; 0.2% Triton-X100) and treated with micrococcal nuclease from *Staphylococcus aureus* (MNase) for 5 min at 37°C. Nuclei were lysed by brief sonication and dialyzed into RIPA buffer (10 mM Tris-HCl, pH 7.6; 1 mM EDTA; 0.1% SDS; 0.1% Na-Deoxycholate; 1% Triton X-100) for 2 hours at 4°C. Soluble material was recovered and subjected to immunoprecipitation using antibody against H3K4me3 (Active Motif; Cell signaling) or H3K27me3 (Millipore; Cell signaling), and Dynabeads Protein A (Invitrogen). Following the final wash, chromatin was eluted with elution buffer (50 mM Tris-HCl, pH 8.0; 10 mM EDTA; 1% SDS) and digested by proteinase K (Roche). ChIP DNA and ChIP input

DNA were then isolated using QIAGEN Qiaquick PCR purification kit. ChIP-seq libraries were prepared according to the Illumina protocol and sequenced with either the Genome analyzer II or HiSeq 2000.

Data analysis

Analysis of ChIP-seq data was carried out within the Galaxy website (http://galaxyproject.org/). Briefly, reads that passed the quality filter were mapped to the human genome (hg19) using Bowtie algorithm (*26*) with default setting. Peak calling was done by Model-based Analysis of ChIP-Seq (MACS) algorithm (*27*) with 500-bp window size. For comparing the level of histone modifications in different groups of promoters, the total number of reads in individual promoters (between +1 kb and -500 bp from transcription start site) was computed and normalized by total read counts. The level at gene-body regions was further normalized by the length of individual transcripts.

Western Blot

Cells were lysed in RIPA Buffer (50mM Tris-HCl, pH 8.0; 120mM NaCl; 5mM EDTA; 0.5% NP-40). Following 30-minute centrifuge at 14000 rpm, supernatant was collected and protein concentration was measured by the Bradford Assay (Bio-Rad). Lysates were boiled for 5 minutes in Laemmli sample buffer and separated by electrophoresis on 4-12% Bis-Tris gel in SDS running buffer for 1.5-2 hours. Protein was transferred to nitrocellulose membrane using the iBlot gel transfer device (Invitrogen). Non-specific protein binding was prevented by blocking the membrane with 4% blocking reagent (Amersham) in TBS-T (0.1% Tween-20 in TBS buffer). Membrane was incubated at 4°C overnight in the blocking buffer with primary antibodies: PDGFRA (1:1000; Cell Signaling), Trimethylated-H3K27 (1:1000; Cell Signaling), b-tubulin (clone DM1A; 1:1000; SantaCruz), GAPDH (1:1000; Cell Signaling), HA-tag (clone 3F10; 1:1000; Roche), H3 (clone 96C10; 1:1000; Cell Signaling), Menin (1:1000; Bethyl Laboratories) and H3.3K27M (1:1000; Millipore). After four washes with TBS-T, the blot was incubated with respective secondary antibodies for Mouse (1:5000) or Rabbit (1:5000) at room temperature for 30 minutes. ECL prime Western Blotting Detection Kit was used for detection according to manufacturer's instruction (Amersham).

Quantitative real-time PCR

Total RNA was extracted using TRIzol (Invitrogen). For each sample, 1 mg of total RNA was reverse transcribed using the SuperScriptIII (Invitrogen). Amplified material was detected using Quantitect SYBR green probes and PCR kit (Qiagen) on a Mastercycler RealPlex2 (Eppendorf). All results were normalized to an Actin control. Sequences of primers are shown in supplementary table.

Vectors and mutagenesis

Human PDGFRA (Addgene #23892)(*28*) was cloned into pLenti PGK Neo DEST vector (Addgene #19067)(*29*). Mutagenesis was performed following the manufacturer's protocol (Promega). Cloning and mutagenesis of H3.3 transgenes were described previously(*9*) . Luciferase-expressing vector (pLenti PGK Blast V5-LUC) was obtained from Addgene (#19166)(*29*), MEN1-expressing vector from Open Biosystems. For the construction of shRNA-expressing vectors, annealed oligos were cloned into H1 vector or pENTR-H1 vector. The shRNA expressing cassette in pENTR-H1 vector was transferred to lentiviral vectors by LR recombination according to manufacturer's instruction (Invitrogen). Target sequences of each shRNA are shown in supplementary table.

Lentivirus production

Lentiviruses were produced in 293T packaging cells, by a slightly modified version of a method described previously(*30*) . Lentiviral vectors were transfected in 293T cells with packaging vectors (pCMV-dR8.2 and pCMV-VSV-G), in the presence of Polyethylenimine (Polysciences). Viral supernatants were collected 72 h after transfection and viral particles were concentrated by ultracentrifugation at 49,000g for 1.5 h at 4 °C.

Assessment of Senescence

Senescence-associated b-galactosidase activity was assessed using the staining kit from Invitrogen according to the manufacturer's instructions.

Statistical analysis

Student's t-test and ANOVA were performed for statistical analysis, unless indicated otherwise.

Figure S1

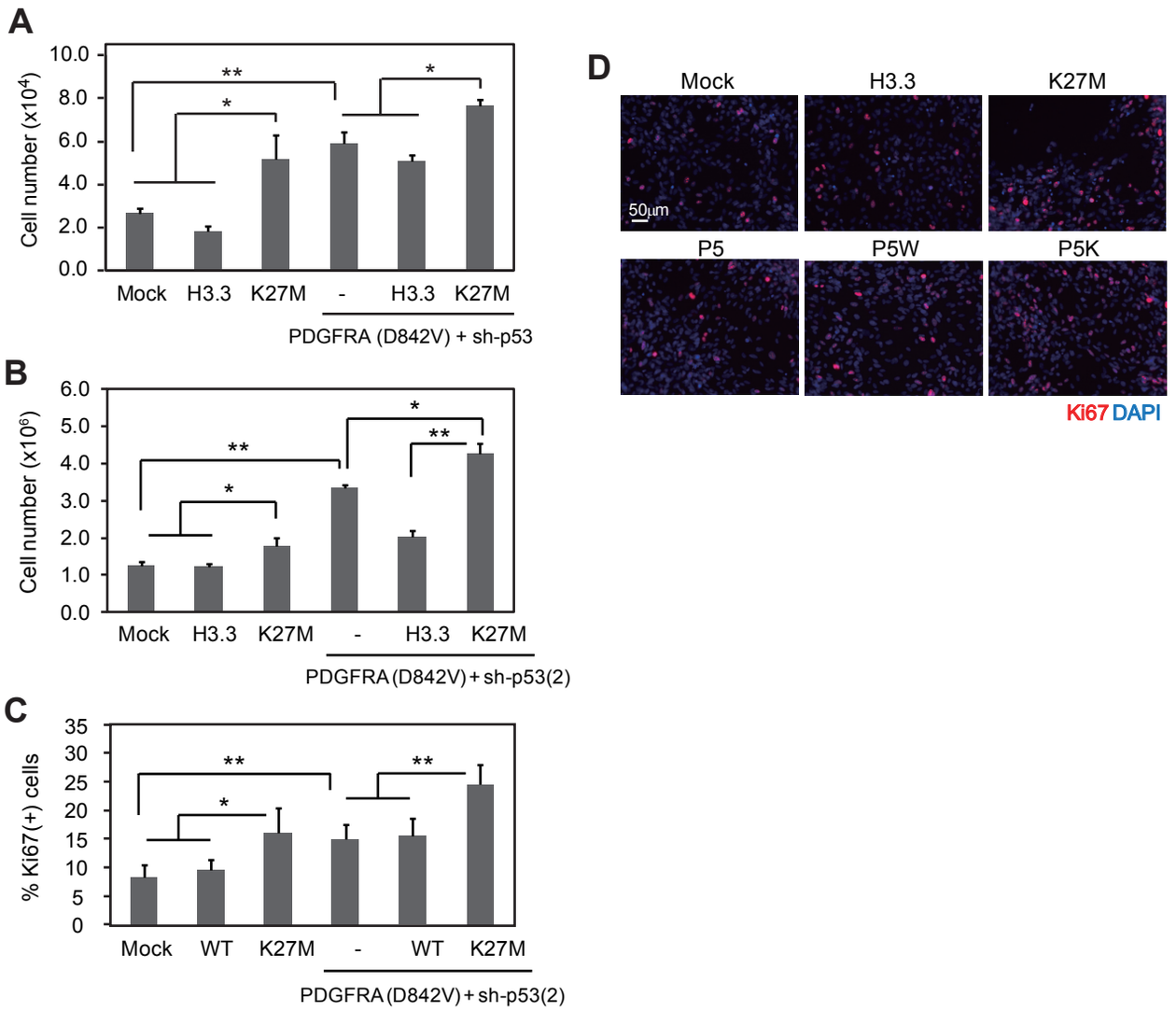
A
Cell number (x10^4)
10.0
8.0
6.0
4.0
2.0
0.0
**
*
*
Mock
H3.3
K27M
-
H3.3
K27M
PDGFRA (D842V) + sh-p53
B
Cell number (x10^6)
6.0
5.0
4.0
3.0
2.0
1.0
0.0
*
**
*
**
Mock
H3.3
K27M
-
H3.3
K27M
PDGFRA (D842V) + sh-p53(2)
C
% Ki67(+) cells
35
30
25
20
15
10
5
0
**
*
**
Mock
WT
K27M
-
WT
K27M
PDGFRA (D842V) + sh-p53(2)
D
Mock
H3.3
K27M
50μm
P5
P5W
P5K
Ki67 DAPI

Fig. S1.

(A,B) Quantification of cell viability (trypan bue) following incubation for 5 days *in vitro*. A second shRNA against p53 was used in B, leading to a similar results. (C) Quantification of proliferation via Ki67 upon transduction of oncogenes combinations and using the second shRNA-p53. (D) Immunohistochemistry for Ki67 in the different cell groups. Bars indicate mean ± S.D. (n = 4~5). *, $p < 0.05$; **, $p < 0.01$.

Figure S2

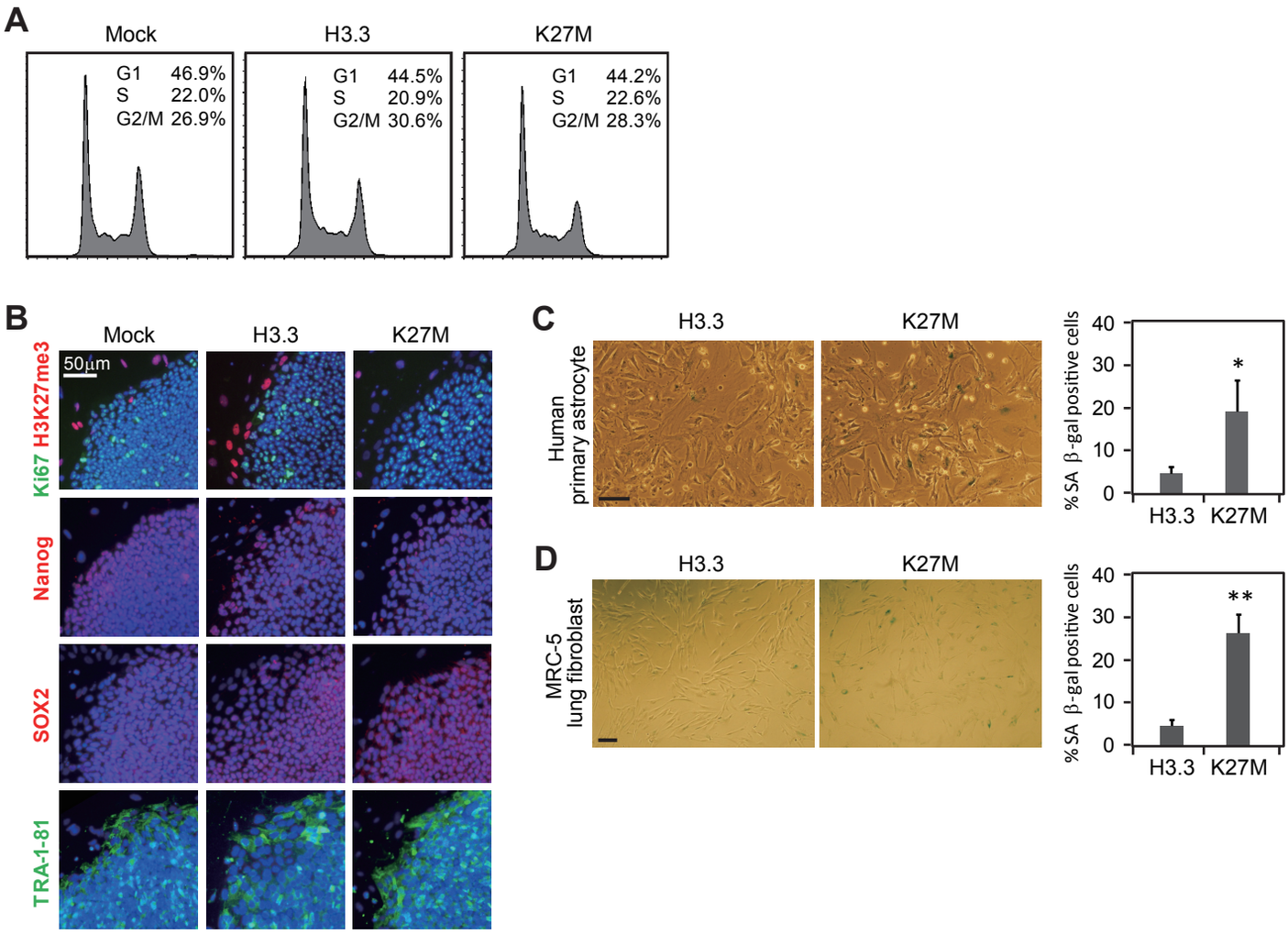
A
Mock
H3.3
K27M
G1 46.9%
S 22.0%
G2/M 26.9%
G1 44.5%
S 20.9%
G2/M 30.6%
G1 44.2%
S 22.6%
G2/M 28.3%
B
Mock
H3.3
K27M
50μm
Ki67 H3K27me3
Nanog
SOX2
TRA-1-81
C
H3.3
K27M
Human primary astrocyte
% SA β-gal positive cells
40
30
20
10
0
*
H3.3
K27M
D
H3.3
K27M
MRC-5 lung fibroblast
% SA β-gal positive cells
40
30
20
10
0
**
H3.3
K27M

Fig. S2

(A) FACS-based cell cycle analysis of human ES cells transduced with WT or K27M mutant form of histone H3.3. (B) Human ES cells expressing WT histone H3.3 or K27M mutant were immunostained with the indicated antibodies, demonstrating absence of H3K27me3 marks, and unchanged expression of pluripotency markers Nanog and TRA1-81 as well as the early transcription factor SOX2. Sporadic expression of H3K27me3 is likely localized to the feeder layer. (C,D) Expression of K27M is associated with a decrease in proliferation and increased senescence in differentiated cells, such as astrocytes (C) and fibroblasts (D). Quantification of senescent cells was performed via analysis of senescence-associated β-galactosidase activity (SA β-gal). Bars indicate mean ± S.D. (n = 4~5). Scales: 100 μm. *, $p < 0.05$; **, $p < 0.01$.

Figure S3

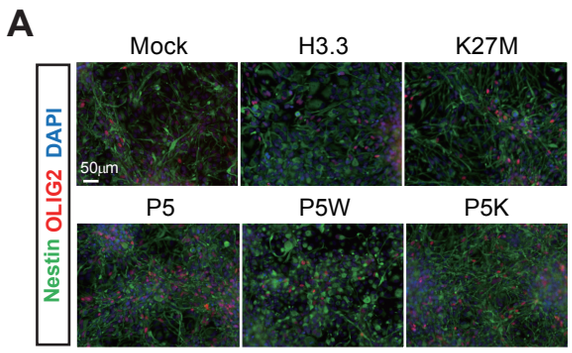
A
Mock
H3.3
K27M
Nestin OLIG2 DAPI
50μm
P5
P5W
P5K

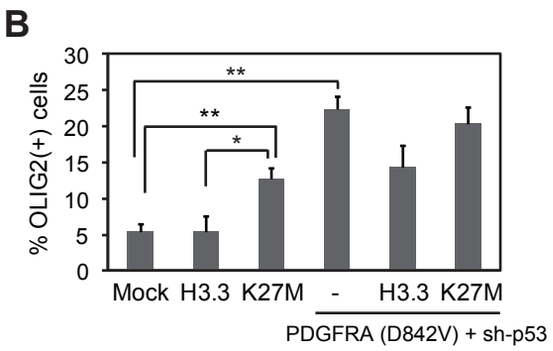
B
% OLIG2(+) cells
30
25
20
15
10
5
0
**
**
*
Mock H3.3 K27M - H3.3 K27M
PDGFRA (D842V) + sh-p53

Fig. S3

(A) NPCs transduced with the indicated lentiviruses were immunostained for Nestin and Olig2. (B) Quantification of immunostaining for Olig2. Bars indicate mean ± S.D. (n = 4~5). *, $p < 0.05$; **, $p < 0.01$.

Figure S4

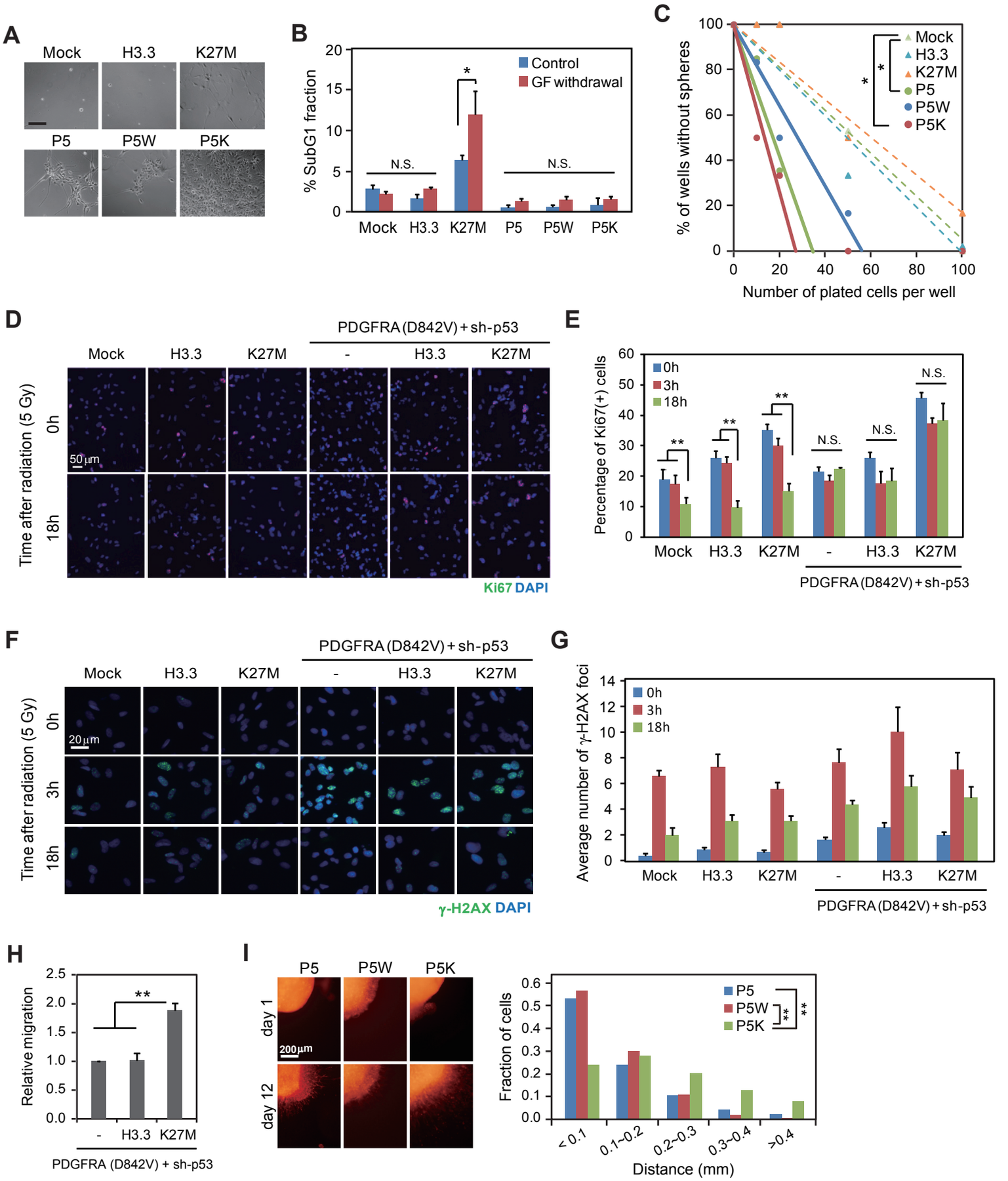
A
Mock
H3.3
K27M
P5
P5W
P5K
B
% SubG1 fraction
Control
GF withdrawal
N.S.
N.S.
*
Mock
H3.3
K27M
P5
P5W
P5K
C
% of wells without spheres
Number of plated cells per well
Mock
H3.3
K27M
P5
P5W
P5K
*
D
PDGFRA (D842V) + sh-p53
Mock
H3.3
K27M
-
H3.3
K27M
Time after radiation (5 Gy)
0h
18h
50 μm
Ki67 DAPI
E
Percentage of Ki67(+) cells
0h
3h
18h
**
**
**
N.S.
N.S.
N.S.
Mock
H3.3
K27M
-
H3.3
K27M
PDGFRA (D842V) + sh-p53
F
PDGFRA (D842V) + sh-p53
Mock
H3.3
K27M
-
H3.3
K27M
Time after radiation (5 Gy)
0h
3h
18h
20 μm
γ-H2AX DAPI
G
Average number of γ-H2AX foci
0h
3h
18h
Mock
H3.3
K27M
-
H3.3
K27M
PDGFRA (D842V) + sh-p53
H
Relative migration
**
-
H3.3
K27M
PDGFRA (D842V) + sh-p53
I
P5
P5W
P5K
day 1
day 12
200 μm
Fraction of cells
P5
P5W
P5K
**
**
< 0.1
0.1~0.2
0.2~0.3
0.3~0.4
>0.4
Distance (mm)

Fig. S4

(A) Bright phase microscopy of transduced NPCs grown at very low density for 4 weeks. (B) FACS analysis for the sub-G1 fraction (apoptotic cells) in transduced NPCs under control conditions and 24 hours following growth factor withdrawal. Bars indicate mean ± S.D. (n = 3). (C) Sphere-forming capacity was assessed by limiting dilution assay. 10~100 cells were plated into a 96-well low-attachment plate. After 12 days of incubation, spheres with more than 5 cells were counted. (D,E) Proliferation of normal and transformed NPCs was assessed following a single dose of radiation (5 Gy) at the indicated time point, by Ki67 staining. Bars in (E) indicate mean ± S.D. (n = 4~5). (F,G) DNA repair kinetics following radiation. Cells were immunostained for phospho-γ-H2A.X at 0, 3 hours and 18 hours following a dose of 5 Gy. The number of positive foci was counted. (H) Cell migration was assessed by the Boyden chamber assay. 3,000 cells were plated in the top chamber and the number of cells that migrated to the bottom chamber was counted by fluorescence microscopy of DAPI stained cells. Bars indicate mean ± S.D. (n = 4). (I) Low magnification immunofluorescence microscopy of RFP-labeled transduced NPCs embedded as spheres in Matrigel. Cells migrating from the spheres were analyzed on day 12 and the distance travelled from the sphere edge was measured. *, $p < 0.05$; **, $p < 0.01$. NS, Not Significant.

Figure S5

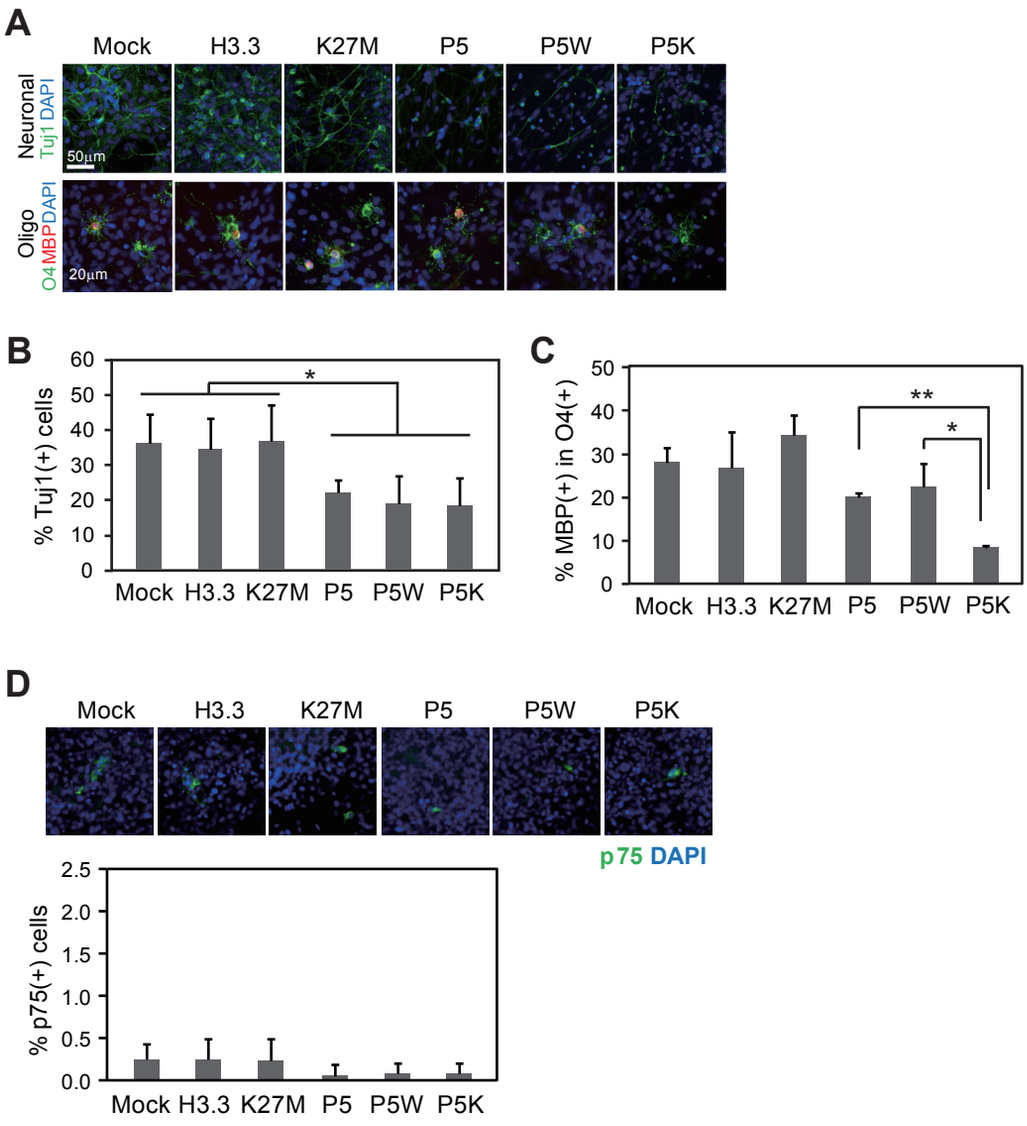
A
Mock
H3.3
K27M
P5
P5W
P5K
Neuronal
Tuj1 DAPI
50μm
Oligo
O4 MBP DAPI
20μm
B
% Tuj1(+) cells
60
50
40
30
20
10
0
*
Mock H3.3 K27M P5 P5W P5K
C
% MBP(+) in O4(+)
50
40
30
20
10
0
**
*
Mock H3.3 K27M P5 P5W P5K
D
Mock
H3.3
K27M
P5
P5W
P5K
p75 DAPI
% p75(+) cells
2.5
2.0
1.5
1.0
0.5
0.0
Mock H3.3 K27M P5 P5W P5K

Fig. S. 5

(A-C) Transduced NPCs were differentiated under neuronal and oligodendrocyte (oligo) conditions. Immunohistochemistry and quantification for the neuronal (TUJ1, B) and oligodendrocyte (O4 and MBP, C) markers, respectively. Bars indicate mean ± S.D. (*n* = 4~5). (D) Spontaneous differentiation to mesenchymal cells was analyzed by p75 immunostaining. *, $p < 0.05$; **, $p < 0.01$.

Figure S6

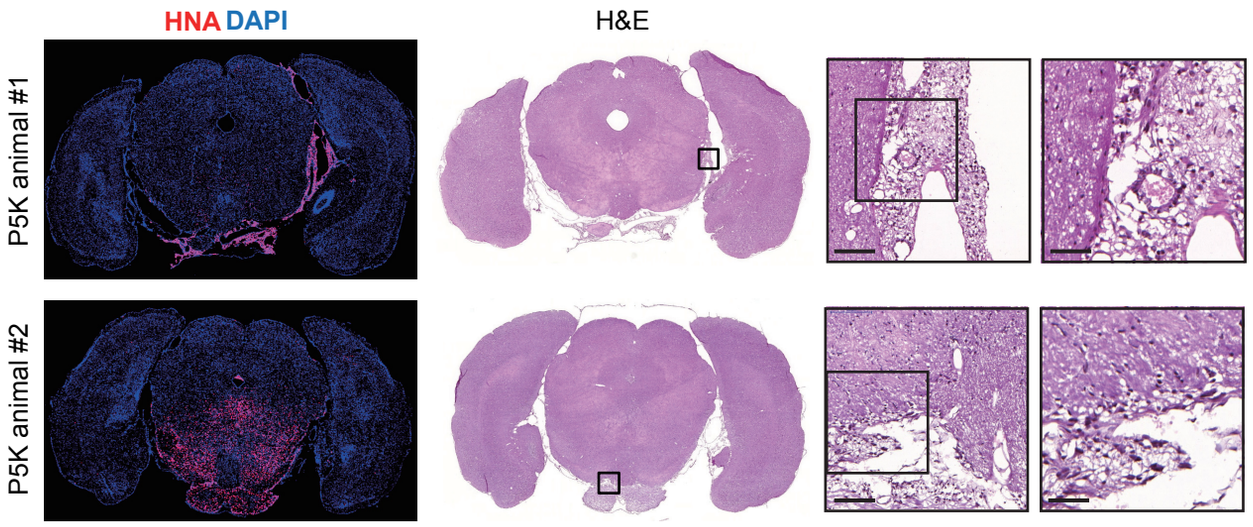

Fig. S6

Representative images of mouse brains transplanted with P5K cells. Low magnification immunofluorescence images of representative sections labeled for human specific nuclear antigen (HNA) and counter-stained with DAPI (left). The consecutive sections were stained with H&E (right). Scale bar, 100 μm (left), 50 μm (right).Note the presence of hydrocephalus secondary to subarachnoidal disease, as well as intraventricular tumor (animal #2).

Figure S7

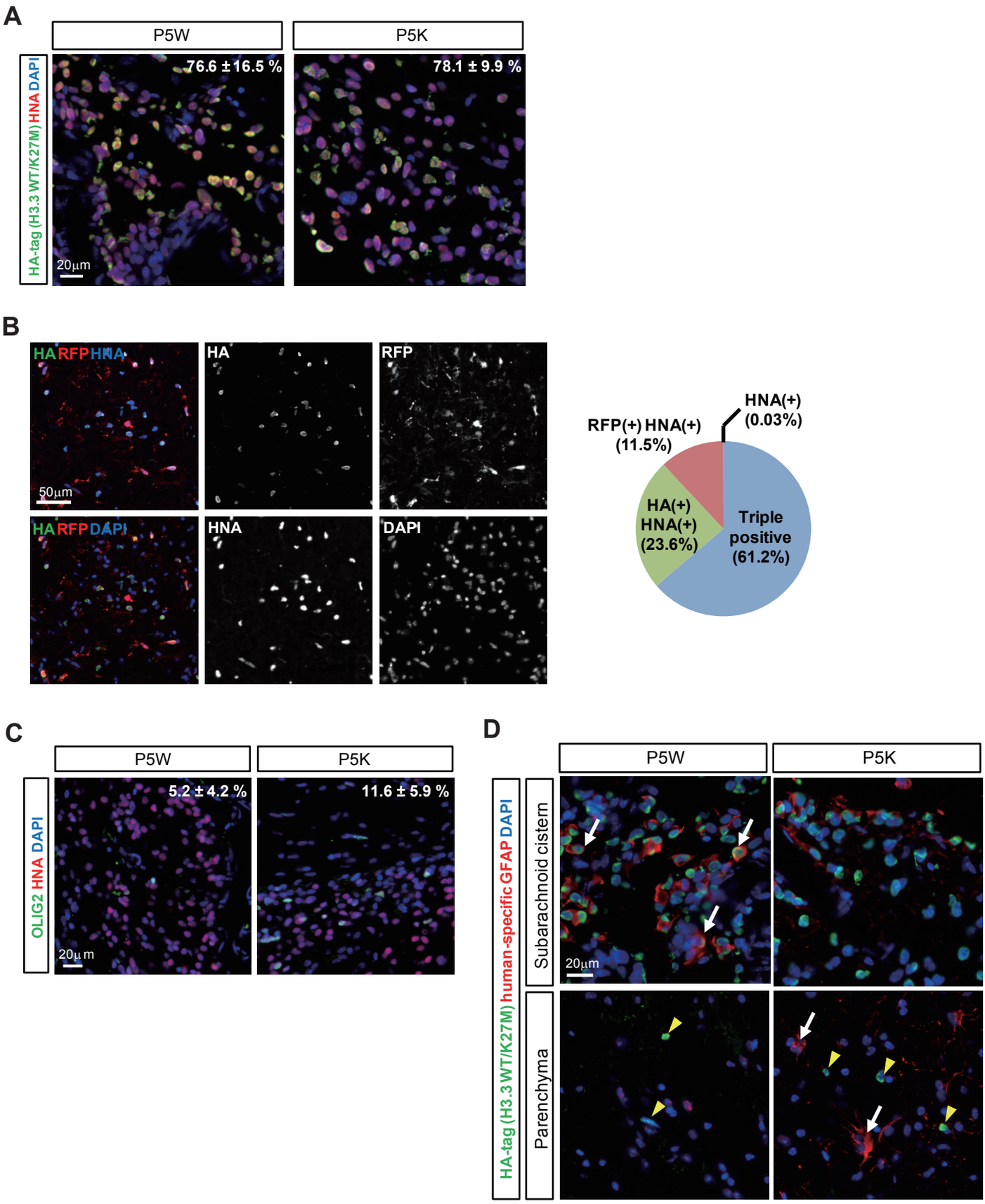

	% hGFAP(+) cells in total human cells	% hGFAP(+)/HA(-) in total hGFAP(+)
P5W	17.3 ± 2.2	18.5 ± 7.6
P5K	7.9 ± 1.0 **	42.5 ± 13.2

Fig. S7

Immunophenotyping of transplanted cells. (A-D) Frozen sections of mouse brains transplanted with P5W or P5K cells were immunostained for the indicated antibodies. Expression of H3.3 WT or K27M was coupled to hemagglutinin (HA) epitope tag, while sh-p53 was associated with a RFP reporter. (A) Immunostaining for the HA-tag showed that the majority of the cells retained the histone transgenes. Numbers indicate the percentage of HA-stained cells relative to HNA-stained cells (mean ± S.E.M., n = 3~4). (B) Silencing of the histone transgene and/or sh-p53 expression in transplanted P5K cells was evaluated by immunostaining for the HA-tag and RFP expression, respectively. (C) Immunohistochemistry for Olig2 demonstrates an increased percentage in the P5K tumors, compared to P5W. Numbers indicate the percentage of Olig2-stained cells relative to HNA-stained cells (mean ± S.E.M., n = 3~4). (D) Astrocytic differentiation of transplanted cells was assessed by immunostaining for human-specific GFAP and the HA-tag. White arrows indicate astrocytes of human origin. Yellow arrowheads indicate transplanted cells that retain histone transgenes. Numbers indicate the percentage of GFAP-stained cells relative to the total number of cells of human origin (HA and/or GFAP-stained cells, mean ± S.E.M., n = 4~6). **, $p < 0.01$.

Figure S8

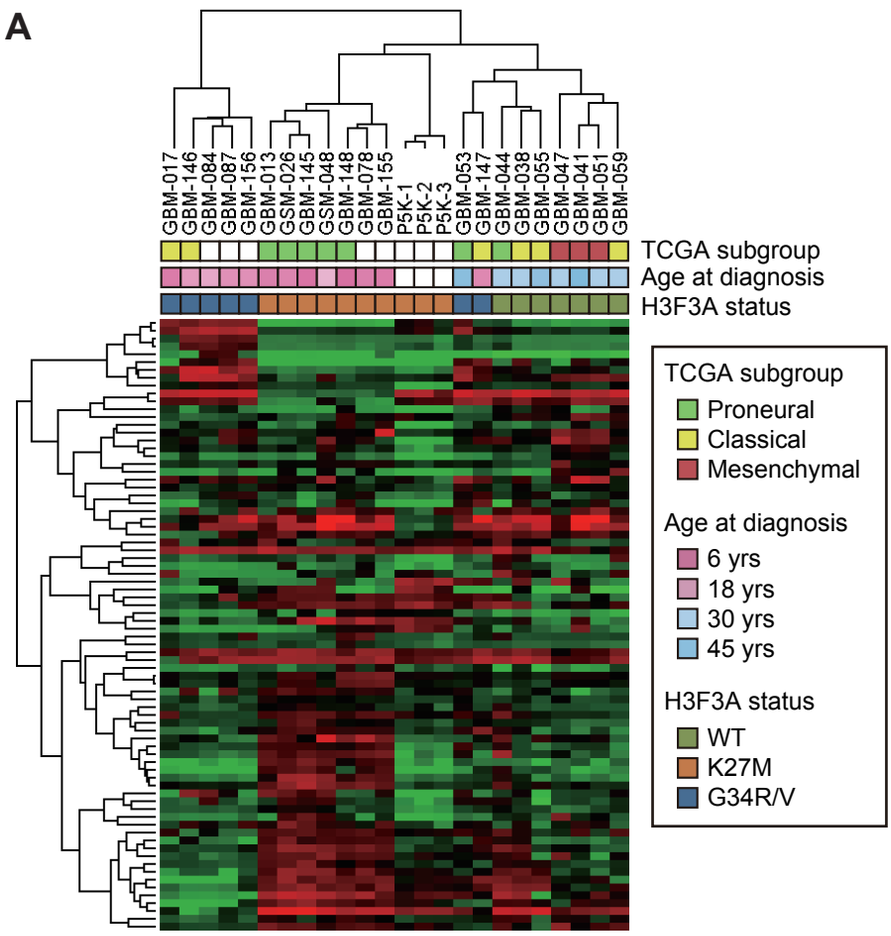

B

	K27M tumor	G34 tumor
P5K "*in vitro*"	R=0.406 $p=2.26 \times 10^{-4}$	R=0.288 p=0.0107
P5K sorted "*in vivo*"	R=0.572 $p=4.36 \times 10^{-8}$	R=0.125 p=0.281
K27M tumor	R=1	R= - 0.110 p=0.3358

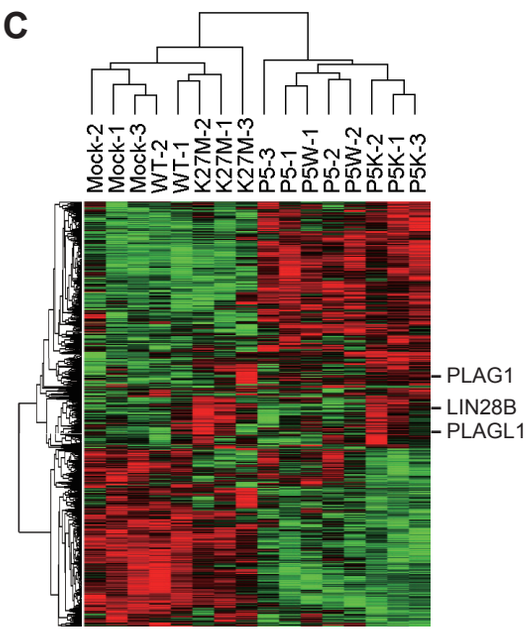

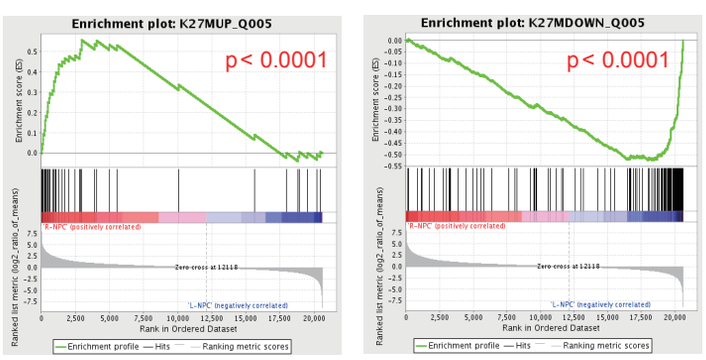

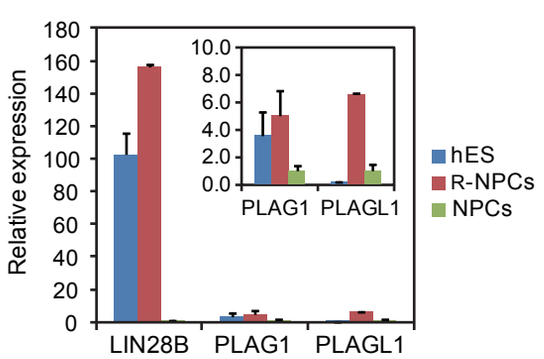

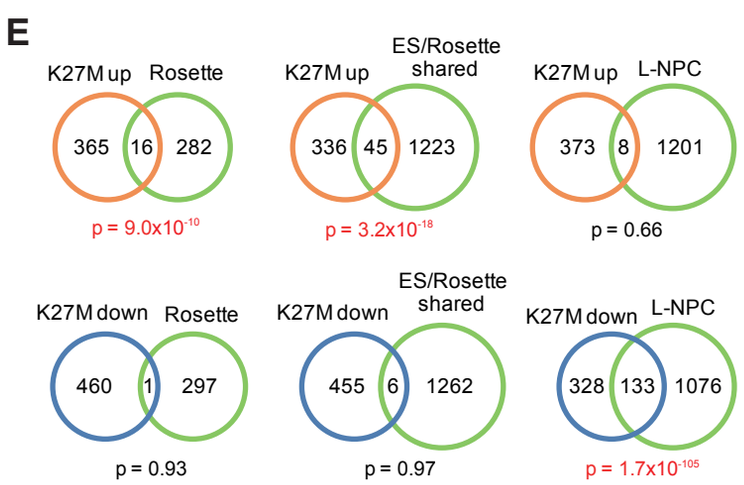

Fig. S8

(A) Hierarchical clustering of microarray data from P5K cells and patient tumor samples bearing the K27M or G34R/V mutations (GSE36245) obtained from (*4*). (B) Pearson's correlation between the two groups was analyzed. (C) Unsupervised hierarchical clustering of microarray data obtained from NPCs transduced with the different H3.3 and oncogene combinations. (D) Gene Set Enrichment Analysis (GSEA) indicates an enrichment of the gene sets that are up or down-regulated by K27M in the expression profile of early-stage (rosette-stage) NPCs compared with late-stage NPCs. (E) Overlap of indicated transcript sets are shown by Venn diagrams. Transcripts that are up or down-regulated for more than 3 folds by K27M ('K27M up' and 'K27M down') were compared with the transcripts that are upregulated in early-stage NPCs ('Rosette'), late-stage NPCs ('Late-NPCs') or shared between early-stage NPCs and undifferentiated ES cells ('ES/Rosette shared'), respectively. P-values were calculated by hyper-geometric test. (F) RT-qPCR demonstrates increased expression levels of LIN28B, PLAG1 and PLAGL1 in human ES cells and rosette-stage NPCs. Bars indicate mean ± S.E.M. (n = 3~4).

Figure S9

A

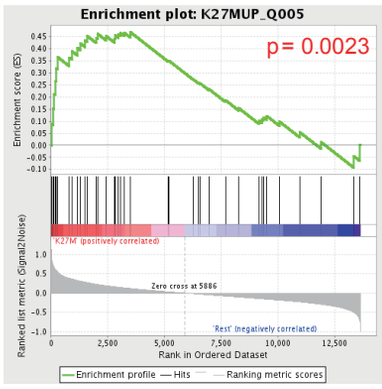
Enrichment plot: K27MUP_Q005
p= 0.0023
Enrichment score (ES)
'K27M' (positively correlated)
Zero cross at 5886
'Rest' (negatively correlated)
Ranked list metric (Signal2Noise)
Rank in Ordered Dataset
Enrichment profile
Hits
Ranking metric scores

B

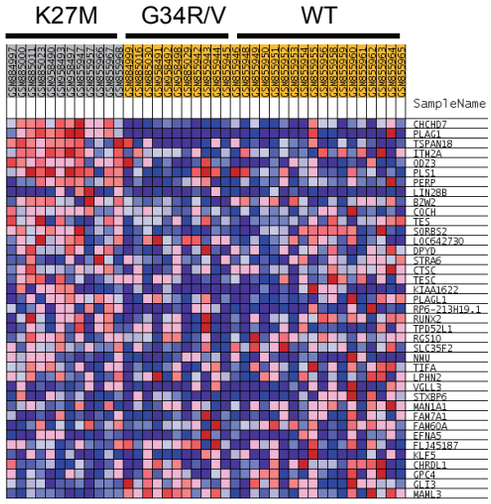
K27M
G34R/V
WT
SampleName
CHCHD7
PLAG1
TSPAN18
ITN2A
OD23
PLS1
PEBP
LIN28B
B2W2
COCH
TES
SORBS2
LOC642730
DPYD
STRA6
CTSC
TESC
KIAA1622
PLAGL1
RP6-213H19.1
RUNX2
TPD52L1
RGS16
SLC35F2
NNU
TIFA
LPHN2
VGLL3
STXBP6
WANK1A1
FAM7A1
FAM60A
EFNA5
FLJ45187
KLF5
CHRDL1
GPC4
GLI3
WAWL3

Fig. S9

(A,B) Gene Set Enrichment Analysis (GSEA) indicates an enrichment of the gene set that is upregulated by K27M in the gene expression profile of patient tumor samples with K27M mutation, compared to G34R/V mutations, and non-histone mutated GBMs.

Figure S10

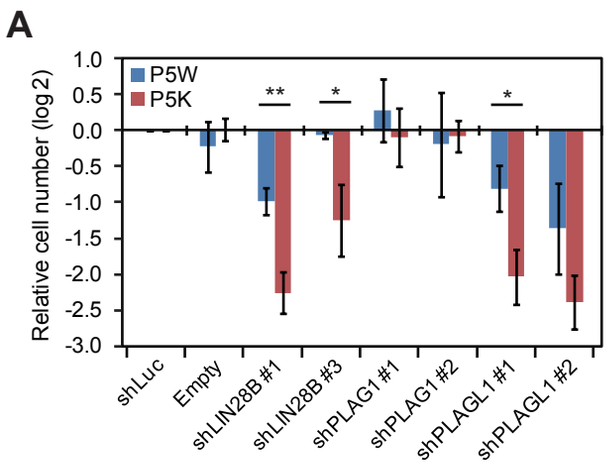
A
Relative cell number (log 2)
P5W
P5K
**
*
*
shLuc
Empty
shLIN28B #1
shLIN28B #3
shPLAG1 #1
shPLAG1 #2
shPLAGL1 #1
shPLAGL1 #2

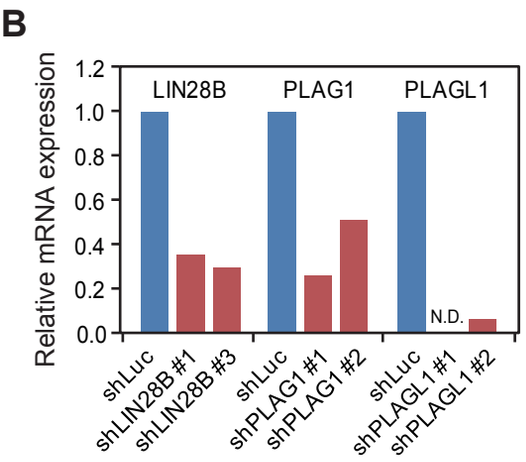
B
Relative mRNA expression
LIN28B
PLAG1
PLAGL1
N.D.
shLuc
shLIN28B #1
shLIN28B #3
shLuc
shPLAG1 #1
shPLAG1 #2
shLuc
shPLAGL1 #1
shPLAGL1 #2

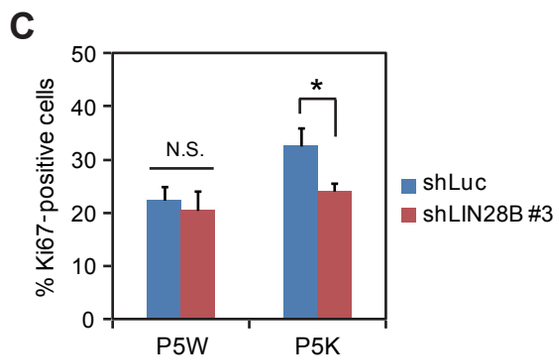
C
% Ki67-positive cells
N.S.
*
shLuc
shLIN28B #3
P5W
P5K

Fig S10

(A) Knockdown of LIN28B and PLAGL1 reduced the number of viable cells in P5K cells. P5W and P5K cells were infected with the indicated shRNA-expressing lentiviruses. Viability was assayed by trypan-blue following 6 days *in vitro*. Values are normalized to control shRNA (shLuc) and log transformed. Bars indicate mean ± S.E.M. (n = 3~6). (B) Confirmation of silencing by real-time RT-qPCR. (C) Knockdown of LIN28B decreased the proliferation of P5K cells. P5W and P5K cells were transduced with control (shLuc) or LIN28B-shRNA expressing (shLIN28B#3) lentiviruses, respectively, and immunostained for Ki67. Bars indicate mean ± S.D. (n = 4~5).

Figure S11

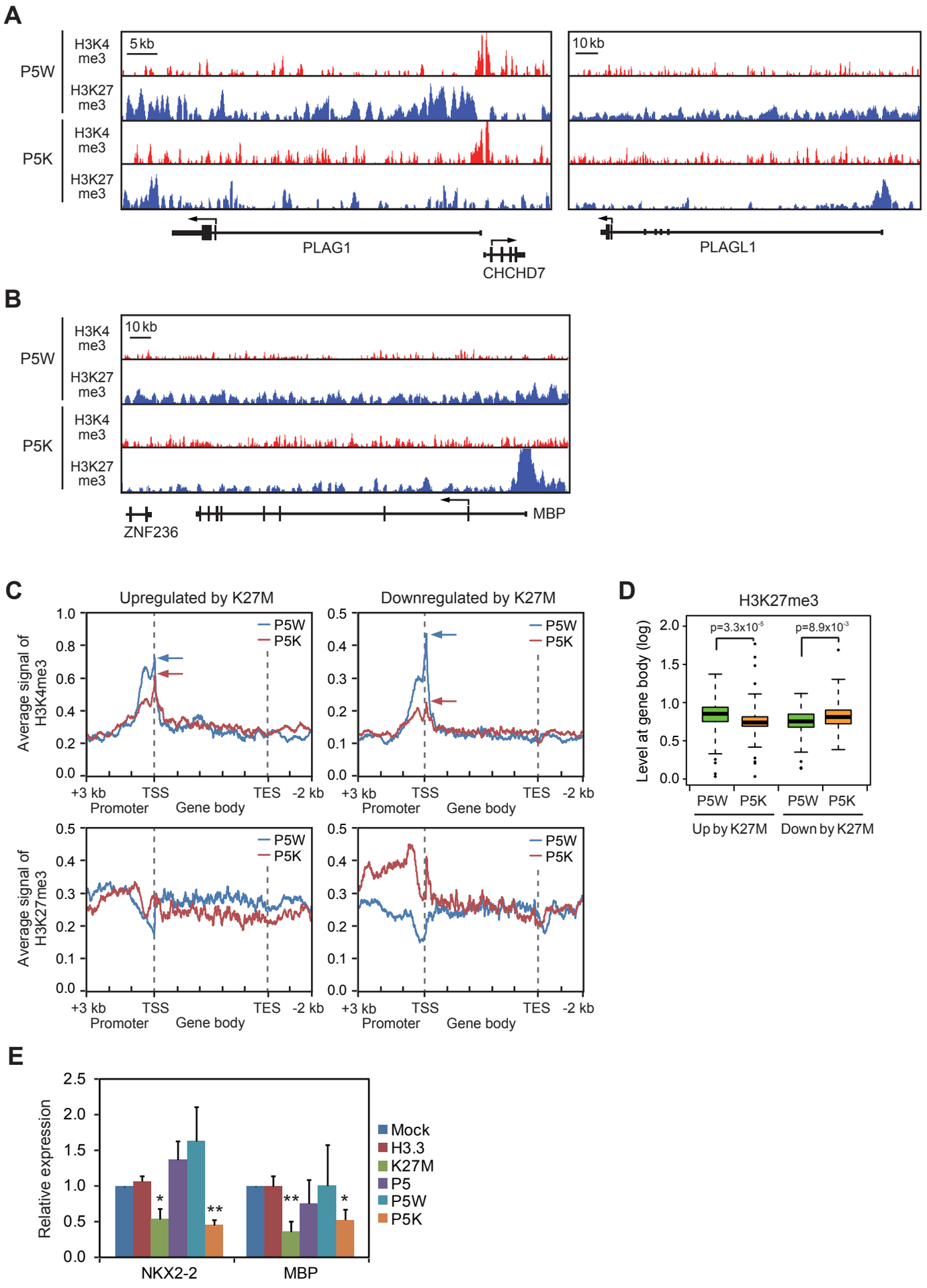
A
P5W
P5K
H3K4 me3
H3K27 me3
5 kb
10 kb
PLAG1
CHCHD7
PLAGL1
B
10 kb
ZNF236
MBP
C
Upregulated by K27M
Downregulated by K27M
Average signal of H3K4me3
Average signal of H3K27me3
P5W
P5K
+3 kb
Promoter
TSS
Gene body
TES
-2 kb
D
H3K27me3
Level at gene body (log)
p=3.3x10-5
p=8.9x10-3
Up by K27M
Down by K27M
E
Relative expression
Mock
H3.3
K27M
P5
P5W
P5K
NKX2-2
MBP

Fig. S11

(A,B) Chromatin landscape of selected genes. H3K4me3 (red) and H3K27me3 (blue) marks are shown for P5W and P5K cells. (C) Profiles of H3K4me3 and H3K27me3 marks over the upregulated (91 genes) or downregulated (80 genes) by K27M (Supplementary Table 3). Blue, P5W cells; red, P5K cells. Arrows indicate the peak of signal intensity. (D) Levels of H3K27me3 marks at the gene-body region of the genes upregulated or downregulated by K27M. P-values were calculated by the Wilcoxon rank-sum test. (E) Decreased expression of Nkx2-2 and MBP was confirmed by RT-qPCR. Bars indicate mean ± S.E.M. (n = 3~5). *, $p < 0.05$; **, $p < 0.01$.

Figure S12

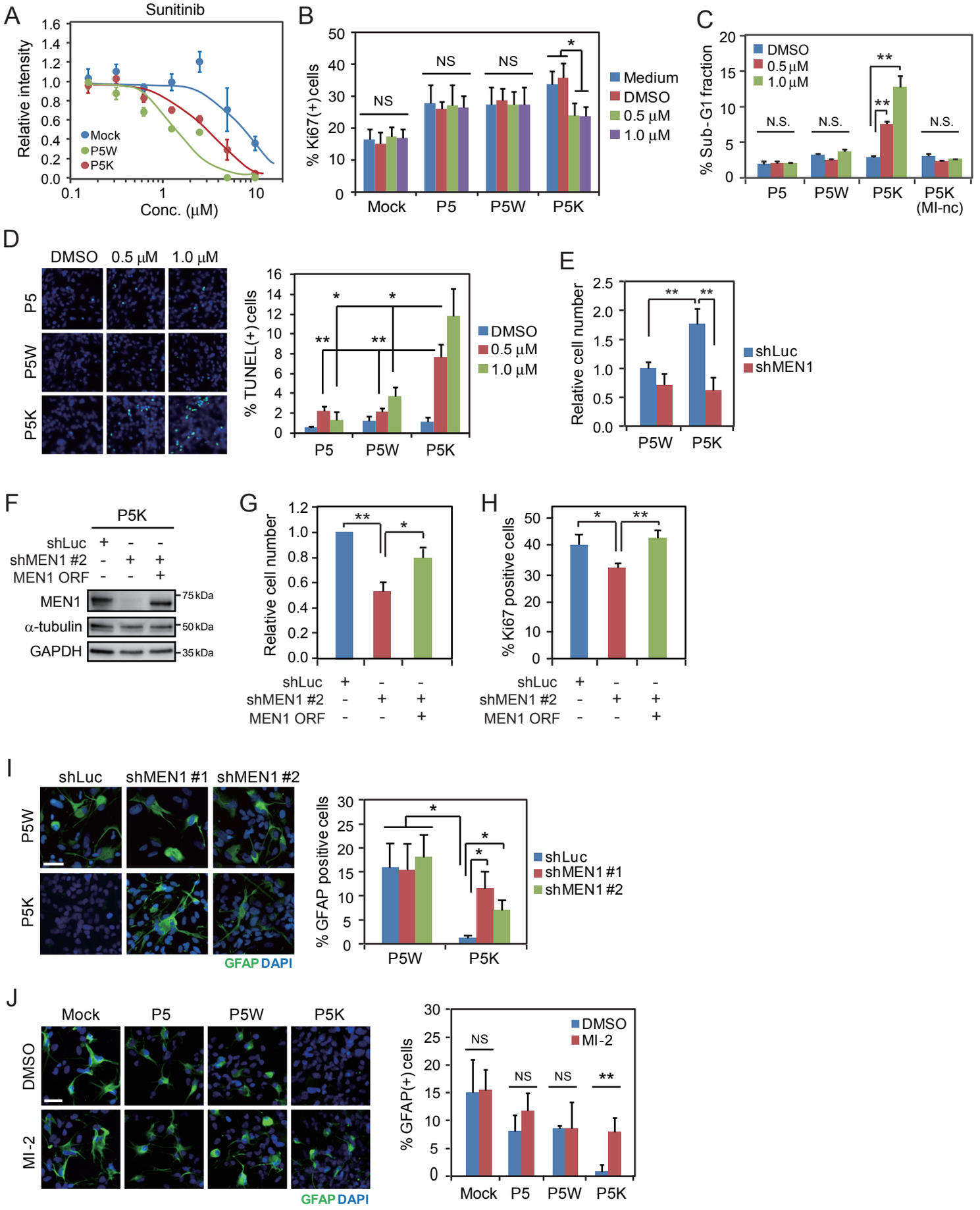
A
Sunitinib
Relative intensity
Conc. (μM)
Mock
P5W
P5K
B
% Ki67(+) cells
NS
NS
NS
*
Medium
DMSO
0.5 μM
1.0 μM
Mock
P5
P5W
P5K
C
% Sub-G1 fraction
DMSO
0.5 μM
1.0 μM
N.S.
N.S.
**
**
N.S.
P5
P5W
P5K
P5K (MI-nc)
D
DMSO
0.5 μM
1.0 μM
P5
P5W
P5K
% TUNEL(+) cells
*
*
**
**
DMSO
0.5 μM
1.0 μM
P5
P5W
P5K
E
Relative cell number
**
**
shLuc
shMEN1
P5W
P5K
F
P5K
shLuc + - -
shMEN1 #2 - + +
MEN1 ORF - - +
MEN1
α-tubulin
GAPDH
75 kDa
50 kDa
35 kDa
G
Relative cell number
**
*
shLuc + - -
shMEN1 #2 - + +
MEN1 ORF - - +
H
% Ki67 positive cells
*
**
shLuc + - -
shMEN1 #2 - + +
MEN1 ORF - - +
I
shLuc
shMEN1 #1
shMEN1 #2
P5W
P5K
GFAP DAPI
% GFAP positive cells
*
*
*
shLuc
shMEN1 #1
shMEN1 #2
P5W
P5K
J
Mock
P5
P5W
P5K
DMSO
MI-2
GFAP DAPI
% GFAP(+) cells
NS
NS
NS
**
DMSO
MI-2
Mock
P5
P5W
P5K

Fig. S12

(A) Representative dose response curves in normal NPCs (Mock, blue), P5W (green) and P5K (red) cells treated with Sunitinib. Error bars indicate S.D. (n = 4). (B) Proliferation assay demonstrates a significant effect of MI-2 on P5K cells, with no impact on normal or P5W cells. Bars indicate mean ± S.D. (n = 4). (C,D) MI-2 treatment induced cell death in P5K cells. After 6 days of treatment, the percentage of dead cells was measured by Sub-G1 assay (C) and TUNEL staining (D). (E) Knockdown of menin decreased the proliferation of P5K cells. The number of viable cells was counted by trypan-blue staining. Bars indicate mean ± S.D. (n = 4). (F) Confirmation of menin knockdown and rescue by western blotting. The expression of menin was suppressed by the shRNA targeting 3' UTR of menin (shMEN1 #2) and rescued by the overexpression of menin ORF (MEN1 ORF) in P5K cells. (G and H) Proliferation of P5K cells was decreased by menin knockdown and rescued by the overexpression of menin ORF. Viability and proliferation were assessed by trypan-blue staining (G) and Ki67 staining (H). Bars indicate mean ± S.D. (n = 4~5). (I,J) Suppression of menin restored astrocytic differentiation in P5K cells. P5K cells transduced with control or menin shRNA-expressing lentiviruses (shMEN #1 and shMEN #2), were cultured under the differentiation condition. Following 14 days *in vitro*, astrocytic differentiation was assessed by immunostaining for GFAP (I). Cells were cultured under the differentiation condition with or without MI-2 (0.5 μM) for 14 days (J). Bars indicate mean ± S.D. (n = 4~5). Scale, 20 μm. *, $p < 0.05$; **, $p < 0.01$. NS, Not Significant.

Figure S13

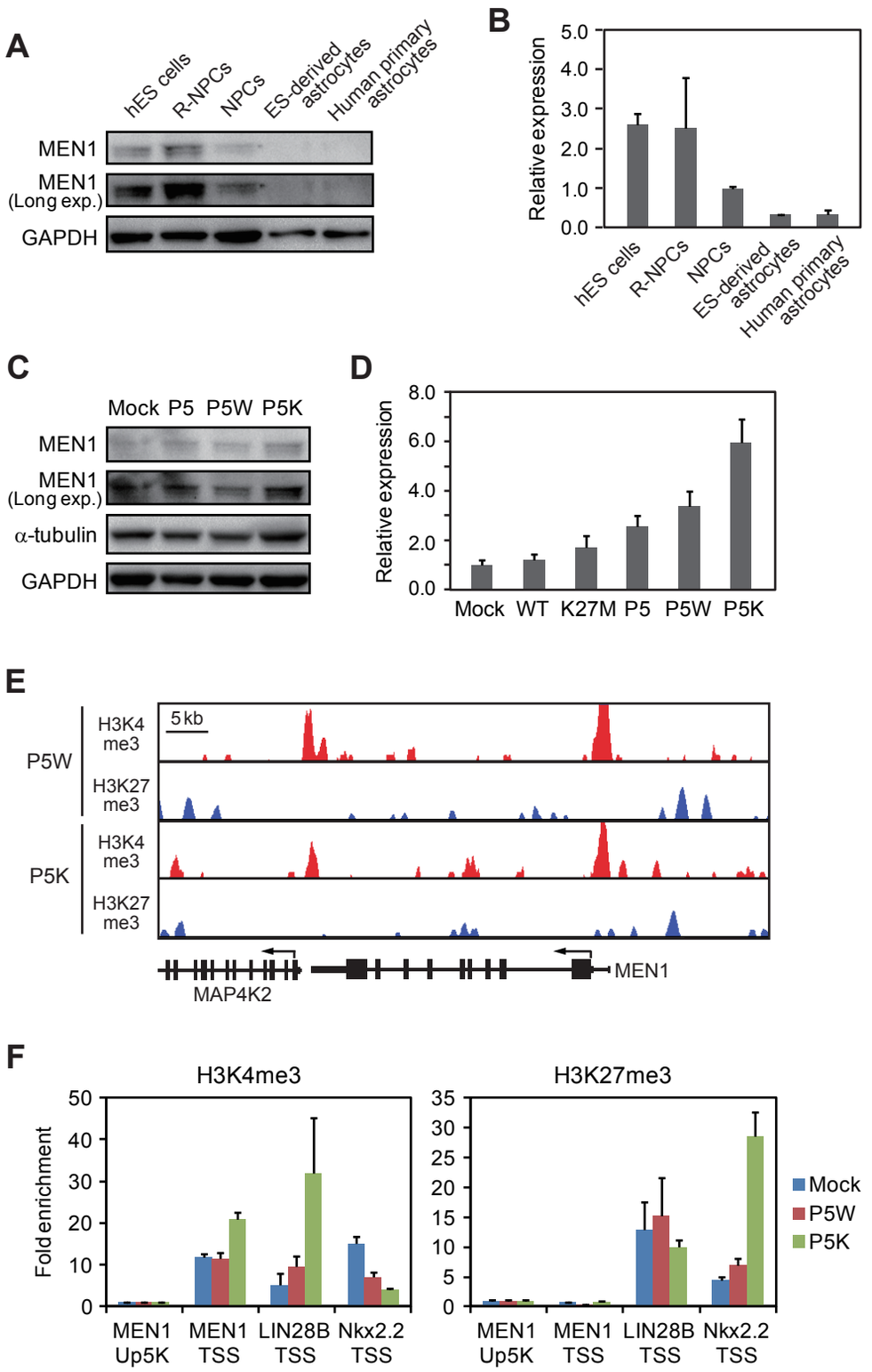
A
hES cells
R-NPCs
NPCs
ES-derived astrocytes
Human primary astrocytes
MEN1
MEN1 (Long exp.)
GAPDH
B
Relative expression
5.0
4.0
3.0
2.0
1.0
0.0
hES cells
R-NPCs
NPCs
ES-derived astrocytes
Human primary astrocytes
C
Mock P5 P5W P5K
MEN1
MEN1 (Long exp.)
α-tubulin
GAPDH
D
Relative expression
8.0
6.0
4.0
2.0
0.0
Mock WT K27M P5 P5W P5K
E
5 kb
P5W
H3K4 me3
H3K27 me3
P5K
H3K4 me3
H3K27 me3
MAP4K2
MEN1
F
H3K4me3
H3K27me3
Fold enrichment
50
40
30
20
10
0
35
30
25
20
15
10
5
0
MEN1 Up5K
MEN1 TSS
LIN28B TSS
Nkx2.2 TSS
Mock
P5W
P5K

Fig. S13

(A,B) Increased expression of menin in P5K cells is shown by western blotting (A) and RT-qPCR (B). (C,D) Expression level of menin is upregulated in human ES cells and rosette-stage NPCs (R-NPCs), whereas downregulated in astrocytes. Bars in (B,D) indicate mean ± S.E.M. (n = 3~5). (E,F) Chromatin landscape of *MEN1* locus in P5W and P5K cells. ChIP-seq data for H3K4me3 (red) and H3K27me3 (blue)(E), and validation by ChIP-PCR (F). Bars indicate mean ± S.D. (n = 3).

Figure S14

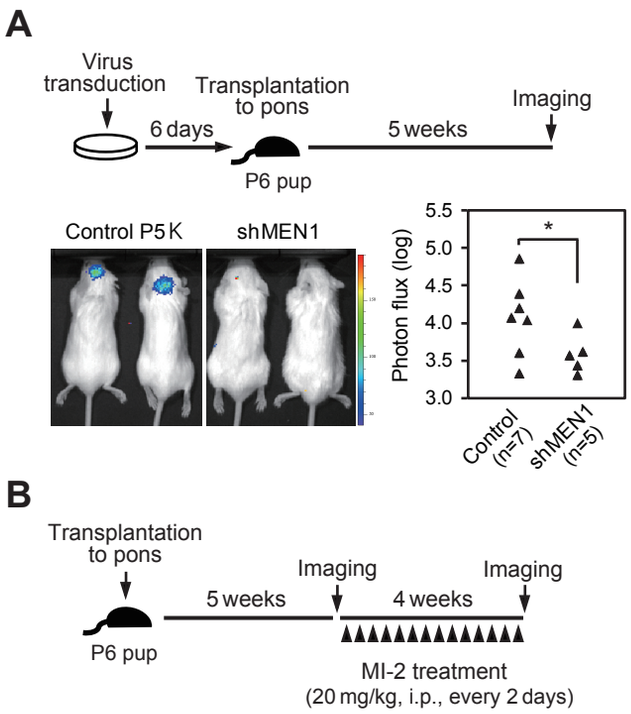
A
Virus transduction
6 days
Transplantation to pons
P6 pup
5 weeks
Imaging
Control P5 K
shMEN1
Photon flux (log)
5.5
5.0
4.5
4.0
3.5
3.0
*
Control (n=7)
shMEN1 (n=5)

B
Transplantation to pons
P6 pup
5 weeks
Imaging
4 weeks
Imaging
MI-2 treatment
(20 mg/kg, i.p., every 2 days)

Fig. S14

(A) Knockdown of menin suppresses *in vivo* growth of P5K cells. Intracranial growth of Luciferase-labeled P5K cells, transduced with control or menin shRNA-expressing (shMEN1) lentiviruses, was measured by quantitative *in vivo* bioluminescence imaging (IVIS). (B) Schematic representation of the drug treatment experiment shown in Fig 4G. *, $p < 0.05$

Figure S15

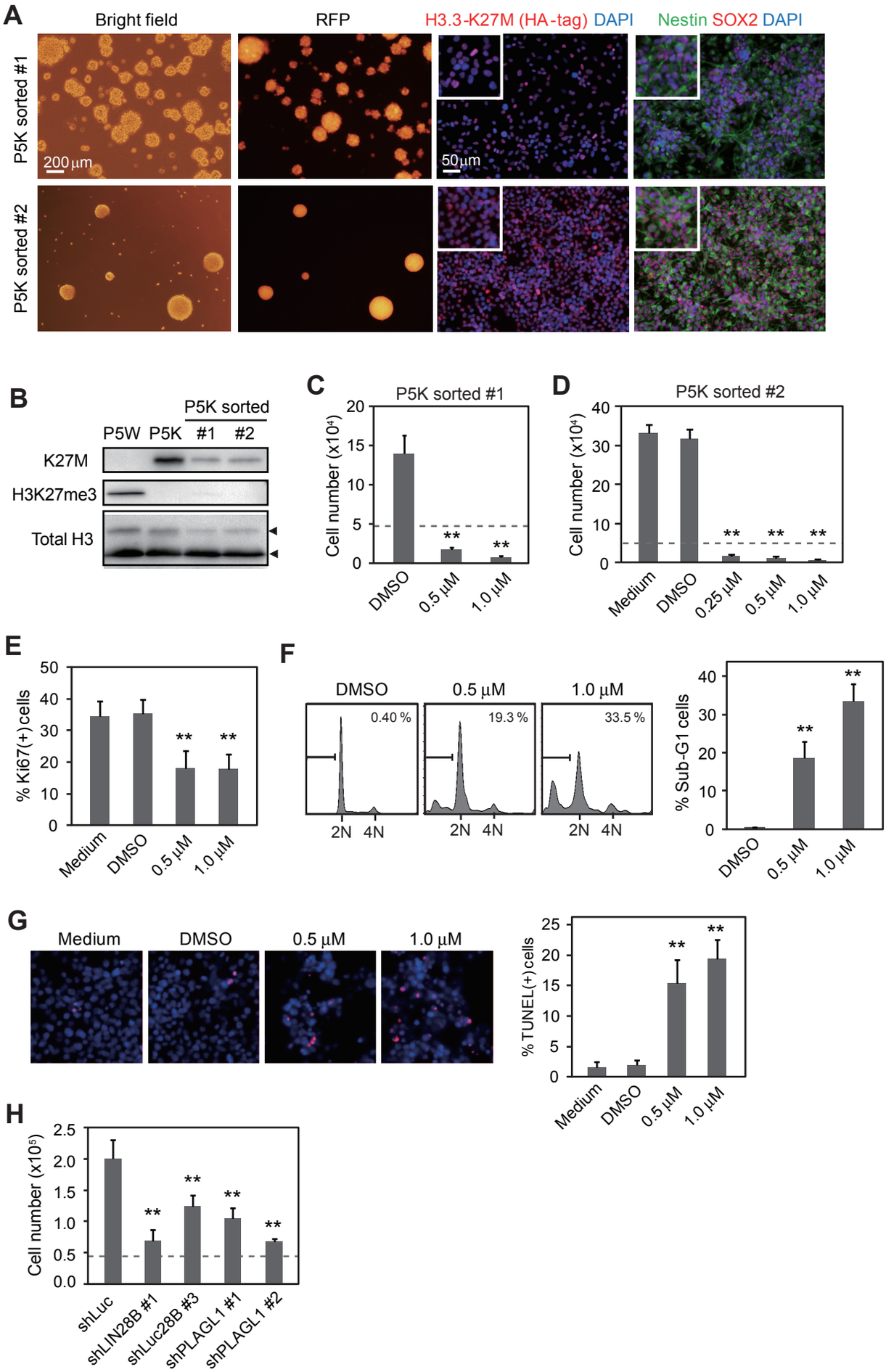
A
Bright field
RFP
H3.3-K27M (HA-tag) DAPI
Nestin SOX2 DAPI
P5K sorted #1
P5K sorted #2
200 μm
50 μm
B
P5K sorted
P5W P5K #1 #2
K27M
H3K27me3
Total H3
C
P5K sorted #1
Cell number (x10⁴)
DMSO
0.5 μM
1.0 μM
D
P5K sorted #2
Cell number (x10⁴)
Medium
DMSO
0.25 μM
0.5 μM
1.0 μM
E
% Ki67(+) cells
Medium
DMSO
0.5 μM
1.0 μM
F
DMSO
0.5 μM
1.0 μM
0.40 %
19.3 %
33.5 %
2N 4N
% Sub-G1 cells
G
Medium
DMSO
0.5 μM
1.0 μM
% TUNEL(+) cells
H
Cell number (x10⁵)
shLuc
shLIN28B #1
shLuc28B #3
shPLAGL1 #1
shPLAGL1 #2

Fig. S15

(A) Characterization of P5K cells sorted from mouse xenografts. Cells can be grown in both sphere (left panels) and adherent-culture (right panels). Immunohistochemistry demonstrates maintenance of SOX2 and Nestin expression as well as H3.3K27M transgene. (B) Western blotting of xenograft-derived P5K cells shows the expression of K27M and loss of H3K27 trimethylation mark (H3K27me3). Higher bands in the total H3 blot indicate hemagglutinin (HA)-tagged H3.3 transgene. (C,D) Sorted P5K cells were treated with MI-2 for 7 days and the number of viable cells was counted by trypan-blue staining. Bars indicate mean ± S.D. (n = 4). (E) MI-2 treatment suppressed the proliferation of sorted P5K cells. Cells were treated with MI-2 at various concentrations for 5 days and immunostained for Ki67. Bars indicate mean ± S.D. (n = 4~5). (F,G) MI-2 treatment induced cell death in sorted P5K cells. Following 6 days of treatment, the percentage of dead cells was measured by Sub-G1 assay (F) and TUNEL staining (G). Bars indicate mean ± S.D. (n = 4). (H) Knockdown of LIN28B and PLAGL1 reduced the number of viable cells in sorted P5K cells. Cells were infected with the indicated shRNA-expressing lentiviruses. Viability was assayed by trypan-blue following 6 days *in vitro*. Bars indicate mean ± S.D. (n = 4). **, $p < 0.01$.

Figure S16

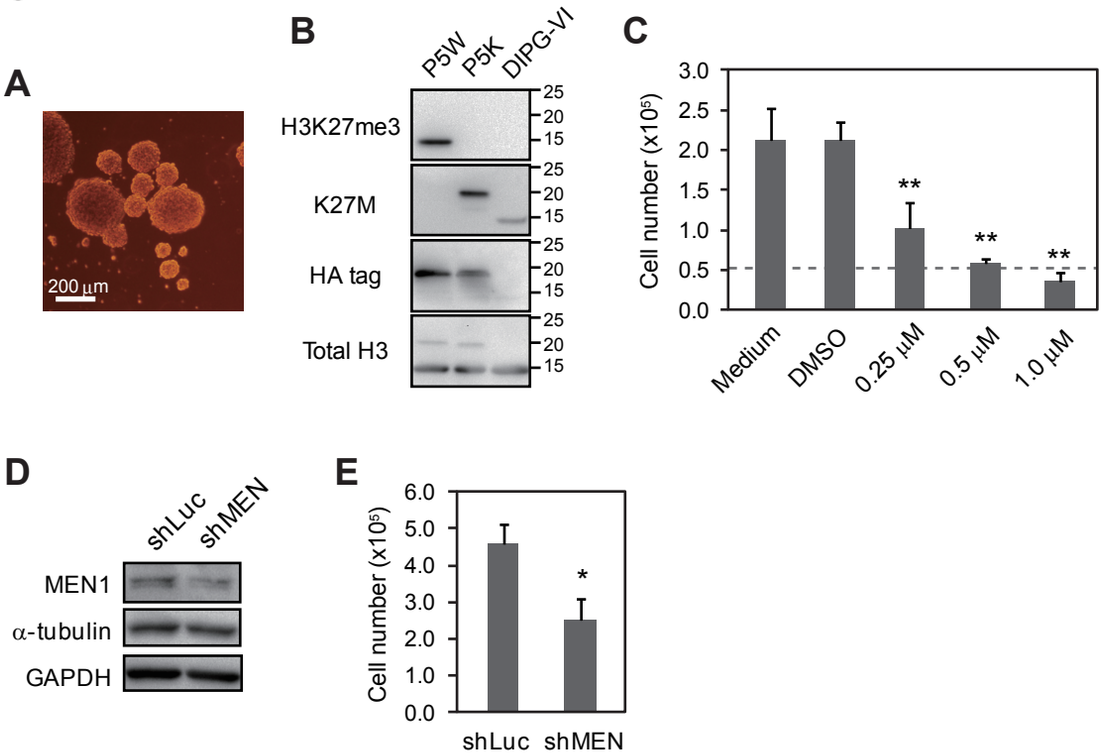
A
200 μm
B
P5W
P5K
DIPG-VI
H3K27me3
K27M
HA tag
Total H3
25
20
15
C
Cell number (x10⁵)
3.0
2.5
2.0
1.5
1.0
0.5
0.0
**
**
**
Medium
DMSO
0.25 μM
0.5 μM
1.0 μM
D
shLuc
shMEN
MEN1
α-tubulin
GAPDH
E
Cell number (x10⁵)
6.0
5.0
4.0
3.0
2.0
1.0
0.0
*
shLuc
shMEN

Fig. S16

(A) Bright phase microscopy of a patient-derived DIPG cell line. (B) Western blotting indicates the presence of H3.3K27M mutation and significant reduction of H3K27 trimethylation mark (H3K27me3) in the DIPG cell line (DIPG-VI). (C) MI-2 treatment suppressed the proliferation of DIPG cell line. Cells were treated with MI-2 for 7 days and the number of viable cells was counted by trypan-blue staining. Bars indicate mean ± S.D. ($n = 4$). (D,E) Knockdown of menin suppressed the proliferation of DIPG cell line. Cells were transduced with control or menin shRNA-expressing (shMEN) lentiviruses. Following 7 days *in vitro*, knockdown of menin was confirmed by western blotting (D) and the number of viable cells was counted by trypan-blue staining (E). Bars indicate mean ± S.D. ($n = 4$). *, $p < 0.05$; **, $p < 0.01$.

Table S1. Genes upregulated in cells expressing the H3.3 K27M mutation (K27M + P5K *vs* all other conditions)

Rank	Gene ID (Affymetrix)	Gene Description	Score (Signal-to-noise ratio)
1	232231_at	runt-related transcription factor 2, RUNX2	9.73
2	205229_s_at	coagulation factor C homolog, cochlin (Limulus polyphemus), COCH	8.15
3	1554242_a_at	coagulation factor C homolog, cochlin (Limulus polyphemus), COCH	7.49
4	222392_x_at	PERP, TP53 apoptosis effector, PERP	6.70
5	218499_at	serine/threonine protein kinase MST4, MST4	6.63
6	243356_at		6.52
7	222701_s_at	coiled-coil-helix-coiled-coil-helix domain containing 7, CHCHD7	6.39
8	206023_at	neuromedin U, NMU	5.87
9	217744_s_at	PERP, TP53 apoptosis effector, PERP	5.74
10	204984_at	glypican 4, GPC4	5.73
11	205372_at	**pleiomorphic adenoma gene 1, PLAG1**	5.72
12	223038_s_at	family with sequence similarity 60, member A, FAM60A	5.66
13	219523_s_at	odz, odd Oz/ten-m homolog 3 (Drosophila), ODZ3	5.22
14	218872_at	tescalcin, TESC	4.95
15	229349_at	**lin-28 homolog B (C. elegans), LIN28B**	4.87
16	229385_s_at	placenta-specific 2 (non-protein coding), PLAC2	4.65
17	220147_s_at	family with sequence similarity 60, member A, FAM60A	4.60
18	233814_at	ephrin-A5, EFNA5	4.51
19	228107_at	hypothetical protein LOC100127983, LOC100127983	4.41
20	205190_at	plastin 1, PLS1	4.40
21	205201_at	GLI family zinc finger 3, GLI3	4.36
22	1559266_s_at	chromosome 10 open reading frame 140, C10orf140	4.26
23	209763_at	chordin-like 1, CHRDL1	4.25
24	227307_at	tetraspanin 18, TSPAN18	4.21
25	1559360_at		4.16
26	227623_at	calcium channel, voltage-dependent, alpha 2/delta subunit 1, CACNA2D1	4.15
27	238865_at	poly(A) binding protein, cytoplasmic 4-like, PABPC4L	4.13
28	227955_s_at	ephrin-A5, EFNA5	4.11
29	207943_x_at	**pleiomorphic adenoma gene-like 1, PLAGL1**	4.10
30	206953_s_at	latrophilin 2, LPHN2	4.06
31	231310_at		4.02
32	214785_at	vacuolar protein sorting 13 homolog A (S. cerevisiae), VPS13A	3.98
33	222900_at	nuclear receptor interacting protein 3, NRIP3	3.97
34	233257_at		3.94
35	217809_at	basic leucine zipper and W2 domains 2, BZW2	3.93
36	214036_at	ephrin-A5, EFNA5	3.92
37	209212_s_at	Kruppel-like factor 5 (intestinal), KLF5	3.92

38	207002_s_at	**pleiomorphic adenoma gene-like 1, PLAGL1**	3.83
39	209318_x_at	**pleiomorphic adenoma gene-like 1, PLAGL1**	3.83
40	1560652_at		3.80
41	1569652_at	mixed-lineage leukemia (trithorax homolog); translocated to, 3, MLLT3	3.79
42	219778_at	zinc finger protein, multitype 2, ZFPM2	3.79
43	221760_at	mannosidase, alpha, class 1A, member 1, MAN1A1	3.78
44	233002_at	protein phosphatase 4, regulatory subunit 4, PPP4R4	3.78
45	226117_at	TRAF-interacting protein with forkhead-associated domain, TIFA	3.76
46	220987_s_at	chromosome 11 open reading frame 17 /// NUAK2	3.72
47	225177_at	RAB11 family interacting protein 1 (class I), RAB11FIP1	3.71
48	204983_s_at	glypican 4, GPC4	3.68
49	225051_at	erythrocyte membrane protein band 4.1 (elliptocytosis 1, RH-linked), EPB41	3.68
50	227415_at	hypothetical protein LOC283508, LOC283508	3.67

Table S2. Genes downregulated in cells expressing the H3.3 K27M mutation (K27M + P5K *vs* all other conditions)

Rank	Gene ID (Affymetrix)	Gene Description	Score (Signal-to-noise ratio)
1	235562_at	chromosome 3 open reading frame 70, C3orf70	-7.45276
2	242447_at	chromosome 3 open reading frame 70, C3orf70	-7.12643
3	227055_at	methyltransferase like 7B, METTL7B	-6.85883
4	240242_at		-6.79264
5	206306_at	ryanodine receptor 3, RYR3	-6.59394
6	207981_s_at	estrogen-related receptor gamma, ESRRG	-6.33449
7	204916_at	receptor (G protein-coupled) activity modifying protein 1, RAMP1	-6.06627
8	203908_at	solute carrier family 4, sodium bicarbonate cotransporter, member 4, SLC4A4	-6.05743
9	229382_at	chromosome 1 open reading frame 183, C1orf183	-6.01959
10	229266_at	shisa homolog 6 (Xenopus laevis), SHISA6	-5.9745
11	213543_at	sarcoglycan, delta (35kDa dystrophin-associated glycoprotein), SGCD	-5.82467
12	1552626_a_at	transmembrane protein 163, TMEM163	-5.65298
13	207093_s_at	oligodendrocyte myelin glycoprotein, OMG	-5.35129
14	227148_at	pleckstrin homology domain containing, family H member 2, PLEKHH2	-5.34979
15	200953_s_at	cyclin D2, CCND2	-5.31529
16	207789_s_at	dipeptidyl-peptidase 6, DPP6	-5.30983
17	231001_at	fin bud initiation factor homolog (zebrafish), FIBIN	-5.24142
18	226769_at	fin bud initiation factor homolog (zebrafish), FIBIN	-5.13636
19	228546_at	dipeptidyl-peptidase 6, DPP6	-5.1138
20	213832_at	potassium voltage-gated channel, Shal-related subfamily, member 3, KCND3	-5.0929
21	220761_s_at	TAO kinase 3, TAOK3	-5.06633
22	231098_at		-5.05854
23	241706_at	copine VIII, CPNE8	-5.04386
24	233129_at		-5.03761
25	232377_at	neurexophilin 1, NXPH1	-4.91254
26	218807_at	vav 3 guanine nucleotide exchange factor, VAV3	-4.91059
27	206462_s_at	neurotrophic tyrosine kinase, receptor, type 3, NTRK3	-4.89773
28	212098_at	mannosyl (α-1,6-)-glycoprotein beta-1,6-N-acetyl-glucosaminyltransferase, MGAT5	-4.88847
29	223923_at	chromosome 21 open reading frame 62, C21orf62	-4.84926
30	239221_at	G protein-coupled receptor 123, GPR123	-4.84522
31	206915_at	**NK2 homeobox 2, NKX2-2**	-4.84372
32	223503_at	transmembrane protein 163, TMEM163	-4.77141
33	212190_at	serpin peptidase inhibitor, clade E (nexin), member 2, SERPINE2	-4.75121
34	223468_s_at	RGM domain family, member A, RGMA	-4.70716

35	206243_at	TIMP metallopeptidase inhibitor 4, TIMP4	-4.68817
36	219564_at	potassium inwardly-rectifying channel, subfamily J, member 16, KCNJ16	-4.67798
37	219049_at	chondroitin sulfate N-acetylgalactosaminyltransferase 1, CSGALNACT1	-4.62745
38	229759_s_at	ventricular zone expressed PH domain homolog 1 (zebrafish), VEPH1	-4.62055
39	202242_at	tetraspanin 7, TSPAN7	-4.59022
40	205475_at	stimulator of chondrogenesis 1, SCRG1	-4.55727
41	238003_at	hepatocyte cell adhesion molecule, HEPACAM	-4.55185
42	220543_at	chromosome 21 open reading frame 62, C21orf62	-4.55149
43	215014_at	potassium voltage-gated channel, Shal-related subfamily, member 3, KCND3	-4.52529
44	217033_x_at	neurotrophic tyrosine kinase, receptor, type 3, NTRK3	-4.51016
45	232235_at	dermatan sulfate epimerase-like, DSEL	-4.46631
46	240458_at		-4.44163
47	236599_at		-4.4402
48	1557143_at	CUB and Sushi multiple domains 2, CSMD2	-4.42817
49	213618_at	ArfGAP with RhoGAP domain, ankyrin repeat and PH domain 2, ARAP2	-4.39381
50	209356_x_at	EGF-containing fibulin-like extracellular matrix protein 2, EFEMP2	-4.38892

Table S3. Levels of H3K4me3 and H3K27me3 at promoter regions of genes that are upregulated or downregulated by K27M.

K4me3	K27me3
>1.0	>0.6
>2.0	>1.0
>3.0	>2.0

Genes upregulated by K27M				
Name	P5W		P5K	
	K4me3	K27me3	K4me3	K27me3
Runx2	0.87	0.34	0.93	0.14
COCH	1.32	0.48	1.02	0.34
PERP	0.63	0.55	0.40	1.00
CHCHD7	1.97	0.11	1.79	0.54
NMU	0.58	0.70	0.77	0.37
MST4	0.63	0.57	1.37	0.66
GPC4	2.21	0.43	1.47	0.29
PLAG1	1.97	0.11	1.88	0.51
FAM60A	1.50	0.30	1.12	0.46
TESC	0.34	0.39	0.56	0.37
LIN28B	0.55	0.95	0.91	1.46
EFNA5	0.97	0.30	1.00	0.66
PLS1	1.74	0.52	0.93	0.29
GLI3	2.13	0.27	0.88	0.20
CHRDL1	1.11	0.43	0.93	0.29
TSPAN18	0.63	0.61	0.53	0.20
CACNA2D1	1.71	0.14	0.95	0.34
PABPC4L	0.95	0.43	0.65	0.23
PLAGL1	0.53	0.50	0.44	1.89
LPHN2	1.39	0.32	1.00	0.31
VPS13A	1.24	0.45	0.74	0.46
BZW2	2.37	0.43	1.35	0.40
KLF5	1.66	0.34	0.98	0.40
MLLT3	1.79	0.20	0.74	0.14
ZFPM2	1.03	0.27	0.63	0.54
MAN1A1	3.11	0.18	1.88	0.80
PPP4R4	0.82	0.27	0.88	0.37
TIFA	0.68	0.43	0.79	0.20
NUAK2	1.26	0.32	1.23	0.46
CDH8	0.47	0.82	0.70	1.03
BCL11A	1.32	0.14	0.58	0.57
RBPMS	2.05	0.23	1.26	0.40

NRIP3	0.87	0.41	0.49	0.57
DACH1	1.50	0.27	0.79	1.66
CDKN1C	0.39	0.18	0.63	0.20
RGS10	0.71	0.27	0.74	0.80
CTSC	1.89	0.41	1.51	0.31
PAK1	0.47	0.09	0.70	0.11
SNAI2	1.05	0.27	0.77	0.29
DPYD	2.47	0.45	1.02	0.49
MAML3	1.47	0.18	0.79	0.14
BSG	1.92	0.25	0.95	0.46
H1FX	1.87	0.43	0.74	0.43
CDH6	1.21	0.41	1.09	0.51
STXBP6	0.92	0.27	0.60	0.37
SSX2IP	1.61	0.20	0.98	0.37
SLC44A1	1.58	0.34	0.60	0.29
SMC4	4.50	0.34	2.09	0.80
H1F0	0.47	0.36	0.40	1.91
RUNX1T1	1.45	0.52	0.72	0.46
SLC35F2	0.84	0.45	1.02	0.26
NID1	1.18	0.25	1.12	0.43
GJA3	0.32	0.34	0.28	3.37
KLF10	2.05	0.16	1.07	0.51
VGLL3	1.74	0.34	1.42	0.69
DDIT4L	1.29	0.39	1.14	0.29
MEF2C	2.26	0.34	1.21	0.69
SLC6A15	1.03	0.82	0.93	0.60
PHIP	2.97	0.23	1.35	0.51
SFRP2	0.79	0.73	0.72	0.63
CALB1	0.71	0.57	0.88	0.43
RRAS2	0.89	0.55	1.23	0.83
NEK2	1.50	0.36	0.95	0.29
PHLDB2	0.45	0.36	0.56	0.63
PPL	0.03	0.32	0.30	0.83
SEMA3A	3.37	0.89	1.98	2.37
TIAM1	2.53	0.36	1.65	0.46
GABRA5	0.63	0.20	0.42	0.31
SNCA	0.53	0.57	1.12	0.54
KLHL14	0.18	0.61	0.42	0.80
CDC14B	1.00	0.23	0.51	0.29
ARL4C	1.00	0.16	0.53	0.26
TMEM38B	1.21	0.48	0.86	1.74
TLE4	1.11	0.23	0.65	0.26
ADAMTS3	2.50	0.16	1.60	0.23
STX3	0.74	0.41	1.02	0.49

PRTG	2.82	0.23	1.40	0.20
SHB	0.74	0.16	0.72	0.66
MSI2	0.50	0.23	0.44	0.34
TXNIP	2.55	0.18	1.42	0.31
HDAC9	0.89	0.50	0.93	0.09
SCEL	0.37	0.41	0.47	0.37
CPS1	1.39	0.25	0.84	0.29
TRIM36	1.45	0.16	0.88	1.94
PDK4	1.34	0.27	1.05	0.23
TPBG	0.79	0.75	0.44	1.29
EMB	0.87	0.45	0.86	0.40
FOXG1	0.11	0.16	0.28	0.54
OTX2	0.71	0.64	1.12	1.97
LIN7A	1.42	0.32	0.95	0.31
HSPB1	1.13	0.45	0.60	0.74

Genes downregulated by K27M				
Name	P5W		P5K	
	K4me3	K27me3	K4me3	K27me3
AQP4	1.16	0.23	0.47	0.43
RYR3	1.39	0.25	1.02	0.49
NKX2-2	0.92	0.18	0.40	3.97
CCND2	1.66	0.43	0.67	4.40
ESRRG-P1	1.03	0.80	0.37	1.91
ESRRG-P2	0.53	0.70	0.28	8.43
DPP6	0.71	0.18	0.33	1.31
VAV3	1.39	0.18	0.56	0.43
PI3KR1	2.42	0.27	1.60	0.66
KAT7	2.63	0.39	1.44	0.54
TMEM163	0.71	0.25	0.44	1.89
CSMD2	1.18	0.39	0.72	1.09
SNRPN	0.34	0.48	0.33	0.71
TRAF4	1.39	0.14	0.67	0.34
FEZ1	1.34	0.34	0.49	0.40
GSTT1	0.87	0.18	0.33	0.26
KAT2B	1.05	0.02	1.26	0.29
BAI3	1.97	0.11	1.40	0.20
IQSEC1	0.39	0.05	0.33	0.14
SLC4A4	2.42	0.20	1.53	0.37
MAPK10	1.58	0.45	0.53	0.34
SLC6A1	1.03	0.23	0.30	1.63

INPP4B	1.79	0.41	1.28	0.23
BLM	3.05	0.43	1.37	0.31
C3orf70	0.71	0.14	0.63	0.34
SHISA6	0.63	0.09	0.05	0.83
SGCD	0.63	0.45	0.19	0.51
PLEKHH2	2.08	0.27	0.93	0.54
FIBIN	0.45	0.34	0.95	0.23
KCND3	1.37	0.16	0.58	0.29
TAOK3	3.76	0.20	1.51	0.29
CPNE8	2.68	0.43	0.91	0.80
NXPH1	1.45	0.36	0.49	1.60
NTRK3	2.34	0.23	0.56	0.37
GPR123	0.55	0.39	0.44	0.40
SERPINE2	2.08	0.25	1.40	0.17
RGMA	1.24	0.39	0.63	0.83
VEPH1	0.21	0.41	0.81	0.20
SCRG1	1.21	0.50	0.53	0.80
DSEL	2.95	0.39	1.72	0.51
ARAP2	2.08	0.32	1.40	0.46
RASSF2	1.66	0.20	0.74	0.43
NLGN3	0.97	0.39	0.53	0.37
CDH10	2.39	0.16	1.12	0.14
LRRK2	0.68	0.30	0.49	0.43
DOCK10	1.26	0.48	0.65	0.60
SRI	2.08	0.25	1.05	0.31
SLC6A11	1.05	0.25	0.40	1.63
SLC6A1	1.03	0.23	0.30	1.63
ITPR2	2.26	0.48	0.56	0.46
DLC1	0.66	0.45	0.53	0.66
GRIA1	2.82	0.55	0.84	0.37
NPAS3	1.79	0.77	1.21	1.34
MYO5C	0.97	0.20	0.72	0.26
DMD	0.82	0.39	0.47	0.40
TRIL	0.84	0.32	0.77	0.66
ZEB1	3.16	0.11	1.70	0.31
ZCCHC24	0.66	0.27	0.30	0.23
TCF12-P1	1.53	0.23	1.07	0.31
TCF12-P2	1.29	0.25	0.53	0.17
PCYT1B	1.24	0.27	0.56	0.31
SALL1	2.47	0.32	0.79	4.31
VSTM2A	0.84	0.27	0.56	0.83
SNTB1	1.18	0.45	0.58	1.29
CST3	1.08	0.25	0.67	0.29
PLD5	1.05	0.27	0.74	1.09

CTH	2.63	0.41	1.53	0.31
SMOC1	1.21	0.30	0.58	0.46
SLC15A2	1.29	0.23	0.72	0.34
RGS6	1.32	0.30	0.47	0.66
PLA2G16	1.37	0.18	0.74	0.09
IGSF11	2.66	0.30	1.07	0.83
SPOCK2	0.82	0.25	0.26	0.31
RIT2	1.32	0.34	0.51	0.37
TRIM9	1.13	0.45	0.77	0.29
ZMAT4	1.08	0.45	0.40	0.34
PHEX	0.16	0.57	0.56	0.74
STAMBPL1	1.32	0.61	1.14	0.54
PTPRE	1.50	0.20	0.77	0.17
SYNE1	0.61	0.55	0.86	1.23
CNKSR2	2.45	0.27	0.98	0.46
ZNF93	2.03	0.16	0.95	0.34

Table S4. List of target genes by H3K27me3 marks or by PRC2 complex

(A) P5W H3K27me3 target	(B) P5K H3K27me3 target	(C) P5K-sepecific H3K27me3 target	(D) Benporath_ESC H3K27me3 target	(E) Benporath_ESC PRC2 target	(C) AND (D) shared	(C) AND (E) shared
AATF	A4GALT	A4GALT	AATF	ABCC8	ACAN	ADAMTS18
ACCSL	AARS2	AARS2	ABCC3	ABTB2	ACTL6B	ADAP2
ACSM4	AATF	ABCE1	ABCC8	ADAMTS15	ADAMTS18	ADARB2
ACTBL2	ABCE1	ACAD9	ABCG4	ADAMTS18	ADAP2	ADCY8
ADCY4	ACAD9	ACAN	ABTB2	ADAP2	ADARB2	ADCYAP1
ADORA3	ACAN	ACHE	ACADL	ADARB2	ADCY8	ADRA1A
AGBL5	ACHE	ACIN1	ACAN	ADCY4	ADCYAP1	ADRB1
AGPAT5	ACIN1	ACOT13	ACCN2	ADCY8	ADRA1A	ADRB3
AHCYL1	ACOT13	ACOXL	ACTL6B	ADCYAP1	ADRB1	AGPAT9
AHCYL2	ACOXL	ACRV1	ADAM15	ADRA1A	ADRB3	ALOX15
ALDH1A2	ACRV1	ACSL1	ADAM22	ADRA2A	AGPAT9	ALX3
AMER3	ACSL1	ACSL5	ADAMTS15	ADRB1	AIM1	ALX4
AMPD1	ACSL5	ACSM1	ADAMTS17	ADRB3	ALOX15	ANKRD18A
ANKRD1	ACSM1	ACSS1	ADAMTS18	AGPAT9	ALX3	ANKRD18B
ANO2	ACSS1	ACTA1	ADAP2	ALOX15	ALX4	ANKRD19P
ANO6	ACTA1	ACTL6A	ADARB2	ALX3	ANKRD18A	ANKRD27
ANXA2P1	ACTL6A	ACTL6B	ADC	ALX4	ANKRD18B	ASCL2
ARSF	ACTL6B	ACVR1C	ADCY4	ANKRD18A	ANKRD19P	ASTN2
ARSH	ACVR1C	ADAM8	ADCY8	ANKRD18B	ANKRD27	ATF3
ASB17	ADAM8	ADAMTS18	ADCYAP1	ANKRD19P	ARID3C	ATOH8
ASCL5	ADAMTS18	ADAMTS2	ADRA1A	ANKRD20A1	ARNTL	BARHL1
ASTL	ADAMTS2	ADAMTS20	ADRA2A	ANKRD20A2	ASCL2	BARHL2
ATOH1	ADAMTS20	ADAMTS8	ADRB1	ANKRD20A3	ASCL4	BARX2
ATP8B4	ADAMTS8	ADAMTSL3	ADRB3	ANKRD20A5P	ASTN2	BATF3
ATXN7L2	ADAMTSL3	ADAP2	ADRBK2	ANKRD20A8P	ATF3	BHLHE23
B4GALNT2	ADAP2	ADARB2	AGAP2	ANKRD27	ATOH8	C17orf102
BARX1	ADARB2	ADCY8	AGPAT9	AQP5	BARHL1	C17orf82
BASP1	ADCY4	ADCYAP1	AIM1	ARHGAP20	BARHL2	C1orf194
BCL6	ADCY8	ADM	ALOX15	ARL9	BARX2	C1orf213
BCL9	ADCYAP1	ADORA2A-AS1	ALOXE3	ASCL1	BATF3	C2CD4A
BHLHE22	ADM	ADPGK	ALX3	ASCL2	BHLHE23	CA10
BMF	ADORA2A-AS1	ADRA1A	ALX4	ASTN1	BMP6	CACNA1B
BMP4	ADPGK	ADRB1	AMELX	ASTN2	C14orf132	CACNA1D
BNC1	ADRA1A	ADRB3	AMN	ATF3	C17orf102	CACNA1E
BPIFA1	ADRB1	AFAP1L2	AMPH	ATOH1	C17orf82	CACNA1G
BPIFA4P	ADRB3	AFF3	ANKRD18A	ATOH8	C1orf194	CAMK2N1
BPIFB4	AFAP1L2	AFM	ANKRD18B	B4GALNT1	C1orf213	CBLN1
BSND	AFF3	AGBL4	ANKRD19P	B4GALNT2	C1orf94	CD34
BTAF1	AFM	AGPAT9	ANKRD20A1	BARHL1	C1QL1	CD70
BTBD11	AGBL4	AHSA2	ANKRD20A2	BARHL2	C2CD4A	CD8A

C10orf11
C10orf126
C12orf57
C14orf23
C14orf39
C16orf95
C17orf47
C1orf185
C1QTNF1-AS1
C1QTNF6
C21orf49
C21orf90
C2CD4B
C2orf71
C2orf78
C3
C4BPA
C7orf50
C7orf71
C9orf53
CACNG2
CALCA
CALHM2
CAMK4
CAPN14
CASC4
CASP8
CCDC112
CCDC140
CCL11
CCL20
CCL27
CCR6
CD160
CD300LB
CELF2
CEP85
CES3
CHRNA3
CHRNB3
CLDN5
CLEC1B
CNIH3
COL20A1
COL25A1
AGBL5
AGPAT5
AGPAT9
AHSA2
AHSP
AIFM1
AIM1
AJAP1
AK5
ALDH1A2
ALDH1A3
ALOX15
ALOX15P1
ALOX5
ALPL
ALX1
ALX3
ALX4
AMER3
AMZ1
ANAPC10
ANAPC15
ANAPC1P1
ANG
ANGEL1
ANK1
ANKH
ANKRD18A
ANKRD18B
ANKRD18DP
ANKRD19P
ANKRD27
ANKRD29
ANKRD34B
ANKRD34C
ANKRD6
ANKS1B
ANO2
ANP32A-IT1
ANP32E
ANXA2
ANXA2R
AP1M2
AP2B1
AP3B1
AHSP
AIFM1
AIM1
AJAP1
AK5
ALDH1A3
ALOX15
ALOX15P1
ALOX5
ALPL
ALX1
ALX3
ALX4
AMZ1
ANAPC10
ANAPC15
ANAPC1P1
ANG
ANGEL1
ANK1
ANKH
ANKRD18A
ANKRD18B
ANKRD18DP
ANKRD19P
ANKRD27
ANKRD29
ANKRD34B
ANKRD34C
ANKRD6
ANKS1B
ANP32A-IT1
ANP32E
ANXA2
ANXA2R
AP1M2
AP2B1
AP3B1
APCDD1L
APCDD1L-AS1
APOBEC3G
ARC
ARHGAP12
ARHGAP22
ARHGAP27
ANKRD20A3
ANKRD20A5P
ANKRD20A8P
ANKRD27
ANKRD35
ANKRD43
APBA1
AQP5
ARHGAP20
ARHGEF38
ARHGEF7
ARID3C
ARID5B
ARL10
ARL5C
ARL9
ARNTL
ASCL1
ASCL2
ASCL4
ASTN1
ASTN2
ATF3
ATOH1
ATOH8
ATP1A3
AVPR1B
B4GALNT1
B4GALNT2
BAI2
BARHL1
BARHL2
BARX1
BARX2
BATF3
BCAN
BCL2
BHLHE22
BHLHE23
BHLHE41
BLVRB
BMP6
BMP8A
BMX
BNC1
BARX1
BARX2
BATF3
BCL2
BHLHE22
BHLHE23
BHLHE41
BMP8A
BNC1
BTG2
C13orf15
C17orf102
C17orf82
C1orf194
C1orf213
C20orf103
C21orf63
C2CD4A
C3orf15
C4orf49
C5orf39
C8orf47
CA10
CACNA1B
CACNA1D
CACNA1E
CACNA1G
CALCA
CAMK2N1
CASZ1
CBLN1
CBLN4
CBR3
CBX8
CCDC140
CD34
CD70
CD8A
CDH23
CDH7
CDK5R2
CDKN2C
CDX2
CGB7
CGB8
CA10
CA7
CACNA1A
CACNA1B
CACNA1D
CACNA1E
CACNA1G
CACNG3
CALCR
CAMK2N1
CBLN1
CBX4
CCNA1
CD34
CD38
CD70
CD8A
CDC20B
CDH7
CDK5R2
CDKN2C
CDX2
CERKL
CH25H
CHD5
CHN2
CHRDL2
CHST8
CLIC5
CLSTN2
CNTNAP5
COL12A1
COL27A1
COL2A1
COLEC12
COMP
CR2
CRLF1
CRTAC1
CRYBA2
CSMD1
CSMD2
CSMD3
CWH43
CXCL16
CDH7
CDK5R2
CDKN2C
CDX2
CH25H
CHRDL2
CHST8
CLSTN2
COL27A1
COL2A1
COLEC12
COMP
CRLF1
CRTAC1
CRYBA2
CSMD1
CSMD3
CXCL16
CYP26A1
CYP26B1
CYP27B1
DACH1
DACH2
DCC
DGKG
DIO3
DKK1
DKK2
DLL4
DLX1
DLX2
DLX3
DLX4
DMRT1
DMRT2
DMRT3
DPF3
DRD5
DSC3
DSCAML1
DUOX1
DUOXA1
ECEL1
EGFL6
EGR4

COL4A3
COL4A4
COL6A5
COX16
CPO
CRH
CRHR2
CRISP3
CSH1
CSTA
CTRB2
CWC25
CXorf28
CXXC4
CYMP
CYP1B1
CYP24A1
CYP2A6
CYP2C9
CYP2F1
CYP2S1
DCAKD
DDC
DDX4
DEFA1
DEFA1B
DEFA3
DEFB104A
DEFB104B
DEFB107A
DEFB107B
DEFB124
DEFB136
DISC2
DLX6-AS1
DMKN
DNM1P35
DNMT3L
DOCK2
DRP2
DUOX2
DUOXA2
DYSF
ECRP
EDIL3
APCDD1L
APCDD1L-AS1
APOBEC3G
ARC
ARHGAP12
ARHGAP22
ARHGAP27
ARHGAP30
ARHGAP6
ARHGAP9
ARHGEF15
ARID3C
ARIH1
ARL15
ARNTL
ARPP21
ARSG
ARX
ASCL2
ASCL3
ASCL4
ASIC2
ASTN2
ATF2
ATF3
ATG5
ATG9B
ATN1
ATOH1
ATOH8
ATP12A
ATP2A3
ATP2B1
ATP2C2
ATP5G3
ATP5J
ATP6V1C2
ATP8B1
ATPIF1
ATXN7L2
AVPR1A
AVPR2
B3GNT1
B3GNT3
B3GNT4
ARHGAP30
ARHGAP6
ARHGAP9
ARHGEF15
ARID3C
ARIH1
ARL15
ARNTL
ARPP21
ARSG
ARX
ASCL2
ASCL3
ASCL4
ASIC2
ASTN2
ATF2
ATF3
ATG5
ATG9B
ATN1
ATOH8
ATP12A
ATP2A3
ATP2B1
ATP2C2
ATP5G3
ATP5J
ATP6V1C2
ATP8B1
ATPIF1
ATXN7L2
AVPR1A
AVPR2
B3GNT1
B3GNT3
B3GNT4
B3GNT7
BAG3
BAG4
BAIAP3
BAMBI
BANCR
BARHL1
BARHL2
BARX2
BTG2
C11orf45
C13orf15
C14orf132
C17orf100
C17orf102
C17orf82
C1orf115
C1orf194
C1orf213
C1orf51
C1orf94
C1QL1
C1QTNF5
C20orf103
C21orf63
C2CD4A
C3orf15
C3orf54
C4orf49
C5orf39
C8orf47
CA10
CA7
CACNA1A
CACNA1B
CACNA1D
CACNA1E
CACNA1G
CACNB3
CACNB4
CACNG3
CACNG8
CADM4
CALCA
CALCR
CAMK2B
CAMK2N1
CAMK2N2
CASZ1
CBLN1
CBLN4
CBR3
CBX4
CBX8
CH25H
CHODL
CHRD
CHRDL2
CHST8
CIDEA
CITED1
CLCN5
CLEC14A
CLSTN2
CMTM2
CNNM1
CNRIP1
CNTFR
COL24A1
COL25A1
COL27A1
COL2A1
COL4A5
COL4A6
COL9A2
COLEC12
COMP
CORO6
CRHR1
CRLF1
CRTAC1
CRYBA2
CSMD1
CSMD3
CTNND2
CXCL14
CXCL16
CYP24A1
CYP26A1
CYP26B1
CYP26C1
CYP27B1
DACH1
DACH2
DCC
DCHS2
DCLK2
DDAH1
DGKG
CYP26A1
CYP26B1
CYP27B1
DACH1
DACH2
DCC
DCX
DGKG
DIO3
DKK1
DKK2
DLK1
DLL4
DLX1
DLX2
DLX3
DLX4
DLX5
DMRT1
DMRT2
DMRT3
DPF3
DPP6
DRD5
DSC3
DSCAML1
DUOX1
DUOXA1
EBF1
EBF3
ECEL1
EGFL6
EGFLAM
EGR4
EIF4E3
ELAVL2
ELMOD1
ELOVL3
EN1
EN2
EPAS1
EPHA10
EPHA3
EPHA5
ELMOD1
EN1
EN2
EPAS1
EPHA5
ESPN
ESX1
FAM163A
FAM19A4
FAM43B
FAM89A
FBLN7
FBXL8
FEZF2
FGF3
FGF5
FGF9
FIGLA
FLI1
FLRT2
FOXB1
FOXD3
FOXD4L3
FOXD4L4
FOXE1
FOXF1
FOXG1
FOXL1
FOXL2
FRMD3
FZD10
GABRA2
GABRA4
GAD2
GALR2
GATA3
GATA4
GATA6
GBX2
GDF6
GDF7
GHR
GHSR
GJB2
GJD2

EOMES	B3GNT7	BATF3	CCDC140	DGKI	ESPN	GPR101
ERICH1-AS1	B4GALNT2	BAZ2A	CCDC50	DHH	ESR1	GPR88
ESRRG	BAG3	BCL2L11	CCDC96	DIO3	ESX1	GRIA2
EVA1A	BAG4	BCL7A	CCNA1	DKK1	FAM163A	GRID1
EVX1	BAIAP3	BDNF	CD34	DKK2	FAM19A4	GRIK3
EXOC3L2	BAMBI	BEAN1	CD38	DLL4	FAM43B	GRM7
FABP4	BANCR	BEGAIN	CD47	DLX1	FAM89A	GSC
FAHD1	BARHL1	BEND4	CD70	DLX2	FBLN7	GSC2
FAIM	BARHL2	BEST2	CD8A	DLX3	FBXL8	GSX1
FAM138A	BARX1	BHLHE23	CDC20B	DLX4	FERD3L	HAND2
FAM138B	BARX2	BHMT	CDH23	DMRT1	FEZF2	HES2
FAM138C	BASP1	BLACE	CDH4	DMRT2	FGF3	HHEX
FAM138F	BATF3	BLK	CDH6	DMRT3	FGF5	HLX
FAM150A	BAZ2A	BLOC1S1	CDH7	DNAJC22	FGF8	HMX2
FAM159B	BCL2L11	BLOC1S1-RDH5	CDK5R2	DOK6	FGF9	HMX3
FAM172BP	BCL7A	BMP2	CDKN2C	DPF3	FIGLA	HOXB3
FAM177B	BCL9	BMP3	CDX1	DPY19L2	FLI1	HOXB7
FAM180A	BDNF	BMP6	CDX2	DPY19L2P2	FLRT2	HOXB8
FAM194B	BEAN1	BMP8B	CERKL	DRD5	FNDC1	HOXC6
FAM72D	BEGAIN	BMPER	CGB7	DSC3	FOXB1	HOXD13
FAM99B	BEND4	BNC2	CGB8	DSCAML1	FOXC1	HOXD8
FBXL21	BEST2	BNIP2	CH25H	DUOX1	FOXD3	HOXD9
FBXO31	BHLHE22	BOD1L1	CHAD	DUOX2	FOXD4L3	HPSE2
FCGR1C	BHLHE23	BRDT	CHD5	DUOXA1	FOXD4L4	HRK
FCGR2A	BHMT	BRE	CHDH	DUOXA2	FOXE1	HS3ST3B1
FCGR3A	BLACE	BRINP2	CHN2	DUSP4	FOXE3	HS6ST3
FEV	BLK	BRINP3	CHODL	ECEL1	FOXF1	HSF4
FFAR1	BLOC1S1	BRIX1	CHRD	EFNA1	FOXF2	HTR1A
FGF4	BLOC1S1-RDH5	BRWD3	CHRDL1	EFNA3	FOXG1	ICAM5
FLI1-AS1	BMP2	BSPRY	CHRDL2	EGFL6	FOXL1	IGF2-AS
FLJ23867	BMP3	BSX	CHST8	EGR3	FOXL2	IKZF3
FLJ36000	BMP4	BTBD1	CIDEA	EGR4	FOXQ1	IL1RAPL2
FMO5	BMP6	BTG4	CITED1	ELMOD1	FRMD3	IL7
FOLR1	BMP8B	BTN1A1	CLCN5	EN1	FRMPD1	INSRR
FOXA2	BMPER	BTNL9	CLEC14A	EN2	FXYD7	IRX3
FOXD2	BNC1	BUB3	CLEC4G	EOMES	FZD10	IRX5
FOXD4L1	BNC2	C10orf131	CLIC5	EPAS1	GAB3	ISL1
GABRA1	BNIP2	C10orf32	CLIP4	EPB41L4A	GABRA2	ITGA4
GAL3ST1	BOD1L1	C10orf32-AS3MT	CLSTN2	EPHA5	GABRA4	ITPKA
GALNTL6	BRDT	C10orf55	CMTM2	EPHB1	GABRB2	KCNA1
GATA2	BRE	C10orf67	CNNM1	EPHB3	GAD2	KCNAB1
GBA	BRINP2	C10orf88	CNNM2	ERBB4	GALR2	KCNC4
GBA3	BRINP3	C11orf44	CNRIP1	ESAM	GATA3	KCNK12
GDNF	BRIX1	C11orf70	CNTFR	ESPN	GATA4	KCNK13

GDNF-AS1	BRWD3	C11orf74	CNTN2	ESX1	GATA6	KCNK2
GFI1	BSND	C11orf88	CNTNAP5	F2R	GBX2	KCNK4
GFOD1	BSPRY	C14orf119	COL12A1	FAM150A	GCM2	KCNMA1
GIPC2	BSX	C14orf132	COL24A1	FAM163A	GDF6	KCNQ3
GJA4	BTAF1	C16orf11	COL25A1	FAM19A4	GDF7	KCNV1
GKN2	BTBD1	C16orf13	COL27A1	FAM43B	GHR	KIAA1324
GLIS1	BTBD11	C17orf102	COL2A1	FAM5B	GHSR	KIRREL3
GLOD5	BTG4	C17orf82	COL4A5	FAM5C	GJB2	KL
GLUD2	BTN1A1	C18orf42	COL4A6	FAM81A	GJD2	KLF4
GPR4	BTNL9	C19orf33	COL8A1	FAM84A	GPR101	KLHL35
GPR68	BUB3	C19orf59	COL9A2	FAM89A	GPR26	LBX1
GPR83	C10orf131	C1orf110	COLEC12	FBLN7	GPR88	LGR5
GPRIN2	C10orf32	C1orf170	COMMD3	FBN2	GRIA2	LHX2
GRHL3	C10orf32-AS3MT	C1orf172	COMP	FBP1	GRID1	LHX4
GRIN3A	C10orf55	C1orf194	CORO6	FBXL8	GRIK3	LHX5
GRM4	C10orf67	C1orf200	COX6B2	FBXO3	GRIN1	LMX1B
GSN	C10orf88	C1orf210	CPM	FEV	GRM6	LOC153684
GSN-AS1	C11orf44	C1orf213	CR2	FEZ1	GRM7	LONRF3
GSX2	C11orf70	C1orf27	CRH	FEZF2	GSC	LPL
GUCY1A3	C11orf74	C1orf53	CRHR1	FGF20	GSC2	LRRC71
GZMA	C11orf88	C1orf61	CRIP1	FGF3	GSX1	LTBP2
H1FOO	C14orf119	C1orf74	CRLF1	FGF5	HAND1	LTK
H2AFX	C14orf132	C1orf94	CRMP1	FGF9	HAND2	LYSMD2
HAGH	C14orf23	C1QC	CRTAC1	FIGLA	HCN4	MAB21L1
HBA1	C14orf39	C1QL1	CRYBA2	FLI1	HES2	MAB21L2
HBA2	C16orf11	C1QL2	CRYL1	FLJ11235	HES3	MAFB
HCG11	C16orf13	C1QL3	CSF1	FLJ32063	HHEX	MAL
HCK	C16orf95	C1QL4	CSMD1	FLJ45983	HLX	MCOLN3
HEMGN	C17orf102	C1QTNF1	CSMD2	FLJ46347	HMX2	MESP1
HEPHL1	C17orf82	C20orf166	CSMD3	FLRT2	HMX3	MKX
HES5	C18orf42	C20orf166-AS1	CTNND2	FOXA2	HOXA1	MSC
HHIPL1	C19orf33	C20orf201	CWH43	FOXB1	HOXA2	MSX1
HIGD1B	C19orf59	C2CD4A	CXCL14	FOXD2	HOXA4	MT1A
HIST1H1A	C1orf110	C3orf58	CXCL16	FOXD3	HOXA6	MT1B
HIST1H1D	C1orf170	C3orf72	CYP24A1	FOXD4L1	HOXB3	MT1DP
HIST1H4H	C1orf172	C3orf80	CYP26A1	FOXD4L3	HOXB7	MT1H
HIST2H2AA3	C1orf194	C3orf84	CYP26B1	FOXD4L4	HOXB8	MT1M
HIST2H2AA4	C1orf200	C4orf19	CYP26C1	FOXE1	HOXC6	MYO5B
HIST2H2BC	C1orf210	C4orf32	CYP27B1	FOXF1	HOXD13	MYOD1
HMBOX1	C1orf213	C5orf38	CYP2A13	FOXG1	HOXD8	NAGS
HMGCLL1	C1orf27	C7orf43	CYP2A6	FOXJ1	HOXD9	NEFL
HNF1B	C1orf53	C8orf31	CYP2A7	FOXL1	HPSE	NELL1
HNRNPCP5	C1orf61	C8orf37	CYP2J2	FOXL2	HPSE2	NEUROD2
HOMER1	C1orf74	C9orf3	CYP39A1	FRMD3	HR	NEUROG1
HOTAIR	C1orf94	C9orf66	DACH1	FRMPD4	HRK	NEUROG2

HOTTIP	C1QC	CA1	DACH2	FUT4	HS3ST2	NEUROG3
HOXA10	C1QL1	CA10	DCC	FZD10	HS3ST3B1	NKX2-1
HOXA10-HOXA9	C1QL2	CA14	DCHS2	FZD2	HS3ST4	NKX2-2
HOXA11	C1QL3	CA4	DCLK1	GABRA2	HS6ST3	NKX2-3
HOXA13	C1QL4	CA7	DCLK2	GABRA4	HSF4	NKX2-8
HOXA3	C1QTNF1	CA8	DCX	GAD2	HTR1A	NKX3-1
HOXA7	C20orf166	CABLES1	DDAH1	GALNTL4	HTR6	NKX3-2
HOXA9	C20orf166-AS1	CABP7	DDX25	GALR2	ICAM5	NKX6-1
HOXA-AS3	C20orf201	CACNA1A	DGKG	GATA2	IGF2-AS	NKX6-2
HOXA-AS4	C21orf49	CACNA1B	DGKI	GATA3	IGFBP3	NPAS1
HOXB1	C2CD4A	CACNA1D	DHH	GATA4	IHH	NPAS4
HOXB13	C2CD4B	CACNA1E	DIO3	GATA6	IKZF3	NPNT
HOXB2	C2orf78	CACNA1G	DKK1	GBX2	IL10RA	NPR3
HOXB4	C3orf58	CACNA1G-AS1	DKK2	GDF6	IL1RAPL2	NPTX1
HOXB5	C3orf72	CACNA2D3	DLK1	GDF7	IL7	NR2F2
HOXB6	C3orf80	CACNG3	DLK2	GDNF	INSRR	NRG2
HOXB-AS1	C3orf84	CACNG6	DLL4	GHR	IRX1	NTNG2
HOXB-AS3	C4orf19	CALCR	DLX1	GHSR	IRX3	NTRK1
HOXC11	C4orf32	CALM1	DLX2	GIMAP5	IRX5	OLIG2
HOXC12	C5orf38	CALN1	DLX3	GJB2	ISL1	ONECUT1
HOXC13	C7orf43	CALY	DLX4	GJD2	ITGA4	ONECUT2
HOXC4	C8orf31	CAMK2N1	DLX5	GLT25D2	ITIH5	OPRD1
HOXC5	C8orf37	CAMP	DMRT1	GNA14	ITPKA	OSR1
HOXC8	C9orf3	CAMTA1	DMRT2	GPC5	KCNA1	OTOP1
HOXC-AS2	C9orf53	CAND1.11	DMRT3	GPM6B	KCNA5	OTOP2
HOXC-AS5	C9orf66	CARTPT	DNAJC22	GPR101	KCNAB1	OTOP3
HOXD1	CA1	CASR	DNER	GPR12	KCNC4	OTP
HOXD10	CA10	CAST	DOK6	GPR88	KCNIP4	OTX1
HOXD12	CA14	CBLN1	DPF3	GRIA2	KCNK12	OTX2
HOXD3	CA4	CBWD1	DPP6	GRID1	KCNK13	PABPC1L2A
HOXD4	CA7	CBWD2	DPY19L2	GRIK1	KCNK17	PAPPA
HPGDS	CA8	CBWD3	DPY19L2P2	GRIK3	KCNK2	PAX1
HS3ST1	CABLES1	CBWD5	DPYSL5	GRIN3A	KCNK4	PAX2
HSPA5	CABP7	CBWD6	DRD4	GRM7	KCNMA1	PAX8
HSPA6	CACNA1A	CBX4	DRD5	GSC	KCNQ1	PAX9
HTR2C	CACNA1B	CCBE1	DSC3	GSC2	KCNQ3	PCDH8
HYLS1	CACNA1D	CCDC108	DSCAML1	GSX1	KCNS2	PDGFRA
ICAM2	CACNA1E	CCDC129	DTNB	GSX2	KCNS3	PDX1
ICAM4	CACNA1G	CCDC17	DUOX1	GUCY1A3	KCNV1	PENK
IFNK	CACNA1G-AS1	CCDC3	DUOX2	GUCY2D	KIAA1324	PGM5
IGF2	CACNA2D3	CCDC59	DUOXA1	HAND2	KIRREL3	PGR
IGFN1	CACNG2	CCDC64B	DUOXA2	HBA1	KIRREL3-AS3	PHOX2A
IGLL5	CACNG3	CCDC68	DUSP15	HBA2	KISS1R	PITX3
IGSF21	CACNG6	CCDC71	DUSP4	HES2	KL	PMP22
IL21R	CALCA	CCDC84	DUSP6	HES7	KLF4	POU3F4

IL23A	CALCR	CCK	DUSP8	HEY1	KLHL35	POU4F1
IL32	CALM1	CCL4	DYNC1I1	HHAT	KLK4	POU4F2
INTS9	CALN1	CCNA1	EBF1	HHEX	LAMB1	POU4F3
IQCF4	CALY	CCND2	EBF3	HHIP	LBX1	PRDM12
IRF4	CAMK2N1	CCNO	ECEL1	HLX	LEF1	PRLHR
IRX4	CAMP	CCNYL1	EFCAB1	HMX2	LGI3	PROK2
ISL2	CAMTA1	CCT6B	EFNA1	HMX3	LGR5	PTF1A
ITGB2	CAND1.11	CCZ1B	EFNA3	HNF1B	LHFPL3	PTGDR
KDR	CARTPT	CD1D	EGFL6	HOXB1	LHX2	PTGER2
KIAA1217	CASC4	CD200R1L	EGFLAM	HOXB13	LHX3	PTGER3
KIAA1239	CASR	CD24	EGR2	HOXB2	LHX4	PTGER4
KIR3DX1	CAST	CD300LF	EGR3	HOXB3	LHX5	PTH2
KISS1	CBLN1	CD302	EGR4	HOXB6	LMX1B	PTHLH
KLF14	CBWD1	CD34	EIF4E3	HOXB7	LOC153684	PTPRT
KNCN	CBWD2	CD38	ELAVL2	HOXB8	LONRF3	PYY
KPNA2	CBWD3	CD4	ELAVL3	HOXC11	LPL	RAB6C
KRT12	CBWD5	CD44	ELMOD1	HOXC12	LRRC71	RASGRF1
KRT34	CBWD6	CD70	ELOVL2	HOXC4	LTBP2	RASSF5
KRT76	CBX4	CD8A	ELOVL3	HOXC5	LTK	RAX
KRTAP13-2	CCBE1	CD8B	EN1	HOXC6	LYSMD2	RBP4
KRTAP4-2	CCDC108	CDA	EN2	HOXC8	MAB21L1	RGS10
L1TD1	CCDC129	CDC20B	ENTPD2	HOXD1	MAB21L2	RGS9BP
LAMA3	CCDC140	CDC5L	ENTPD3	HOXD12	MAFB	RIPK3
LBX2	CCDC17	CDCA5	EOMES	HOXD13	MAL	RSPO2
LEUTX	CCDC3	CDCP1	EPAS1	HOXD3	MCOLN3	SCTR
LHX6	CCDC59	CDH13	EPB41L4A	HOXD4	MECOM	SFRP1
LHX8	CCDC64B	CDH15	EPHA10	HOXD8	MEIS1	SFRP5
LILRA5	CCDC68	CDH22	EPHA3	HOXD9	MEOX2	SGPP2
LILRB2	CCDC71	CDH7	EPHA4	HPCAL4	MESP1	SHH
LINC00111	CCDC84	CDK5R2	EPHA5	HPSE2	MFSD4	SHISA6
LINC00489	CCK	CDKN2A	EPHB1	HRK	MICB	SHOX
LINC00554	CCL11	CDKN2B	EPHB3	HS3ST3B1	MKX	SHOX2
LINC00861	CCL4	CDKN2B-AS1	ERBB4	HS6ST1P1	MLPH	SIDT1
LINC00900	CCNA1	CDKN2C	ERO1LB	HS6ST3	MLXIPL	SIM2
LINC00910	CCND2	CDX2	ESAM	HSF4	MSC	SIX1
LINC00942	CCNO	CEACAM19	ESPN	HSPA6	MSX1	SIX2
LINC01020	CCNYL1	CEP192	ESR1	HTR1A	MSX2	SIX3
LINC01056	CCT6B	CEP85L	ESX1	HTR2C	MT1A	SLC1A2
LIPC	CCZ1B	CERKL	ETV7	HTR7	MT1B	SLC24A4
LMF1	CD1D	CFTR	EVX1	ICAM5	MT1DP	SLC30A2
LOC100128239	CD200R1L	CH25H	EXOC3L2	IGF2-AS	MT1H	SLC30A3
LOC100132174	CD24	CHAT	EYA4	IGSF21	MT1M	SLC32A1
LOC100289473	CD300LF	CHD5	F2R	IKZF3	MYO5B	SLC35F3
LOC100506178	CD302	CHN2	FAM115C	IL1RAPL2	MYOD1	SLC6A1
LOC100506241	CD34	CHRDL2	FAM123A	IL7	NAGS	SLC6A3

LOC100506730	CD38	CHRM2	FAM129A	ILDR2	NCCRP1	SLC6A5
LOC100507003	CD4	CHST13	FAM150A	INA	NDRG1	SLC9A2
LOC100507489	CD44	CHST8	FAM159A	INSM2	NEFH	SLC9A3
LOC100652768	CD70	CISTR-ACT	FAM163A	INSRR	NEFL	SLCO5A1
LOC100996758	CD8A	CKMT1A	FAM167A	IRX3	NELL1	SLFN11
LOC148696	CD8B	CLDN14	FAM19A4	IRX4	NEUROD2	SLITRK3
LOC150622	CDA	CLDN7	FAM43B	IRX5	NEUROG1	SORCS1
LOC152586	CDC20B	CLEC2L	FAM5B	ISL1	NEUROG2	SORCS3
LOC284757	CDC5L	CLEC4GP1	FAM5C	ISL2	NEUROG3	SOX14
LOC285696	CDCA5	CLIC5	FAM70B	ITGA4	NGF	SOX17
LOC286094	CDCP1	CLIC6	FAM78A	ITPKA	NGFR	SOX7
LOC286297	CDH13	CLNS1A	FAM81A	JUN	NKX2-1	SPAG6
LOC286437	CDH15	CLOCK	FAM84A	KAZALD1	NKX2-2	SPON1
LOC339240	CDH22	CLSTN2	FAM89A	KCNA1	NKX2-3	SRD5A2
LOC340073	CDH7	CLTC	FBLN5	KCNA3	NKX2-5	SSTR2
LOC389033	CDK5R2	CLVS2	FBLN7	KCNAB1	NKX2-8	STMN2
LOC641515	CDKN2A	CMA1	FBN1	KCNC2	NKX3-1	SUSD4
LOC643802	CDKN2B	CMTM7	FBN2	KCNC4	NKX3-2	SV2B
LOC727924	CDKN2B-AS1	CMTR1	FBP1	KCND3	NKX6-1	TBR1
LOC729218	CDKN2C	CNGA3	FBXL14	KCNH1	NKX6-2	TBX1
LOC729737	CDX2	CNOT2	FBXL8	KCNH3	NOTUM	TBX2
LPAR3	CEACAM19	CNPY1	FBXO25	KCNK12	NPAS1	TBX3
LRRC26	CELF2	CNTNAP5	FBXO3	KCNK13	NPAS4	THBD
LRRC72	CEP192	COL12A1	FERD3L	KCNK2	NPNT	TLL1
LRTM1	CEP85	COL14A1	FEV	KCNK4	NPR1	TLX1
LRTM2	CEP85L	COL15A1	FEZ1	KCNMA1	NPR3	TLX2
LTBP1	CERKL	COL21A1	FEZF2	KCNQ3	NPTX1	TMEM132E
LTF	CFTR	COL27A1	FGF11	KCNV1	NPY5R	TMEM30B
LYZL6	CH25H	COL2A1	FGF20	KIAA1199	NR2E1	TMEM59L
LZTS1-AS1	CHAT	COL5A3	FGF3	KIAA1324	NR2F2	TMOD2
MALL	CHD5	COLEC12	FGF5	KIRREL3	NRG2	TP73
MAPRE3	CHN2	COMMD4	FGF8	KL	NRIP3	TRADD
MAST4	CHRDL2	COMP	FGF9	KLF4	NRN1	TRH
MEP1A	CHRM2	COPS7A	FIGLA	KLHL35	NRXN1	TRIM36
MIR10A	CHRNA3	CPAMD8	FLI1	KY	NTNG2	TRIM67
MIR10B	CHST13	CPLX2	FLJ11235	LAYN	NTRK1	TRPC5
MIR1-1	CHST8	CPNE1	FLJ32063	LBX1	NXPH4	TSLP
MIR1252	CISTR-ACT	CPNE7	FLJ39739	LGALS3	OLIG2	UCN
MIR1258	CKMT1A	CPT1A	FLJ45983	LGR5	OLIG3	UCP1
MIR196A1	CLDN14	CPXM2	FLJ46347	LHX2	ONECUT1	UNC5C
MIR196A2	CLDN7	CPZ	FLRT2	LHX4	ONECUT2	USH1G
MIR196B	CLEC2L	CR1	FNDC1	LHX5	OPRD1	VAX1
MIR200B	CLEC4GP1	CR2	FNDC5	LHX6	OSR1	VAX2
MIR206	CLIC5	CRABP1	FOXA2	LHX8	OSR2	VDR
MIR3131	CLIC6	CRB3	FOXB1	LINC00268	OTOP1	WNT1

MIR3185
MIR3646
MIR3907
MIR4276
MIR4420
MIR4423
MIR4461
MIR4493
MIR4713
MIR4727
MIR4730
MIR4778
MIR4801
MIR5092
MIR5093
MIR5188
MIR518B
MIR520C
MIR520G
MIR520H
MIR663A
MIR888
MIR890
MIR891A
MNX1
MRGPRX4
MROH5
MS4A10
MSGN1
MSX2P1
MT1G
MT1L
MTFR1
MTHFSD
MTRNR2L7
MUC12
MUC13
MYH4
MYL3
MYOM2
MYOT
NAA30
NASP
NDRG4
NEBL
CLNS1A
CLOCK
CLSTN2
CLTC
CLVS2
CMA1
CMTM7
CMTR1
CNGA3
CNIH3
CNOT2
CNPY1
CNTNAP5
COL12A1
COL14A1
COL15A1
COL21A1
COL25A1
COL27A1
COL2A1
COL4A3
COL4A4
COL5A3
COL6A5
COLEC12
COMMD4
COMP
COPS7A
COX16
CPAMD8
CPLX2
CPNE1
CPNE7
CPT1A
CPXM2
CPZ
CR1
CR2
CRABP1
CRB3
CREB3L2
CREG2
CRHBP
CRHR2
CRIM1
CREB3L2
CREG2
CRHBP
CRIM1
CRLF1
CRNDE
CRTAC1
CRYBA2
CRYM
CSE1L
CSGALNACT1
CSMD1
CSMD2
CSMD3
CSRNP2
CSRP2
CTAGE11P
CTDSP1
CTSE
CUX2
CWC15
CWH43
CXCL12
CXCL16
CXCL6
CYB5R2
CYP11B1
CYP26A1
CYP26B1
CYP27B1
CYP2A13
CYP4F2
CYP4X1
CYS1
DACH1
DACH2
DACT1
DBX1
DBX2
DCC
DCX
DDX17
DDX51
DEFB119
DEGS2
FOXC1
FOXD2
FOXD3
FOXD4L1
FOXD4L3
FOXD4L4
FOXE1
FOXE3
FOXF1
FOXF2
FOXG1
FOXJ1
FOXL1
FOXL2
FOXQ1
FRAT1
FRMD3
FRMPD1
FRMPD4
FUCA1
FUT4
FUT9
FXYD7
FZD1
FZD10
FZD2
GAB3
GABBR2
GABRA2
GABRA4
GABRB2
GABRG3
GAD2
GALNTL1
GALNTL4
GALR2
GAST
GATA2
GATA3
GATA4
GATA6
GBX2
GCC1
GCM2
GDF6
LMX1B
LOC153684
LONRF3
LPHN3
LPL
LPPR1
LRCH2
LRFN5
LRP2
LRRC71
LRRTM1
LTBP2
LTK
LYSMD2
MAB21L1
MAB21L2
MAFB
MAL
MAPK4
MAPT
MCOLN3
MESP1
METRNL
MGC39545
MIR137HG
MKX
MLLT3
MNX1
MSC
MSX1
MT1A
MT1B
MT1DP
MT1H
MT1M
MYF6
MYO5B
MYOD1
NAGS
NAV2
NBPF11
NCAM1
NDUFA4L2
NEFL
NEFM
OTOP2
OTOP3
OTP
OTX1
OTX2
OVOL1
PABPC1L2A
PADI2
PAPPA
PAX1
PAX2
PAX8
PAX9
PCDH8
PCSK2
PDGFRA
PDX1
PENK
PGM5
PGR
PHOX2A
PITX3
PMP22
POMC
POU3F4
POU4F1
POU4F2
POU4F3
PPP1R14C
PRDM12
PRDM13
PRKCB
PRKCH
PRLHR
PROK2
PRUNE2
PSD2
PTF1A
PTGDR
PTGER2
PTGER3
PTGER4
PTH2
PTHLH
PTPRT
WNT10A
WNT11
WNT2
WNT3A
WNT6
WNT7A
WRAP73
ZCCHC16
ZFHX3
ZFYVE28
ZIC1
ZIC4
ZMYND15
ZNF436
ZNF503

NEUROD1	CRLF1	DENND6A	GDF7	NELL1	PYY
NEUROD4	CRNDE	DGKG	GDNF	NEUROD1	RAB6C
NFIX	CRTAC1	DGKK	GHR	NEUROD2	RASGRF1
NFS1	CRYBA2	DHDDS	GHSR	NEUROG1	RASSF5
NMT1	CRYM	DHDH	GIMAP5	NEUROG2	RAX
NOTO	CSE1L	DIO3	GJB2	NEUROG3	RBP4
NPAS3	CSGALNACT1	DKFZP434I0714	GJD2	NFIX	RBP7
NPFFR1	CSMD1	DKFZp686K1684	GKAP1	NKX2-1	REEP1
NPY4R	CSMD2	DKK1	GLB1L2	NKX2-2	RFX6
NR2F1	CSMD3	DKK2	GLIPR2	NKX2-3	RGS10
NR2F1-AS1	CSRNP2	DLK1	GLT25D2	NKX2-8	RGS9BP
NSG1	CSRP2	DLL1	GNA14	NKX3-1	RIPK3
NUBPL	CTAGE11P	DLL4	GNAO1	NKX3-2	RSPO2
NXPE2	CTDSP1	DLX1	GPC3	NKX6-1	RSPO3
OAZ3	CTSE	DLX2	GPC5	NKX6-2	RTBDN
OCA2	CUX2	DLX3	GPD1L	NOL4	SAMD11
OLFM3	CWC15	DLX4	GPM6B	NPAS1	SCTR
OLFM4	CWC25	DLX5	GPR101	NPAS4	SEZ6
OPALIN	CWH43	DLX6	GPR12	NPNT	SFRP1
OR10J1	CXCL12	DMBT1	GPR124	NPR3	SFRP5
OR11H6	CXCL16	DMRT1	GPR150	NPTX1	SFTPC
OR13C8	CXCL6	DMRT2	GPR174	NPY1R	SGPP2
OR1I1	CXXC4	DMRT3	GPR26	NR2F2	SH3GL2
OR1J4	CYB5R2	DMRTA2	GPR6	NR4A3	SHH
OR1L3	CYP11B1	DNAH11	GPR62	NRG1	SHISA6
OR1N1	CYP1B1	DNAJB11	GPR88	NRG2	SHOX
OR2A5	CYP24A1	DNTT	GRB10	NT5C1A	SHOX2
OR4B1	CYP26A1	DOC2B	GRHL3	NTN1	SIDT1
OR4C3	CYP26B1	DOCK10	GRIA2	NTNG2	SIM2
OR4C6	CYP27B1	DOCK3	GRID1	NTRK1	SIX1
OR4F16	CYP2A13	DOCK8	GRIK1	NTRK2	SIX2
OR4F29	CYP2S1	DPF3	GRIK3	O3FAR1	SIX3
OR4F3	CYP4F2	DPP10	GRIN1	OAF	SKAP1
OR4F5	CYP4X1	DPP6	GRIN2D	OCA2	SLC17A6
OR4L1	CYS1	DPP9	GRIN3A	OLFML2B	SLC17A7
OR4N3P	DACH1	DPRX	GRK5	OLIG2	SLC1A2
OR51E1	DACH2	DPY19L2P1	GRM6	ONECUT1	SLC24A4
OR52E6	DACT1	DPYSL2	GRM7	ONECUT2	SLC26A5
OR52W1	DBX1	DRD1	GSC	OPRD1	SLC30A2
OR56B1	DBX2	DRD2	GSC2	OSR1	SLC30A3
OR5B17	DCC	DRD5	GSN	OTOP1	SLC32A1
OR5H14	DCX	DRGX	GSX1	OTOP2	SLC35D3
OR6P1	DDC	DSC3	GSX2	OTOP3	SLC35F3
OR6X1	DDX17	DSCAM-IT1	GUCY1A3	OTP	SLC6A1

OR8D1	DDX51	DSCAML1	GUCY2D	OTX1	SLC6A11
OR8G1	DEFB119	DSP	HAND1	OTX2	SLC6A3
OR8G2	DEGS2	DTL	HAND2	OXCT2	SLC6A5
OR8G5	DENND6A	DUOX1	HBA1	PABPC1L2A	SLC9A2
OR9Q2	DGKG	DUOXA1	HBA2	PAPPA	SLC9A3
OTOA	DGKK	DUSP1	HCG9	PARM1	SLCO5A1
OTX2-AS1	DHDDS	DUSP5P1	HCN4	PAX1	SLFN11
OVOL2	DHDH	DUX2	HES2	PAX2	SLIT3
PABPC4L	DIO3	DUX4	HES3	PAX3	SLITRK3
PADI6	DKFZP434I0714	DUX4L2	HES5	PAX6	SMOC2
PAK7	DKFZp686K1684	DUX4L3	HES7	PAX7	SNTB1
PALLD	DKK1	DUX4L5	HEY1	PAX8	SORCS1
PAMR1	DKK2	DUX4L6	HEYL	PAX9	SORCS3
PAPL	DLK1	DUX4L7	HHAT	PCDH17	SOX14
PAPPA-AS1	DLL1	EBF1	HHEX	PCDH8	SOX17
PATL2	DLL4	EBF2	HHIP	PDE4DIP	SOX7
PAX3	DLX1	EBF3	HIC1	PDGFRA	SPAG6
PAX5	DLX2	ECEL1	HLA-A	PDX1	SPON1
PAX6	DLX3	ECEL1P2	HLA-B	PDZD2	SPON2
PAX7	DLX4	EDA	HLA-C	PENK	SRD5A2
PAXBP1	DLX5	EDN3	HLA-F	PGM5	SSTR2
PDCL	DLX6	EEF1A1	HLX	PGR	ST8SIA5
PDCL2	DLX6-AS1	EEF2	HMX2	PHOX2A	STC2
PDE1B	DMBT1	EFCAB6	HMX3	PHOX2B	STMN2
PDE4A	DMKN	EFCC1	HNF1B	PIGZ	SUSD4
PDE4DIP	DMRT1	EFNA5	HOXA1	PIP5K1B	SV2B
PDIA4	DMRT2	EGFL6	HOXA10	PIR	SYNE1
PDPR	DMRT3	EGFLAM	HOXA13	PITX1	SYT6
PEG3-AS1	DMRTA2	EGR4	HOXA2	PITX2	T
PER4	DNAH11	EHD1	HOXA3	PITX3	TACR1
PF4V1	DNAJB11	EIF3E	HOXA4	PKNOX2	TBR1
PGLYRP4	DNTT	EIF3M	HOXA6	PKP1	TBX1
PGM5-AS1	DOC2B	EIF4E3	HOXA7	PLEC	TBX2
PGPEP1L	DOCK10	ELAVL2	HOXA9	PLXNA2	TBX20
PGRMC2	DOCK3	ELMOD1	HOXB1	PMP22	TBX3
PHACTR3	DOCK8	ELOVL3	HOXB13	PODN	TGFA
PHLDA1	DPF3	ELOVL7	HOXB2	POLE	THBD
PHOX2B	DPP10	ELP3	HOXB3	POU3F1	TLL1
PI16	DPP6	EMC1	HOXB6	POU3F4	TLX1
PIK3IP1	DPP9	EMILIN2	HOXB7	POU4F1	TLX2
PITX1	DPRX	EMX1	HOXB8	POU4F2	TLX3
PITX2	DPY19L2P1	EMX2	HOXC11	POU4F3	TMEM132E
PKD2L1	DPYSL2	EMX2OS	HOXC12	PPM1E	TMEM163
PLA2G7	DRD1	EN1	HOXC4	PRAC	TMEM30B

PLXNC1
PNLIP
PNPLA8
PPEF2
PPIP5K1
PPP1R26-AS1
PPP2R2C
PRAC2
PRAMEF10
PRAMEF2
PRDM14
PRG3
PRICKLE2-AS2
PRKCZ
PRR9
PRSS16
PRSS22
PRSS3
PRSS30P
PTPRD
PVALB
RAB7L1
RAPGEF5
RBP2
REXO1L1
REXO1L2P
RGS3
RNASE7
RNF128
RNPS1
ROBO1
ROBO3
ROMO1
RPL24
RPSAP52
RRAD
RSPO1
RSPO4
S100A6
SAMD7
SATB2
SCARNA6
SELL
SEMA3A
SERPINB13
DRD2
DRD5
DRGX
DSC3
DSCAM-IT1
DSCAML1
DSP
DTL
DUOX1
DUOX2
DUOXA1
DUOXA2
DUSP1
DUSP5P1
DUX2
DUX4
DUX4L2
DUX4L3
DUX4L5
DUX4L6
DUX4L7
DYSF
EBF1
EBF2
EBF3
ECEL1
ECEL1P2
EDA
EDIL3
EDN3
EEF1A1
EEF2
EFCAB6
EFCC1
EFNA5
EGFL6
EGFLAM
EGR4
EHD1
EIF3E
EIF3M
EIF4E3
ELAVL2
ELMOD1
ELOVL3
EN2
ENTHD1
ENTPD6
EPAS1
EPB41L3
EPB42
EPHA10
EPHA2
EPHA3
EPHA5
EPHA8
EPO
EPPIN
EPPIN-WFDC6
ERAP1
ERG
ERVMER34-1
ESPN
ESPNL
ESR1
ESRP1
ESX1
ESYT3
ETS1
EVX2
EXOSC9
EYA2
F11R
F13A1
FADS6
FAM118B
FAM135B
FAM150B
FAM155B
FAM161A
FAM163A
FAM189A2
FAM196A
FAM19A4
FAM201A
FAM210A
FAM212A
FAM21A
FAM21C
FAM32A
HOXC5
HOXC6
HOXC8
HOXD1
HOXD12
HOXD13
HOXD3
HOXD4
HOXD8
HOXD9
HPCAL4
HPSE
HPSE2
HR
HRK
HS3ST2
HS3ST3B1
HS3ST4
HS6ST1P1
HS6ST3
HSF4
HSPA1A
HSPA1B
HSPA1L
HSPA6
HTR1A
HTR2C
HTR6
HTR7
HTRA3
ICAM4
ICAM5
IGF2-AS
IGFBP1
IGFBP3
IGSF21
IHH
IKZF3
IL10RA
IL11
IL17D
IL17RB
IL1RAPL2
IL7
ILDR2
PRDM12
PRKCE
PRKG1
PRLHR
PROK2
PTF1A
PTGDR
PTGER2
PTGER3
PTGER4
PTGFR
PTH2
PTHLH
PTPRT
PTPRU
PXMP2
PYY
RAB6C
RASGRF1
RASL10A
RASSF5
RAX
RBP4
REPS2
RGS10
RGS20
RGS9BP
RIMBP3
RIMBP3B
RIMBP3C
RIMKLA
RIPK3
RNF128
ROBO3
RPRML
RPS6KA6
RSPO1
RSPO2
RTN4RL2
RYR3
SCD5
SCN4B
SCNN1G
SCTR
SEMA6D
TMEM59L
TMOD2
TNFSF9
TP73
TRADD
TRH
TRIM36
TRIM67
TRPC5
TSLP
TWIST1
UCN
UCP1
ULBP1
ULBP2
UNC5C
USH1G
VAX1
VAX2
VDR
WNT1
WNT10A
WNT11
WNT2
WNT3A
WNT6
WNT7A
WRAP73
ZACN
ZCCHC16
ZFHX3
ZFYVE28
ZIC1
ZIC4
ZMYND15
ZNF436
ZNF503

SERTAD1	ELOVL7	FAM43B	IMPDH1	SERTM1
SIM1	ELP3	FAM69C	INA	SFRP1
SIRPB1	EMC1	FAM78B	INSM2	SFRP5
SIX6	EMILIN2	FAM83F	INSRR	SGPP2
SKOR2	EMX1	FAM83H	INTS4L1	SHC4
SLC13A4	EMX2	FAM89A	IRF4	SHH
SLC14A2	EMX2OS	FAM95C	IRX1	SHISA6
SLC18A2	EN1	FASTK	IRX3	SHOX
SLC22A9	EN2	FBLN7	IRX4	SHOX2
SLC26A4	ENTHD1	FBXL16	IRX5	SIDT1
SLC27A6	ENTPD6	FBXL20	ISL1	SIM2
SLC28A3	EOMES	FBXL8	ISL2	SIX1
SLC4A11	EPAS1	FBXW2	ITGA4	SIX2
SLC5A7	EPB41L3	FBXW7	ITIH5	SIX3
SLC6A12	EPB42	FCER1G	ITPKA	SIX6
SLC6A2	EPHA10	FCER2	JUN	SLC10A4
SLC6A20	EPHA2	FCHSD2	KAZALD1	SLC1A2
SLC6A7	EPHA3	FCRL6	KCNA1	SLC1A4
SLPI	EPHA5	FCRLB	KCNA3	SLC24A4
SMC5	EPHA8	FENDRR	KCNA5	SLC26A4
SMC5-AS1	EPO	FERD3L	KCNAB1	SLC27A2
SMUG1	EPPIN	FEZF1	KCNC2	SLC30A2
SNAR-A1	EPPIN-WFDC6	FEZF1-AS1	KCNC4	SLC30A3
SNAR-A10	ERAP1	FEZF2	KCND3	SLC30A4
SNAR-A11	ERG	FFAR4	KCNF1	SLC32A1
SNAR-A12	ERICH1-AS1	FGD2	KCNH1	SLC35F3
SNAR-A13	ERVMER34-1	FGF1	KCNH3	SLC6A1
SNAR-A14	ESPN	FGF10	KCNH7	SLC6A3
SNAR-A2	ESPNL	FGF14	KCNIP2	SLC6A5
SNAR-A3	ESR1	FGF17	KCNIP4	SLC9A2
SNAR-A4	ESRP1	FGF19	KCNJ10	SLC9A3
SNAR-A5	ESRRG	FGF23	KCNJ3	SLCO2A1
SNAR-A6	ESX1	FGF3	KCNJ4	SLCO5A1
SNAR-A7	ESYT3	FGF5	KCNJ9	SLFN11
SNAR-A8	ETS1	FGF7	KCNK12	SLIT1
SNAR-A9	EVA1A	FGF8	KCNK13	SLIT2
SNAR-C1	EVX1	FGF9	KCNK17	SLITRK1
SNAR-C2	EVX2	FGFR2	KCNK2	SLITRK3
SNAR-C4	EXOC3L2	FGL2	KCNK3	SORCS1
SNAR-C5	EXOSC9	FIBCD1	KCNK4	SORCS3
SNHG7	EYA2	FIGLA	KCNMA1	SOX14
SNORA45	F11R	FLI1	KCNQ1	SOX17
SNORD113-6	F13A1	FLJ12825	KCNQ3	SOX7
SNRPA1	FADS6	FLJ20518	KCNQ5	SPAG6
SNX16	FAHD1	FLJ31813	KCNS2	SPOCK3

SNX29P1	FAIM	FLJ44511	KCNS3	SPON1
SOX18	FAM118B	FLRT2	KCNV1	SRD5A2
SOX5	FAM135B	FLT1	KIAA1191	SSTR1
SOX8	FAM150A	FLT3	KIAA1199	SSTR2
SP6	FAM150B	FLT4	KIAA1324	ST8SIA2
SP8	FAM155B	FNDC1	KIRREL3	STK32B
SPDEF	FAM159B	FNIP1	KIRREL3-AS3	STMN2
SPDYE3	FAM161A	FOXA1	KISS1R	STXBP6
SPERT	FAM163A	FOXA3	KL	SUSD4
SPINK8	FAM189A2	FOXB1	KLF4	SV2B
SPOCK3	FAM196A	FOXB2	KLHL1	SYT12
SRP9	FAM19A4	FOXC1	KLHL13	TAL1
SRSF7	FAM201A	FOXC2	KLHL14	TBR1
SSTR1	FAM210A	FOXD1	KLHL17	TBX1
SSTR5	FAM212A	FOXD2-AS1	KLHL35	TBX2
ST14	FAM21A	FOXD3	KLK4	TBX21
ST5	FAM21C	FOXD4	KY	TBX3
STX6	FAM32A	FOXD4L2	LAMB1	TBX5
SYCP1	FAM43B	FOXD4L3	LAYN	TCEA3
TAAR1	FAM69C	FOXD4L4	LBX1	TET2
TAC1	FAM78B	FOXD4L5	LEF1	TFAP2E
TAGAP	FAM83F	FOXD4L6	LEKR1	THBD
TAL1	FAM83H	FOXE1	LGALS3	TLL1
TARBP1	FAM89A	FOXE3	LGI3	TLX1
TAS2R39	FAM95C	FOXF1	LGR5	TLX2
TBC1D3	FASTK	FOXF2	LHFPL3	TMEFF2
TBC1D3C	FBLN7	FOXG1	LHX2	TMEM132E
TBC1D3F	FBXL16	FOXI2	LHX3	TMEM27
TBC1D3H	FBXL20	FOXI3	LHX4	TMEM30B
TBC1D3P5	FBXL21	FOXL1	LHX5	TMEM59L
TBX15	FBXL8	FOXL2	LHX6	TMEM88
TBX4	FBXW2	FOXO3	LHX8	TMOD2
TBX5	FBXW7	FOXP2	LINC00268	TP73
TBX5-AS1	FCER1G	FOXQ1	LMO1	TPPP3
TCF21	FCER2	FREM3	LMOD1	TRADD
TES	FCGR1C	FRG2B	LMX1B	TRH
TFAP2A	FCHSD2	FRG2C	LOC100131554	TRIM36
TFAP2B	FCRL6	FRMD3	LOC153684	TRIM67
TFAP2D	FCRLB	FRMD4B	LOC154761	TRIM9
TGM5	FENDRR	FRMPD1	LOC84931	TRPC5
TGM6	FERD3L	FSHR	LONRF3	TSLP
TIGD2	FEV	FSIP2	LPHN3	TTYH1
TMEM132B	FEZF1	FST	LPL	UCN
TMEM174	FEZF1-AS1	FSTL4	LPPR1	UCP1
TMEM45B	FEZF2	FTCDNL1	LRAT	UNC5C

TNFAIP2
TNFSF11
TNS4
TOB1
TPI1P3
TPM3
TREML4
TRPA1
UBC
UCA1
UPK1A-AS1
UPK3A
USHBP1
USP16
USP44
USP46
USPL1
VGLL2
VSIG10L
VSX1
VSX2
VTCN1
WDR72
WIPF3
WNT10B
WNT16
WNT8B
WT1
WT1-AS
XDH
ZAN
ZMYM3
ZMYM4
ZNF260
ZNF280A
ZNF420
ZNF462
ZNF503-AS1
ZNF534
ZNF555
ZNF676
ZPBP2

FFAR4
FGD2
FGF1
FGF10
FGF14
FGF17
FGF19
FGF23
FGF3
FGF4
FGF5
FGF7
FGF8
FGF9
FGFR2
FGL2
FIBCD1
FIGLA
FLI1
FLI1-AS1
FLJ12825
FLJ20518
FLJ31813
FLJ36000
FLJ44511
FLRT2
FLT1
FLT3
FLT4
FNDC1
FNIP1
FOXA1
FOXA2
FOXA3
FOXB1
FOXB2
FOXC1
FOXC2
FOXD1
FOXD2
FOXD2-AS1
FOXD3
FOXD4
FOXD4L1
FOXD4L2

FUOM
FUS
FXYD2
FXYD5
FXYD7
FZD10
FZD10-AS1
GAB3
GABPA
GABRA2
GABRA4
GABRB2
GABRE
GAD2
GADD45G
GAGE12F
GAGE12I
GAGE2A
GAGE2B
GAGE2C
GAGE2E
GAGE4
GAGE5
GAGE7
GAGE8
GAL
GALNT3
GALNT6
GALNT9
GALR1
GALR2
GAN
GAP43
GAS2
GATA3
GATA3-AS1
GATA4
GATA5
GATA6
GATA6-AS1
GBX1
GBX2
GCGR
GCM2
GDE1

LRBA
LRCH2
LRFN2
LRFN5
LRP2
LRRC71
LRRTM1
LTBP2
LTK
LY6H
LYSMD2
MAB21L1
MAB21L2
MADCAM1
MAFB
MAL
MAN1C1
MAP6
MAPK4
MAPK8IP2
MAPT
MAST4
MCOLN3
MECOM
MED31
MEIS1
MEOX2
MESP1
METRNL
MFSD4
MGC39545
MICB
MIR137HG
MKX
MLLT3
MLPH
MLXIPL
MMD2
MMP2
MNX1
MSC
MSX1
MSX2
MT1A
MT1B

USH1G
VASH1
VAX1
VAX2
VDR
VSX1
VSX2
WNT1
WNT10A
WNT10B
WNT11
WNT16
WNT2
WNT3A
WNT6
WNT7A
WRAP73
WT1
WT1-AS
ZADH2
ZBTB16
ZCCHC16
ZEB2
ZFHX3
ZFYVE28
ZIC1
ZIC4
ZMYND15
ZNF436
ZNF503

FOXD4L3	GDF6	MT1DP
FOXD4L4	GDF7	MT1H
FOXD4L5	GET4	MT1M
FOXD4L6	GFI1B	MT3
FOXE1	GFRA1	MXRA7
FOXE3	GFRA4	MYB
FOXF1	GGT8P	MYF6
FOXF2	GHR	MYO5B
FOXG1	GHRL	MYOD1
FOXI2	GHSR	NAGS
FOXI3	GIMAP4	NAV2
FOXL1	GINS3	NBL1
FOXL2	GIPC1	NBPF11
FOXO3	GJA3	NCAM1
FOXP2	GJB2	NCCRP1
FOXQ1	GJB3	NDRG1
FREM3	GJB4	NDUFA4L2
FRG2B	GJB6	NEFH
FRG2C	GJD2	NEFL
FRMD3	GLB1L	NEFM
FRMD4B	GLB1L3	NEGR1
FRMPD1	GLP1R	NELL1
FSHR	GLYAT	NEURL
FSIP2	GMFB	NEUROD1
FST	GNAL	NEUROD2
FSTL4	GNAS	NEUROG1
FTCDNL1	GNE	NEUROG2
FUOM	GNG13	NEUROG3
FUS	GNN	NFIA
FXYD2	GOLGA3	NFIC
FXYD5	GOLGA7B	NFIX
FXYD7	GPAM	NGF
FZD10	GPR101	NGFR
FZD10-AS1	GPR139	NIM1
GAB3	GPR149	NIN
GABPA	GPR158	NKAIN2
GABRA1	GPR26	NKPD1
GABRA2	GPR27	NKX2-1
GABRA4	GPR50	NKX2-2
GABRB2	GPR64	NKX2-3
GABRE	GPR78	NKX2-5
GAD2	GPR88	NKX2-8
GADD45G	GRAP2	NKX3-1
GAGE12F	GRB7	NKX3-2
GAGE12I	GREM1	NKX6-1

GAGE2A
GAGE2B
GAGE2C
GAGE2E
GAGE4
GAGE5
GAGE7
GAGE8
GAL
GALNT3
GALNT6
GALNT9
GALR1
GALR2
GAN
GAP43
GAS2
GATA2
GATA3
GATA3-AS1
GATA4
GATA5
GATA6
GATA6-AS1
GBA
GBX1
GBX2
GCGR
GCM2
GDE1
GDF6
GDF7
GDNF
GDNF-AS1
GET4
GFI1
GFI1B
GFOD1
GFRA1
GFRA4
GGT8P
GHR
GHRL
GHSR
GIMAP4
GRIA2
GRID1
GRIK3
GRIN1
GRIN2C
GRIN3B
GRM1
GRM6
GRM7
GRM8
GRP
GSC
GSC2
GSDMC
GSG1L
GSG2
GSTA3
GSTZ1
GSX1
H1F0
H1FX
H1FX-AS1
H3F3B
HAND1
HAND2
HAND2-AS1
HAP1
HAPLN4
HAUS2
HBM
HBZ
HCFC2
HCN4
HCRTR2
HCST
HDAC9
HDHD2
HDLBP
HECW1
HELT
HERC4
HERC5
HES2
HES3
HEY2
NKX6-2
NOC2L
NOL4
NOTUM
NOVA2
NOXO1
NPAS1
NPAS2
NPAS4
NPNT
NPR1
NPR3
NPTX1
NPY1R
NPY5R
NR2E1
NR2F2
NR4A3
NRG1
NRG2
NRGN
NRIP3
NRN1
NRXN1
NT5C1A
NTN1
NTNG2
NTRK1
NTRK2
NXPH4
O3FAR1
OAF
OCA2
OLFML2B
OLIG2
OLIG3
ONECUT1
ONECUT2
OPRD1
OSBP2
OSR1
OSR2
OTOP1
OTOP2
OTOP3

GINS3	HHEX	OTP
GIPC1	HHIP-AS1	OTX1
GIPC2	HHLA1	OTX2
GJA3	HIST1H1C	OVOL1
GJB2	HIST1H1E	OXCT2
GJB3	HIST1H2AC	P2RX5
GJB4	HIST1H2AE	PABPC1L2A
GJB6	HIST1H2BC	PADI2
GJD2	HIST1H2BG	PAPL
GLB1L	HIST1H3J	PAPPA
GLB1L3	HLA-J	PARD3B
GLIS1	HLF	PARM1
GLP1R	HLX	PARP8
GLYAT	HMBS	PAX1
GMFB	HMGA2	PAX2
GNAL	HMGCS1	PAX3
GNAS	HMGCS2	PAX5
GNE	HMHA1	PAX6
GNG13	HMX1	PAX7
GNN	HMX2	PAX8
GOLGA3	HMX3	PAX9
GOLGA7B	HNRNPA1L2	PCDH17
GPAM	HOPX	PCDH8
GPR101	HOTAIRM1	PCDHGC4
GPR139	HOXA1	PCGF5
GPR149	HOXA11-AS	PCSK2
GPR158	HOXA2	PDE10A
GPR26	HOXA4	PDE1B
GPR27	HOXA5	PDE4DIP
GPR4	HOXA6	PDE8A
GPR50	HOXB3	PDE8B
GPR64	HOXB7	PDGFRA
GPR78	HOXB8	PDX1
GPR88	HOXB9	PDZD2
GRAP2	HOXC10	PENK
GRB7	HOXC6	PGM5
GREM1	HOXC9	PGR
GRIA2	HOXC-AS1	PHLDB1
GRID1	HOXD11	PHOX2A
GRIK3	HOXD13	PHOX2B
GRIN1	HOXD8	PHYHIPL
GRIN2C	HOXD9	PIGZ
GRIN3A	HOXD-AS1	PIP5K1B
GRIN3B	HOXD-AS2	PIR
GRM1	HPCA	PITX1

GRM4
GRM6
GRM7
GRM8
GRP
GSC
GSC2
GSDMC
GSG1L
GSG2
GSTA3
GSTZ1
GSX1
GSX2
H1F0
H1FX
H1FX-AS1
H2AFX
H3F3B
HAGH
HAND1
HAND2
HAND2-AS1
HAP1
HAPLN4
HAUS2
HBA1
HBA2
HBM
HBZ
HCFC2
HCK
HCN4
HCRTR2
HCST
HDAC9
HDHD2
HDLBP
HECW1
HELT
HEMGN
HERC4
HERC5
HES2
HES3
HPGD
HPN-AS1
HPSE
HPSE2
HR
HRC
HRH1
HRH2
HRH3
HRK
HS3ST2
HS3ST3A1
HS3ST3B1
HS3ST4
HS3ST6
HS6ST3
HSF4
HSP90AA1
HSP90B1
HSPB1
HSPH1
HTR1A
HTR1B
HTR4
HTR6
ICAM1
ICAM5
ICOSLG
ID3
ID4
IDO2
IFIH1
IFITM10
IFNG
IFNL4
IFT27
IGF2-AS
IGFBP3
IGFL1
IHH
IKZF1
IKZF3
IL10RA
IL15RA
IL17REL
PITX2
PITX3
PKNOX2
PKP1
PLEC
PLLP
PLP1
PLXNA2
PLXNC1
PMP22
PODN
POLE
POLR3GL
POMC
POU3F1
POU3F2
POU3F4
POU4F1
POU4F2
POU4F3
PPM1E
PPP1R13B
PPP1R14C
PRAC
PRDM12
PRDM13
PRKAG2
PRKCB
PRKCE
PRKCH
PRKD1
PRKG1
PRLHR
PROK2
PRR18
PRRT1
PRSS12
PRUNE2
PSD2
PTF1A
PTGDR
PTGER2
PTGER3
PTGER4
PTGFR

HEY2	IL1F10	PTH2
HHEX	IL1RAPL2	PTHLH
HHIP-AS1	IL20RA	PTPRN2
HHLA1	IL22RA2	PTPRT
HIST1H1A	IL6R	PTPRU
HIST1H1C	IL7	PXMP2
HIST1H1D	IL9R	PYY
HIST1H1E	ILF2	RAB11FIP3
HIST1H2AC	IMP3	RAB33A
HIST1H2AE	IMPACT	RAB40B
HIST1H2BC	INCA1	RAB6C
HIST1H2BG	INSL5	RAB9B
HIST1H3J	INSM1	RAMP1
HIST2H2AA3	INSRR	RAPGEF4
HIST2H2AA4	INTS4L2	RARA
HIST2H2BC	INTS6	RARRES2
HLA-J	INTS6-AS1	RASGEF1C
HLF	INTS7	RASGRF1
HLX	IQGAP2	RASL10A
HMBS	IQSEC2	RASSF5
HMGA2	IQSEC3	RAX
HMGCS1	IRF5	RBBP7
HMGCS2	IRF8	RBP4
HMHA1	IRX1	RBP7
HMX1	IRX2	RCSD1
HMX2	IRX3	REEP1
HMX3	IRX5	REPS2
HNF1B	IRX6	RFX4
HNRNPA1L2	ISL1	RFX6
HOPX	ISLR2	RGAG4
HOTAIR	ISM1	RGS10
HOTAIRM1	ITGA11	RGS20
HOTTIP	ITGA4	RGS9
HOXA1	ITGA8	RGS9BP
HOXA10	ITGB2-AS1	RIMBP3
HOXA10-HOXA9	ITIH5	RIMBP3B
HOXA11	ITPKA	RIMBP3C
HOXA11-AS	ITPR3	RIMKLA
HOXA13	ITPRIPL1	RIMS4
HOXA2	IVNS1ABP	RIPK3
HOXA3	JPH3	RIPPLY2
HOXA4	JUND	RNF128
HOXA5	KANK4	RNF2
HOXA6	KBTBD12	RNPEPL1
HOXA7	KBTBD13	ROBO3

HOXA9
HOXA-AS3
HOXA-AS4
HOXB1
HOXB13
HOXB2
HOXB3
HOXB4
HOXB5
HOXB6
HOXB7
HOXB8
HOXB9
HOXB-AS1
HOXB-AS3
HOXC10
HOXC11
HOXC12
HOXC13
HOXC4
HOXC5
HOXC6
HOXC8
HOXC9
HOXC-AS1
HOXC-AS2
HOXC-AS5
HOXD1
HOXD10
HOXD11
HOXD12
HOXD13
HOXD3
HOXD4
HOXD8
HOXD9
HOXD-AS1
HOXD-AS2
HPCA
HPGD
HPN-AS1
HPSE
HPSE2
HR
HRC
KCNA1
KCNA10
KCNA2
KCNA5
KCNA7
KCNAB1
KCNAB2
KCNB2
KCNC4
KCNE2
KCNH2
KCNH4
KCNH5
KCNIP2-AS1
KCNIP3
KCNIP4
KCNJ12
KCNJ5
KCNK1
KCNK10
KCNK12
KCNK13
KCNK15
KCNK17
KCNK2
KCNK4
KCNK6
KCNK9
KCNMA1
KCNMB4
KCNN2
KCNQ1
KCNQ3
KCNS2
KCNS3
KCNV1
KDM1A
KDM3B
KDM4A
KDM4D
KIAA0087
KIAA0226L
KIAA1009
KIAA1024
KIAA1211L
RPRML
RPS6KA2
RPS6KA6
RSPO1
RSPO2
RSPO3
RTBDN
RTN4RL2
RUNX2
RXRG
RYR3
SAMD11
SATB2
SCD5
SCIN
SCN4B
SCNN1G
SCTR
SCUBE3
SECTM1
SEMA3B
SEMA4F
SEMA6D
SERTM1
SEZ6
SFRP1
SFRP4
SFRP5
SFTPC
SGPP2
SH3GL2
SHC4
SHH
SHISA6
SHOX
SHOX2
SIDT1
SIM1
SIM2
SIX1
SIX2
SIX3
SIX6
SKAP1
SLC10A4

HRH1	KIAA1244	SLC16A11
HRH2	KIAA1324	SLC17A6
HRH3	KIF1C	SLC17A7
HRK	KIF5B	SLC1A2
HS3ST1	KIRREL3	SLC1A4
HS3ST2	KIRREL3-AS3	SLC22A3
HS3ST3A1	KISS1R	SLC24A4
HS3ST3B1	KIT	SLC25A27
HS3ST4	KL	SLC26A4
HS3ST6	KLF1	SLC26A5
HS6ST3	KLF4	SLC27A2
HSF4	KLF6	SLC30A10
HSP90AA1	KLHDC9	SLC30A2
HSP90B1	KLHL24	SLC30A3
HSPA5	KLHL30	SLC30A4
HSPA6	KLHL32	SLC32A1
HSPB1	KLHL35	SLC35D3
HSPH1	KLK1	SLC35F3
HTR1A	KLK10	SLC35G1
HTR1B	KLK13	SLC40A1
HTR2C	KLK4	SLC6A1
HTR4	KLK9	SLC6A11
HTR6	KLRG2	SLC6A2
ICAM1	KMT2A	SLC6A20
ICAM4	KNTC1	SLC6A3
ICAM5	KPNA4	SLC6A5
ICOSLG	KRT1	SLC9A2
ID3	KRT19	SLC9A3
ID4	KRT19P2	SLCO2A1
IDO2	KRT25	SLCO3A1
IFIH1	KRT36	SLCO5A1
IFITM10	KRT7	SLFN11
IFNG	KRT71	SLIT1
IFNL4	KRT78	SLIT2
IFT27	KRT83	SLIT3
IGF2	KRTAP13-1	SLITRK1
IGF2-AS	KRTAP5-9	SLITRK3
IGFBP3	KRTCAP2	SMOC2
IGFL1	L1CAM	SMPD3
IGSF21	LACE1	SNAI2
IHH	LAD1	SNCAIP
IKZF1	LAMB1	SNTB1
IKZF3	LAMP5	SORCS1
IL10RA	LARP1B	SORCS3
IL15RA	LARS	SOX14

IL17REL
IL1F10
IL1RAPL2
IL20RA
IL22RA2
IL6R
IL7
IL9R
ILF2
IMP3
IMPACT
INCA1
INSL5
INSM1
INSRR
INTS4L2
INTS6
INTS6-AS1
INTS7
IQGAP2
IQSEC2
IQSEC3
IRF4
IRF5
IRF8
IRX1
IRX2
IRX3
IRX4
IRX5
IRX6
ISL1
ISL2
ISLR2
ISM1
ITGA11
ITGA4
ITGA8
ITGB2
ITGB2-AS1
ITIH5
ITPKA
ITPR3
ITPRIPL1
IVNS1ABP
LASP1
LBH
LBX1
LBX1-AS1
LBX2-AS1
LDB2
LEF1
LEF1-AS1
LEPR
LFNG
LGALS4
LGI1
LGI3
LGR5
LGR6
LHFPL3
LHFPL4
LHX1
LHX2
LHX3
LHX4
LHX5
LHX9
LIAS
LIF
LILRA6
LIMS2
LIN28A
LIN28B
LINC00114
LINC00115
LINC00210
LINC00221
LINC00222
LINC00261
LINC00273
LINC00461
LINC00466
LINC00473
LINC00475
LINC00485
LINC00599
LINC00608
LINC00617
LINC00629
SOX17
SOX7
SOX8
SOX9
SPAG6
SPOCK3
SPON1
SPON2
SPTB
SPTBN4
SRD5A2
SRRM4
SSBP4
SSTR1
SSTR2
ST8SIA2
ST8SIA4
ST8SIA5
STC2
STK32B
STMN2
STX1A
STXBP6
SUSD4
SV2B
SYNE1
SYT12
SYT6
SYT7
T
TAC1
TACR1
TACSTD2
TAL1
TAP1
TBR1
TBX1
TBX2
TBX20
TBX21
TBX3
TBX5
TBXAS1
TCEA3
TCEAL1

JPH3	LINC00643	TCEAL8
JUND	LINC00682	TCF21
KANK4	LINC00693	TCTE1
KBTBD12	LINC00707	TET2
KBTBD13	LINC00940	TFAP2B
KCNA1	LINC00943	TFAP2D
KCNA10	LINC00951	TFAP2E
KCNA2	LINC00960	TGFA
KCNA5	LINC00966	THBD
KCNA7	LINC01024	THBS2
KCNAB1	LINC01081	TIGD3
KCNAB2	LINGO2	TLE2
KCNB2	LIPI	TLL1
KCNC4	LIPJ	TLX1
KCNE2	LMTK3	TLX2
KCNH2	LMX1A	TLX3
KCNH4	LMX1B	TMEFF2
KCNH5	LNX1	TMEM106C
KCNIP2-AS1	LOC100128770	TMEM132E
KCNIP3	LOC100129148	TMEM151A
KCNIP4	LOC100129175	TMEM163
KCNJ12	LOC100129917	TMEM185A
KCNJ5	LOC100130476	TMEM27
KCNK1	LOC100130539	TMEM30B
KCNK10	LOC100130992	TMEM54
KCNK12	LOC100131320	TMEM59L
KCNK13	LOC100132111	TMEM88
KCNK15	LOC100132215	TMOD2
KCNK17	LOC100132891	TNFRSF1B
KCNK2	LOC100134391	TNFSF9
KCNK4	LOC100144602	TP73
KCNK6	LOC100190940	TPPP3
KCNK9	LOC100240734	TRADD
KCNMA1	LOC100240735	TRH
KCNMB4	LOC100268168	TRIM28
KCNN2	LOC100288069	TRIM36
KCNQ1	LOC100288637	TRIM67
KCNQ3	LOC100288748	TRIM7
KCNS2	LOC100288842	TRIM9
KCNS3	LOC100288866	TRPC5
KCNV1	LOC100288911	TSLP
KDM1A	LOC100505622	TTLL7
KDM3B	LOC100505782	TTLL9
KDM4A	LOC100506127	TTPA
KDM4D	LOC100506551	TTYH1

KIAA0087	LOC100506810	TWIST1
KIAA0226L	LOC100653046	UCN
KIAA1009	LOC100996485	UCP1
KIAA1024	LOC101054525	ULBP1
KIAA1211L	LOC145474	ULBP2
KIAA1217	LOC145845	UNC5B
KIAA1239	LOC146513	UNC5C
KIAA1244	LOC152578	USH1G
KIAA1324	LOC153684	VASH1
KIF1C	LOC283299	VAV3
KIF5B	LOC283731	VAX1
KIRREL3	LOC284395	VAX2
KIRREL3-AS3	LOC284412	VDR
KISS1	LOC284801	VGLL2
KISS1R	LOC285084	VSX1
KIT	LOC285547	VSX2
KL	LOC285548	WNT1
KLF1	LOC340017	WNT10A
KLF14	LOC348761	WNT10B
KLF4	LOC375295	WNT11
KLF6	LOC388242	WNT16
KLHDC9	LOC389023	WNT2
KLHL24	LOC389895	WNT3A
KLHL30	LOC392232	WNT5B
KLHL32	LOC399829	WNT6
KLHL35	LOC400043	WNT7A
KLK1	LOC400456	WRAP73
KLK10	LOC401463	WSCD1
KLK13	LOC402160	WT1
KLK4	LOC440461	WT1-AS
KLK9	LOC440896	XYLT1
KLRG2	LOC440925	YAF2
KMT2A	LOC493754	ZACN
KNTC1	LOC613038	ZADH2
KPNA2	LOC63930	ZBTB16
KPNA4	LOC642366	ZBTB7A
KRT1	LOC643201	ZCCHC16
KRT19	LOC643837	ZEB2
KRT19P2	LOC643923	ZFHX3
KRT25	LOC648987	ZFPM1
KRT36	LOC654342	ZFYVE28
KRT7	LOC728463	ZIC1
KRT71	LOC728739	ZIC4
KRT76	LOC728989	ZMYND15
KRT78	LOC729911	ZNF436

KRT83
KRTAP13-1
KRTAP5-9
KRTCAP2
L1CAM
L1TD1
LACE1
LAD1
LAMA3
LAMB1
LAMP5
LARP1B
LARS
LASP1
LBH
LBX1
LBX1-AS1
LBX2
LBX2-AS1
LDB2
LEF1
LEF1-AS1
LEPR
LFNG
LGALS4
LGI1
LGI3
LGR5
LGR6
LHFPL3
LHFPL4
LHX1
LHX2
LHX3
LHX4
LHX5
LHX6
LHX8
LHX9
LIAS
LIF
LILRA5
LILRA6
LIMS2
LIN28A
LONRF3
LOR
LPIN1
LPL
LPPR4
LRG1
LRRC18
LRRC38
LRRC57
LRRC71
LRRK1
LSR
LTA4H
LTBP2
LTK
LUZP2
LYSMD1
LYSMD2
MAB21L1
MAB21L2
MAFB
MAGEC2
MAGED1
MAL
MAL2
MANBAL
MAP3K13
MAPKAPK2
MAPKAPK5
MAPRE2
MAPT-AS1
MAPT-IT1
MATK
MBIP
MBL2
MBNL3
MBP
MC5R
MCHR2
MCHR2-AS1
MCIDAS
MCOLN2
MCOLN3
MCRS1
MDGA1
ZNF503

LIN28B	MECOM
LINC00114	MECR
LINC00115	MED1
LINC00210	MED8
LINC00221	MEFV
LINC00222	MEIS1
LINC00261	MEIS1-AS3
LINC00273	MEIS2
LINC00461	MEOX2
LINC00466	MEPCE
LINC00473	MESP1
LINC00475	MET
LINC00485	METTL12
LINC00489	METTL25
LINC00554	MFSD4
LINC00599	MGC12916
LINC00608	MGC39584
LINC00617	MGEA5
LINC00629	MGME1
LINC00643	MICAL2
LINC00682	MICB
LINC00693	MIR124-1
LINC00707	MIR124-2
LINC00910	MIR124-3
LINC00940	MIR1247
LINC00943	MIR1253
LINC00951	MIR128-1
LINC00960	MIR129-2
LINC00966	MIR144
LINC01024	MIR1469
LINC01081	MIR183
LINGO2	MIR188
LIPI	MIR190B
LIPJ	MIR203
LMF1	MIR302F
LMTK3	MIR3115
LMX1A	MIR3120
LMX1B	MIR3188
LNX1	MIR3193
LOC100128770	MIR3196
LOC100129148	MIR31HG
LOC100129175	MIR34B
LOC100129917	MIR34C
LOC100130476	MIR3545
LOC100130539	MIR3621

LOC100130992	MIR3652
LOC100131320	MIR3663
LOC100132111	MIR3687
LOC100132215	MIR375
LOC100132891	MIR378D2
LOC100134391	MIR378E
LOC100144602	MIR424
LOC100190940	MIR4287
LOC100240734	MIR4297
LOC100240735	MIR4304
LOC100268168	MIR4436A
LOC100288069	MIR4453
LOC100288637	MIR4471
LOC100288748	MIR4515
LOC100288842	MIR4520A
LOC100288866	MIR4520B
LOC100288911	MIR4634
LOC100505622	MIR4638
LOC100505782	MIR4645
LOC100506127	MIR4656
LOC100506551	MIR4700
LOC100506810	MIR4732
LOC100507003	MIR4752
LOC100653046	MIR4770
LOC100996485	MIR4781
LOC101054525	MIR4785
LOC145474	MIR4787
LOC145845	MIR4792
LOC146513	MIR483
LOC152578	MIR503
LOC153684	MIR503HG
LOC283299	MIR5091
LOC283731	MIR532
LOC284395	MIR548AO
LOC284412	MIR548N
LOC284801	MIR5580
LOC285084	MIR598
LOC285547	MIR615
LOC285548	MIR622
LOC285696	MIR632
LOC340017	MIR9-1
LOC348761	MIR933
LOC375295	MIR936
LOC388242	MIR944
LOC389023	MIR96

LOC389895	MKX
LOC392232	MLNR
LOC399829	MLPH
LOC400043	MLST8
LOC400456	MLXIPL
LOC401463	MME
LOC402160	MMP25
LOC440461	MMP9
LOC440896	MNAT1
LOC440925	MNX1-AS1
LOC493754	MOGAT3
LOC613038	MOS
LOC63930	MOSPD2
LOC642366	MOXD1
LOC643201	MPP2
LOC643837	MPP5
LOC643923	MPZ
LOC648987	MPZL2
LOC654342	MRPL13
LOC728463	MRPL18
LOC728739	MRPL22
LOC728989	MRPL33
LOC729911	MRPL35
LONRF3	MRPS14
LOR	MRTO4
LPAR3	MRVI1-AS1
LPIN1	MSC
LPL	MSMO1
LPPR4	MSX1
LRG1	MSX2
LRRC18	MT1A
LRRC26	MT1B
LRRC38	MT1DP
LRRC57	MT1E
LRRC71	MT1F
LRRK1	MT1H
LSR	MT1JP
LTA4H	MT1M
LTBP2	MTBP
LTF	MTUS1
LTK	MUC17
LUZP2	MUSTN1
LYSMD1	MXRA5
LYSMD2	MYCNOS
MAB21L1	MYCT1

MAB21L2
MAFB
MAGEC2
MAGED1
MAL
MAL2
MANBAL
MAP3K13
MAPKAPK2
MAPKAPK5
MAPRE2
MAPT-AS1
MAPT-IT1
MARCH11
MAST4
MATK
MBIP
MBL2
MBNL3
MBP
MC5R
MCHR2
MCHR2-AS1
MCIDAS
MCOLN2
MCOLN3
MCRS1
MDGA1
MECOM
MECR
MED1
MED8
MEFV
MEIS1
MEIS1-AS3
MEIS2
MEOX2
MEPCE
MESP1
MET
METTL12
METTL25
MFSD4
MGC12916
MGC39584
MYH10
MYH11
MYH13
MYO5B
MYOCD
MYOD1
MYRIP
MYT1
NAGK
NAGS
NAT10
NAT16
NAV1
NBEA
NBEAP1
NCCRP1
NCLN
NCOA7
NCR1
NCR2
NDP
NDRG1
NEFH
NEFL
NELL1
NEUROD2
NEUROG1
NEUROG2
NEUROG3
NEXN
NFE2L3
NFRKB
NGB
NGF
NGFR
NHLH2
NID2
NKAIN4
NKX1-2
NKX2-1
NKX2-1-AS1
NKX2-2
NKX2-3
NKX2-4
NKX2-5

MGEA5
MGME1
MICAL2
MICB
MIR10A
MIR10B
MIR124-1
MIR124-2
MIR124-3
MIR1247
MIR1253
MIR1258
MIR128-1
MIR129-2
MIR144
MIR1469
MIR183
MIR188
MIR190B
MIR196A1
MIR196A2
MIR196B
MIR203
MIR302F
MIR3115
MIR3120
MIR3131
MIR3185
MIR3188
MIR3193
MIR3196
MIR31HG
MIR34B
MIR34C
MIR3545
MIR3621
MIR3652
MIR3663
MIR3687
MIR375
MIR378D2
MIR378E
MIR424
MIR4287
MIR4297
NKX2-6
NKX2-8
NKX3-1
NKX3-2
NKX6-1
NKX6-2
NMNAT3
NMUR2
NOC4L
NODAL
NOL3
NOL7
NOS1
NOTCH2NL
NOTUM
NPAS1
NPAS4
NPBWR1
NPHP4
NPHS2
NPNT
NPPB
NPPC
NPR1
NPR3
NPTX1
NPTX2
NPW
NPY
NPY5R
NR0B1
NR2E1
NR2F2
NR2F2-AS1
NR3C2
NR5A2
NRG2
NRG3
NRIP3
NRK
NRN1
NRSN1
NRXN1
NRXN3
NT5E

MIR4304	NTF3
MIR4436A	NTN4
MIR4453	NTNG2
MIR4471	NTRK1
MIR4515	NTSR1
MIR4520A	NUDT22
MIR4520B	NUFIP2
MIR4634	NUPL2
MIR4638	NUSAP1
MIR4645	NXPH1
MIR4656	NXPH2
MIR4700	NXPH3
MIR4727	NXPH4
MIR4732	NXT2
MIR4752	OIP5
MIR4770	OLFML2A
MIR4781	OLIG2
MIR4785	OLIG3
MIR4787	ONECUT1
MIR4792	ONECUT2
MIR4801	ONECUT3
MIR483	OPA1
MIR503	OPCML
MIR503HG	OPN1LW
MIR5091	OPRD1
MIR5188	OPRK1
MIR532	OPRL1
MIR548AO	OPRM1
MIR548N	OR10A6
MIR5580	OR10G2
MIR598	OR13C3
MIR615	OR13C5
MIR622	OR1F2P
MIR632	OR1G1
MIR663A	OR2W5
MIR9-1	OR4D1
MIR933	OR4D2
MIR936	OR4D5
MIR944	OR4F15
MIR96	OR5B12
MKX	OR5H15
MLNR	OR6B2
MLPH	OR6C68
MLST8	OR6C76
MLXIPL	OR7D2

MME
MMP25
MMP9
MNAT1
MNX1
MNX1-AS1
MOGAT3
MOS
MOSPD2
MOXD1
MPP2
MPP5
MPZ
MPZL2
MRPL13
MRPL18
MRPL22
MRPL33
MRPL35
MRPS14
MRTO4
MRVI1-AS1
MSC
MSMO1
MSX1
MSX2
MSX2P1
MT1A
MT1B
MT1DP
MT1E
MT1F
MT1G
MT1H
MT1JP
MT1M
MTBP
MTUS1
MUC12
MUC17
MUSTN1
MXRA5
MYCNOS
MYCT1
MYH10
OR9I1
OSBPL10
OSR1
OSR2
OTOP1
OTOP2
OTOP3
OTP
OTX1
OTX2
OVOL1
OXTR
P2RX2
P4HA1
PABPC1L2A
PABPC1L2B
PADI2
PAK3
PANK3
PAPPA
PAQR5
PARP10
PARP11
PARP2
PATE4
PAX1
PAX2
PAX4
PAX8
PAX9
PCDH11X
PCDH11Y
PCDH19
PCDH8
PCDH9
PCED1B-AS1
PCP4L1
PCSK2
PCSK9
PDE1C
PDE2A
PDE4B
PDE4D
PDGFA
PDGFB

MYH11	PDGFRA
MYH13	PDLIM5
MYO5B	PDP1
MYOCD	PDX1
MYOD1	PDX1-AS1
MYRIP	PDYN
MYT1	PENK
NAGK	PEPD
NAGS	PET117
NAT10	PEX5L
NAT16	PGCP1
NAV1	PGLS
NBEA	PGM5
NBEAP1	PGM5P2
NCCRP1	PGR
NCLN	PGS1
NCOA7	PHOX2A
NCR1	PID1
NCR2	PIGV
NDP	PIK3CD
NDRG1	PIK3R1
NDRG4	PIK3R5
NEFH	PINX1
NEFL	PIP4K2A
NELL1	PITX3
NEUROD1	PKP2
NEUROD2	PLA2G10
NEUROD4	PLA2G2A
NEUROG1	PLAGL1
NEUROG2	PLB1
NEUROG3	PLCG2
NEXN	PLD1
NFE2L3	PLD5
NFIX	PLEKHA8
NFRKB	PLEKHD1
NGB	PLS3
NGF	PLXDC1
NGFR	PMP22
NHLH2	PNOC
NID2	PNPLA5
NKAIN4	POC1B
NKX1-2	POC1B-GALNT4
NKX2-1	POLR2A
NKX2-1-AS1	POLR3A
NKX2-2	POLR3E

NKX2-3
NKX2-4
NKX2-5
NKX2-6
NKX2-8
NKX3-1
NKX3-2
NKX6-1
NKX6-2
NMNAT3
NMUR2
NOC4L
NODAL
NOL3
NOL7
NOS1
NOTCH2NL
NOTO
NOTUM
NPAS1
NPAS3
NPAS4
NPBWR1
NPFFR1
NPHP4
NPHS2
NPNT
NPPB
NPPC
NPR1
NPR3
NPTX1
NPTX2
NPW
NPY
NPY5R
NR0B1
NR2E1
NR2F1
NR2F1-AS1
NR2F2
NR2F2-AS1
NR3C2
NR5A2
NRG2
POM121L2
POMC
POMT2
POP4
POU1F1
POU2F2
POU2F3
POU3F4
POU4F1
POU4F2
POU4F3
PP12613
PPAPDC1A
PPARG
PPFIBP2
PPM1D
PPM1J
PPM1N
PPP1R12B
PPP1R14C
PPP1R15A
PPP6R3
PRAC1
PRDM12
PRDM13
PRDM6
PRDM8
PRDX3
PRG2
PRICKLE2-AS1
PRIMA1
PRKAB2
PRKCB
PRKCH
PRKCQ-AS1
PRKG2
PRKRIR
PRLHR
PRMT3
PRMT8
PROK2
PROKR1
PROKR2
PROM1
PROX1

NRG3	PRPF31	
NRIP3	PRPH	
NRK	PRR15	
NRN1	PRR21	
NRSN1	PRRG1	
NRXN1	PRRX1	
NRXN3	PRSS45	
NSG1	PRUNE2	
NT5E	PSAP	
NTF3	PSD2	
NTN4	PTAR1	
NTNG2	PTF1A	
NTRK1	PTGDR	
NTSR1	PTGER2	
NUBPL	PTGER3	
NUDT22	PTGER4	
NUFIP2		PTGER4P2-CDK2AP2P2
NUPL2	PTGS2	
NUSAP1	PTH2	
NXPH1	PTHLH	
NXPH2	PTK2B	
NXPH3	PTPN1	
NXPH4	PTPN23	
NXT2	PTPN3	
OIP5	PTPN5	
OLFM3	PTPRN	
OLFML2A	PTPRT	
OLIG2	PTRF	
OLIG3	PUM1	
ONECUT1	PURA	
ONECUT2	PYDC1	
ONECUT3	PYY	
OPA1	QRFPR	
OPCML	QRSL1	
OPN1LW	RAB37	
OPRD1	RAB3B	
OPRK1	RAB6B	
OPRL1	RAB6C	
OPRM1	RABGAP1L	
OR10A6	RACGAP1P	
OR10G2	RAD1	
OR13C3	RAD51AP2	
OR13C5	RAD54B	
OR1F2P	RAET1K	
OR1G1	RAI14	

OR1I1
OR1L3
OR2W5
OR4B1
OR4D1
OR4D2
OR4D5
OR4F15
OR5B12
OR5H15
OR6B2
OR6C68
OR6C76
OR7D2
OR9I1
OSBPL10
OSR1
OSR2
OTOP1
OTOP2
OTOP3
OTP
OTX1
OTX2
OTX2-AS1
OVOL1
OVOL2
OXTR
P2RX2
P4HA1
PABPC1L2A
PABPC1L2B
PADI2
PAK3
PANK3
PAPL
PAPPA
PAQR5
PARP10
PARP11
PARP2
PATE4
PAX1
PAX2
PAX3
RAI2
RAPSN
RARB
RASEF
RASGEF1A
RASGRF1
RASGRF2
RASL11B
RASSF10
RASSF5
RAX
RBFOX1
RBKS
RBM11
RBM14
RBM14-RBM4
RBM20
RBM4
RBM42
RBMS1
RBP4
RBP7
RBPJ
RC3H2
RDH13
RDH8
RDM1
REEP1
RELN
RESP18
RET
RFC1
RFPL2
RFPL4B
RFTN2
RFX3
RFX6
RFX7
RFXAP
RGCC
RGL3
RGS10
RGS6
RGS7
RGS7BP

PAX4
PAX5
PAX6
PAX7
PAX8
PAX9
PAXBP1
PCDH11X
PCDH11Y
PCDH19
PCDH8
PCDH9
PCED1B-AS1
PCP4L1
PCSK2
PCSK9
PDCL
PDE1C
PDE2A
PDE4A
PDE4B
PDE4D
PDE4DIP
PDGFA
PDGFB
PDGFRA
PDLIM5
PDP1
PDX1
PDX1-AS1
PDYN
PENK
PEPD
PET117
PEX5L
PGCP1
PGLS
PGM5
PGM5-AS1
PGM5P2
PGR
PGS1
PHACTR3
PHOX2A
PHOX2B
RGS9BP
RHOU
RIPK1
RIPK3
RIPK4
RNASE4
RND1
RNF141
RNF207
RNF220
RNF6
RNMT
RNU11
ROCK1P1
ROR1
ROR2
RPF1
RPH3A
RPL10A
RPL23
RPL26L1
RPL27
RPL29
RPL31
RPL34
RPL34-AS1
RPL5
RPL9
RPP25
RPPH1
RPRD2
RPS12
RPS26
RPS27
RPUSD4
RRAS2
RRP1
RSPO2
RSPO3
RSRC1
RSRC2
RTBDN
RTN2
RTN4IP1
RTN4RL1

PID1	RUNX1
PIGV	RUNX1T1
PIK3CD	RUNX3
PIK3R1	RYR2
PIK3R5	S100A12
PINX1	S100A14
PIP4K2A	S100A7
PITX1	S100A7A
PITX2	S100A8
PITX3	SAE1
PKD2L1	SALL1
PKP2	SALL2
PLA2G10	SAMD11
PLA2G2A	SART1
PLAGL1	SATB1
PLB1	SATB2-AS1
PLCG2	SCAMP5
PLD1	SCARNA10
PLD5	SCGN
PLEKHA8	SCN5A
PLEKHD1	SCNM1
PLS3	SCNN1B
PLXDC1	SCP2
PMP22	SCRIB
PNOC	SCRT1
PNPLA5	SCRT2
POC1B	SCTR
POC1B-GALNT4	SDE2
POLR2A	SDF2L1
POLR3A	SEC16B
POLR3E	SEC22A
POM121L2	SEMA3F
POMC	SENP7
POMT2	SERPINA7
POP4	SERPINB6
POU1F1	SERTAD4
POU2F2	SERTAD4-AS1
POU2F3	SEZ6
POU3F4	SFMBT2
POU4F1	SFRP1
POU4F2	SFRP5
POU4F3	SFTA3
PP12613	SFTPC
PPAPDC1A	SGPP2
PPARG	SH2D1B

PPFIBP2
PPIP5K1
PPM1D
PPM1J
PPM1N
PPP1R12B
PPP1R14C
PPP1R15A
PPP2R2C
PPP6R3
PRAC1
PRAC2
PRDM12
PRDM13
PRDM14
PRDM6
PRDM8
PRDX3
PRG2
PRICKLE2-AS1
PRIMA1
PRKAB2
PRKCB
PRKCH
PRKCQ-AS1
PRKCZ
PRKG2
PRKRIR
PRLHR
PRMT3
PRMT8
PROK2
PROKR1
PROKR2
PROM1
PROX1
PRPF31
PRPH
PRR15
PRR21
PRRG1
PRRX1
PRSS16
PRSS22
PRSS45
SH2D3A
SH2D3C
SH3BP5
SH3GL2
SH3RF3
SH3RF3-AS1
SHE
SHF
SHH
SHISA2
SHISA3
SHISA6
SHISA7
SHISA8
SHISA9
SHOX
SHOX2
SIDT1
SIGIRR
SIGLEC14
SIGMAR1
SIM2
SIX1
SIX2
SIX3
SIX3-AS1
SKAP1
SKAP2
SKOR1
SLC12A4
SLC15A1
SLC16A12
SLC16A6
SLC17A6
SLC17A7
SLC18A3
SLC1A2
SLC22A31
SLC24A2
SLC24A3
SLC24A4
SLC25A18
SLC25A48
SLC26A10
SLC26A4-AS1

PRUNE2	SLC26A5
PSAP	SLC30A2
PSD2	SLC30A3
PTAR1	SLC32A1
PTF1A	SLC35D3
PTGDR	SLC35F3
PTGER2	SLC35F4
PTGER3	SLC35F5
PTGER4	SLC38A3
PTGER4P2-CDK2AP2P2	SLC38A4
PTGS2	SLC38A6
PTH2	SLC4A1
PTHLH	SLC4A8
PTK2B	SLC5A8
PTPN1	SLC6A1
PTPN23	SLC6A11
PTPN3	SLC6A17
PTPN5	SLC6A3
PTPRD	SLC6A4
PTPRN	SLC6A5
PTPRT	SLC7A10
PTRF	SLC7A14
PUM1	SLC7A2
PURA	SLC7A5P2
PVALB	SLC8A3
PYDC1	SLC9A2
PYY	SLC9A3
QRFPR	SLCO4A1
QRSL1	SLCO5A1
RAB37	SLFN11
RAB3B	SLFN12L
RAB6B	SLFN14
RAB6C	SLIT3
RABGAP1L	SLITRK3
RACGAP1P	SMAD5
RAD1	SMDT1
RAD51AP2	SMEK2
RAD54B	SMIM14
RAET1K	SMOC2
RAI14	SNAP25
RAI2	SNAP25-AS1
RAPSN	SNAR-B1
RARB	SNAR-B2
RASEF	SND1-IT1
RASGEF1A	SNED1

RASGRF1
RASGRF2
RASL11B
RASSF10
RASSF5
RAX
RBFOX1
RBKS
RBM11
RBM14
RBM14-RBM4
RBM20
RBM4
RBM42
RBMS1
RBP4
RBP7
RBPJ
RC3H2
RDH13
RDH8
RDM1
REEP1
RELN
RESP18
RET
REXO1L2P
RFC1
RFPL2
RFPL4B
RFTN2
RFX3
RFX6
RFX7
RFXAP
RGCC
RGL3
RGS10
RGS6
RGS7
RGS7BP
RGS9BP
RHOU
RIPK1
RIPK3
SNORA21
SNORA57
SNORA76
SNORD101
SNORD114-3
SNORD114-4
SNORD116-28
SNORD1A
SNORD1B
SNTB1
SNTG2
SNX31
SNX5
SOCS2
SOCS2-AS1
SORBS2
SORCS1
SORCS3
SOWAHA
SOWAHB
SOX1
SOX14
SOX17
SOX3
SOX7
SP5
SP7
SP9
SPAG6
SPATA2
SPATA31C1
SPATA31D4
SPCS2
SPHKAP
SPINT1
SPNS2
SPOCK1
SPON1
SPON2
SRC
SRD5A2
SRGAP2-AS1
SRP68
SRSF3
SST

RIPK4
RNASE4
RND1
RNF128
RNF141
RNF207
RNF220
RNF6
RNMT
RNPS1
RNU11
ROBO3
ROCK1P1
ROR1
ROR2
RPF1
RPH3A
RPL10A
RPL23
RPL26L1
RPL27
RPL29
RPL31
RPL34
RPL34-AS1
RPL5
RPL9
RPP25
RPPH1
RPRD2
RPS12
RPS26
RPS27
RPSAP52
RPUSD4
RRAD
RRAS2
RRP1
RSPO1
RSPO2
RSPO3
RSPO4
RSRC1
RSRC2
RTBDN
SSTR2
ST3GAL6-AS1
ST6GAL1
ST6GAL2
ST6GALNAC1
ST6GALNAC2
ST8SIA5
ST8SIA6
STAC
STAM
STC2
STK16
STK3
STMN2
STX11
STX8
SUPT5H
SURF6
SUSD4
SUSD5
SUV420H2
SV2B
SV2C
SYCP2L
SYK
SYMPK
SYN3
SYNDIG1
SYNE1
SYNPR
SYT15
SYT2
SYT3
SYT6
SZT2
T
TACR1
TARBP2
TARS
TBC1D1
TBC1D21
TBC1D30
TBC1D8B
TBCCD1
TBR1

RTN2
RTN4IP1
RTN4RL1
RUNX1
RUNX1T1
RUNX3
RYR2
S100A12
S100A14
S100A7
S100A7A
S100A8
SAE1
SALL1
SALL2
SAMD11
SART1
SATB1
SATB2
SATB2-AS1
SCAMP5
SCARNA10
SCGN
SCN5A
SCNM1
SCNN1B
SCP2
SCRIB
SCRT1
SCRT2
SCTR
SDE2
SDF2L1
SEC16B
SEC22A
SELL
SEMA3A
SEMA3F
SENP7
SEPT2
SERPINA7
SERPINB6
SERTAD4
SERTAD4-AS1
SEZ6
TBX1
TBX18
TBX2
TBX20
TBX3
TC2N
TCEAL6
TCERG1L
TCF15
TCF24
TCP1
TDGF1
TDP2
TDRD10
TECTA
TERF2
TESK1
TEX10
TFAP2A-AS1
TFAP2C
TFCP2L1
TFPT
TGFA
TGFBI
TGFBR3L
THBD
THRB
THRB-AS1
THSD7B
TIA1
TIFAB
TLE6
TLL1
TLR2
TLX1
TLX1NB
TLX2
TLX3
TMEM132C
TMEM132D
TMEM132E
TMEM155
TMEM163
TMEM171
TMEM176A

SFMBT2
SFRP1
SFRP5
SFTA3
SFTPC
SGPP2
SH2D1B
SH2D3A
SH2D3C
SH3BP5
SH3GL2
SH3RF3
SH3RF3-AS1
SHE
SHF
SHH
SHISA2
SHISA3
SHISA6
SHISA7
SHISA8
SHISA9
SHOX
SHOX2
SIDT1
SIGIRR
SIGLEC14
SIGMAR1
SIM1
SIM2
SIX1
SIX2
SIX3
SIX3-AS1
SIX6
SKAP1
SKAP2
SKOR1
SKOR2
SLC12A4
SLC15A1
SLC16A12
SLC16A6
SLC17A6
SLC17A7
TMEM176B
TMEM18
TMEM215
TMEM229A
TMEM229B
TMEM233
TMEM235
TMEM30B
TMEM38B
TMEM59
TMEM59L
TMEM61
TMEM66
TMEM79
TMOD1
TMOD2
TMPRSS2
TMX1
TNFRSF11A
TNFRSF19
TNFRSF8
TNFSF9
TNK1
TOP1P2
TP73
TPBG
TPR
TPRKB
TRABD2A
TRABD2B
TRADD
TRH
TRHDE-AS1
TRIM34
TRIM35
TRIM36
TRIM41
TRIM46
TRIM54
TRIM67
TRIM72
TRMT5
TRPC5
TRPC6
TRPM4

SLC18A2
SLC18A3
SLC1A2
SLC22A31
SLC24A2
SLC24A3
SLC24A4
SLC25A18
SLC25A48
SLC26A10
SLC26A4
SLC26A4-AS1
SLC26A5
SLC27A6
SLC30A2
SLC30A3
SLC32A1
SLC35D3
SLC35F3
SLC35F4
SLC35F5
SLC38A3
SLC38A4
SLC38A6
SLC4A1
SLC4A11
SLC4A8
SLC5A7
SLC5A8
SLC6A1
SLC6A11
SLC6A17
SLC6A2
SLC6A20
SLC6A3
SLC6A4
SLC6A5
SLC6A7
SLC7A10
SLC7A14
SLC7A2
SLC7A5P2
SLC8A3
SLC9A2
SLC9A3
TRPT1
TSC22D2
TSGA13
TSLP
TSPEAR
TTC39A
TTLL6
TUBA4A
TUBA4B
TWIST1
UBASH3B
UBE2D3
UBE2F
UBE2F-SCLY
UBE4A
UBTD2
UCN
UCP1
UG0898H09
ULBP1
ULBP2
UNC5A
UNC5B-AS1
UNC5C
UNC5D
UNCX
UPB1
UQCRC2
USH1G
USP42
USP50
UTF1
UTRN
VAV3-AS1
VAX1
VAX2
VDR
VENTX
VGF
VGLL4
VIPR1
VIPR2
VMA21
VPS33A
VPS51

SLCO4A1	VRK3
SLCO5A1	VSIG2
SLFN11	VSTM2B
SLFN12L	VTRNA2-1
SLFN14	VWA2
SLIT3	VWA5B2
SLITRK3	VWC2
SMAD5	VWC2L-IT1
SMDT1	WASH2P
SMEK2	WBSCR17
SMIM14	WDR16
SMOC2	WDR33
SMUG1	WDR4
SNAP25	WIF1
SNAP25-AS1	WLS
SNAR-A1	WNT1
SNAR-A10	WNT10A
SNAR-A11	WNT11
SNAR-A14	WNT2
SNAR-A2	WNT2B
SNAR-A3	WNT3
SNAR-A4	WNT3A
SNAR-A5	WNT6
SNAR-A6	WNT7A
SNAR-A7	WNT7B
SNAR-A8	WNT9B
SNAR-A9	WRAP73
SNAR-B1	WTH3DI
SNAR-B2	XIRP1
SNAR-C1	XKR7
SNAR-C2	XRRA1
SNAR-C5	YBX3P1
SND1-IT1	YWHAE
SNED1	ZACN
SNHG7	ZBTB4
SNORA21	ZCCHC16
SNORA57	ZCWPW1
SNORA76	ZDHHC22
SNORD101	ZDHHC5
SNORD114-3	ZFAND5
SNORD114-4	ZFHX3
SNORD116-28	ZFP91
SNORD1A	ZFP91-CNTF
SNORD1B	ZFPL1
SNRPA1	ZFPM2

SNTB1
SNTG2
SNX16
SNX31
SNX5
SOCS2
SOCS2-AS1
SORBS2
SORCS1
SORCS3
SOWAHA
SOWAHB
SOX1
SOX14
SOX17
SOX18
SOX3
SOX5
SOX7
SOX8
SP5
SP6
SP7
SP8
SP9
SPAG6
SPATA2
SPATA31C1
SPATA31D4
SPCS2
SPHKAP
SPINT1
SPNS2
SPOCK1
SPON1
SPON2
SRC
SRD5A2
SRGAP2-AS1
SRP68
SRSF3
SRSF7
SST
SSTR1
SSTR2
ZFYVE28
ZIC1
ZIC2
ZIC3
ZIC4
ZIC5
ZMYND15
ZNF106
ZNF207
ZNF259
ZNF385B
ZNF436
ZNF471
ZNF473
ZNF484
ZNF503
ZNF503-AS2
ZNF546
ZNF706
ZNF77
ZNF775
ZNF804B
ZNF827
ZNF830
ZNF860
ZSCAN5B
ZSWIM6

SSTR5
ST14
ST3GAL6-AS1
ST5
ST6GAL1
ST6GAL2
ST6GALNAC1
ST6GALNAC2
ST8SIA5
ST8SIA6
STAC
STAM
STC2
STK16
STK3
STMN2
STX11
STX6
STX8
SUPT5H
SURF6
SUSD4
SUSD5
SUV420H2
SV2B
SV2C
SYCP2L
SYK
SYMPK
SYN3
SYNDIG1
SYNE1
SYNPR
SYT15
SYT2
SYT3
SYT6
SZT2
T
TAC1
TACR1
TAL1
TARBP2
TARS
TBC1D1

TBC1D21
TBC1D3
TBC1D30
TBC1D3C
TBC1D3F
TBC1D3H
TBC1D8B
TBCCD1
TBR1
TBX1
TBX15
TBX18
TBX2
TBX20
TBX3
TBX4
TBX5
TBX5-AS1
TC2N
TCEAL6
TCERG1L
TCF15
TCF21
TCF24
TCP1
TDGF1
TDP2
TDRD10
TECTA
TERF2
TESK1
TEX10
TFAP2A
TFAP2A-AS1
TFAP2B
TFAP2C
TFAP2D
TFCP2L1
TFPT
TGFA
TGFBI
TGFBR3L
TGM5
THBD
THRB

THRB-AS1
THSD7B
TIA1
TIFAB
TLE6
TLL1
TLR2
TLX1
TLX1NB
TLX2
TLX3
TMEM132C
TMEM132D
TMEM132E
TMEM155
TMEM163
TMEM171
TMEM176A
TMEM176B
TMEM18
TMEM215
TMEM229A
TMEM229B
TMEM233
TMEM235
TMEM30B
TMEM38B
TMEM45B
TMEM59
TMEM59L
TMEM61
TMEM66
TMEM79
TMOD1
TMOD2
TMPRSS2
TMX1
TNFRSF11A
TNFRSF19
TNFRSF8
TNFSF11
TNFSF9
TNK1
TNS4
TOP1P2

TP73
TPBG
TPM3
TPR
TPRKB
TRABD2A
TRABD2B
TRADD
TRH
TRHDE-AS1
TRIM34
TRIM35
TRIM36
TRIM41
TRIM46
TRIM54
TRIM67
TRIM72
TRMT5
TRPA1
TRPC5
TRPC6
TRPM4
TRPT1
TSC22D2
TSGA13
TSLP
TSPEAR
TTC39A
TTLL6
TUBA4A
TUBA4B
TWIST1
UBASH3B
UBC
UBE2D3
UBE2F
UBE2F-SCLY
UBE4A
UBTD2
UCN
UCP1
UG0898H09
ULBP1
ULBP2

UNC5A
UNC5B-AS1
UNC5C
UNC5D
UNCX
UPB1
UQCRC2
USH1G
USP42
USP44
USP50
USPL1
UTF1
UTRN
VAV3-AS1
VAX1
VAX2
VDR
VENTX
VGF
VGLL2
VGLL4
VIPR1
VIPR2
VMA21
VPS33A
VPS51
VRK3
VSIG2
VSTM2B
VSX1
VSX2
VTRNA2-1
VWA2
VWA5B2
VWC2
VWC2L-IT1
WASH2P
WBSCR17
WDR16
WDR33
WDR4
WIF1
WLS
WNT1

WNT10A
WNT10B
WNT11
WNT16
WNT2
WNT2B
WNT3
WNT3A
WNT6
WNT7A
WNT7B
WNT8B
WNT9B
WRAP73
WT1
WT1-AS
WTH3DI
XIRP1
XKR7
XRRA1
YBX3P1
YWHAE
ZACN
ZBTB4
ZCCHC16
ZCWPW1
ZDHHC22
ZDHHC5
ZFAND5
ZFHX3
ZFP91
ZFP91-CNTF
ZFPL1
ZFPM2
ZFYVE28
ZIC1
ZIC2
ZIC3
ZIC4
ZIC5
ZMYND15
ZNF106
ZNF207
ZNF259
ZNF385B

ZNF436
ZNF462
ZNF471
ZNF473
ZNF484
ZNF503
ZNF503-AS2
ZNF546
ZNF555
ZNF706
ZNF77
ZNF775
ZNF804B
ZNF827
ZNF830
ZNF860
ZSCAN5B
ZSWIM6

Table S5. IC_{50} of compounds* used in the chemical screen

Name	IC_{50} (-log mM)		
	Normal	P5K	Δ
MI-2 (hydrochloride)	2.18	3.81	1.64
Sinefungin	<1.5	2.43	0.93
CAY10591	1.95	2.55	0.60
MS-275	1.87	2.46	0.59
Tubastatin A (trifluoroacetate salt)	1.61	2.07	0.46
Tenovin-6	2.53	2.82	0.30
Decitabine	<1.5	1.80	0.30
(−)-Neplanocin A	<1.5	1.68	0.18
UNC0224	2.49	2.61	0.12
4-iodo-SAHA	2.31	2.41	0.10
HC Toxin	3.07	3.17	0.09
AGK2	2.06	2.12	0.06
UNC0638	2.54	2.59	0.05
CAY10398	2.47	2.49	0.02
Piceatannol	1.94	1.94	0.00
Apicidin	2.90	2.89	-0.01
SB 939	2.73	2.71	-0.02
Trichostatin A	2.75	2.68	-0.08
M 344	2.50	2.40	-0.10
Suberohydroxamic Acid	2.18	2.07	-0.11
SAHA	2.38	2.23	-0.15
Chidamide	2.51	2.28	-0.23
2,4-Pyridinedicarboxylic Acid	1.75	<1.5	-0.25
(S)-HDAC-42	2.58	2.32	-0.27
Ellagic Acid	2.07	<1.5	-0.57
Mirin	2.65	2.07	-0.58
Oxamflatin	2.10	<1.5	-0.60
Pyroxamide	2.13	<1.5	-0.63
Tenovin-1	2.14	<1.5	-0.64
(−)-JQ1	<1.5	<1.5	NA
(+)-JQ1	<1.5	<1.5	NA
2',3',5'-triacetyl-5-Azacytidine	<1.5	<1.5	NA
2,4-DPD	<1.5	<1.5	NA
2-PCPA (hydrochloride)	<1.5	<1.5	NA
3-amino Benzamide	<1.5	<1.5	NA
3-Deazaneplanocin A	<1.5	<1.5	NA
5-Azacytidine	<1.5	<1.5	NA
AG-014699	<1.5	<1.5	NA
AMI-1 (sodium salt)	<1.5	<1.5	NA

Anacardic Acid	<1.5	<1.5	NA
BSI-201	<1.5	<1.5	NA
C646	<1.5	<1.5	NA
CAY10433	<1.5	<1.5	NA
CAY10603	<1.5	<1.5	NA
CBHA	<1.5	<1.5	NA
Cl-Amidine	<1.5	<1.5	NA
Daminozide	<1.5	<1.5	NA
Delphinidin chloride	<1.5	<1.5	NA
DMOG	<1.5	<1.5	NA
EX-527	<1.5	<1.5	NA
F-Amidine (trifluoroacetate salt)	<1.5	<1.5	NA
Garcinol	<1.5	<1.5	NA
Gemcitabine	<1.5	<1.5	NA
GSK-J1 (sodium salt)	<1.5	<1.5	NA
GSK-J4 (hydrochloride)	<1.5	<1.5	NA
HNHA	<1.5	<1.5	NA
IOX1	<1.5	<1.5	NA
Isoliquiritigenin	<1.5	<1.5	NA
JGB1741	<1.5	<1.5	NA
Lomeguatrib	<1.5	<1.5	NA
MI-nc (hydrochloride)	<1.5	<1.5	NA
Nicotinamide	<1.5	<1.5	NA
N-Oxalylglycine	<1.5	<1.5	NA
PCI 4051	<1.5	<1.5	NA
PFI-1	<1.5	<1.5	NA
Phthalazinone pyrazole	<1.5	<1.5	NA
Pimelic Diphenylamide 106	<1.5	<1.5	NA
RG-108	<1.5	<1.5	NA
S-Adenosylhomocysteine	<1.5	<1.5	NA
Salermide	<1.5	<1.5	NA
Scriptaid	<1.5	<1.5	NA
Sirtinol	<1.5	<1.5	NA
Sodium Butyrate	<1.5	<1.5	NA
Splitomicin	<1.5	<1.5	NA
Suramin (sodium salt)	<1.5	<1.5	NA
trans-Resveratrol	<1.5	<1.5	NA
UNC0321 (trifluoroacetate salt)	<1.5	<1.5	NA
UNC1215	<1.5	<1.5	NA
Valproic Acid (sodium salt)	<1.5	<1.5	NA
Zebularine	<1.5	<1.5	NA

*selected from an epigenetic chemical library from Cayman Chemicals (cat. No. 11076)

Table S6. Oligonucleotide sequences

shRNA target sequences

Name	Target sequence
shLuc	CTTACGCTGAGTACTTCGA
sh-p53	GACTCCAGTGGTAATCTACT
sh-p53#2	GTAATCTACTGGGACGGAA
shLIN28B#1	GCAGGCATAATAAGCAAGTTA
shLIN28B#3	GGATTCATCTCCATGATAAAC
shPLAG1#1	GGAAGAAGCACATTCTTCTGT
shPLAG1#2	GCAAGAACTACAATACCAAGC
shPLAGL1#1	GAGAAGACGTTCAACCGGAAA
shPLAGL1#2	GTCAGTTACAATATGAGAAAG
shMEN1#1	GATCTACAAGGAGTTCTTTGA
shMEN1#2	GAGTACAGTCTGTATCAAACC

Primer sequences for RT-qPCR

Name	Sequence
LIN28B_Fw	GAAGACCCAAAGGGAAGACAC
LIN28B_Rv	TTCTTTGGCTGAGGAGGTAGA
PLAG1_Fw	ATTGTGATCGCCGGTTCTAC
PLAG1_Rv	ATCCTTTCGCCCAAATCTCT
PLAGL1_Fw	CAGACCGGAGACCTTCTGAG
PLAGL1_Rv	TCTGGGCAGAAGCTCCTAAA
Nkx2-2_Fw	AGTACTCCCTGCACGGTCTG
Nkx2-2_Rv	GGGTCTCCTTGTCATTGTCC
MBP_Fw	CCCACATGTAGTAAGCCACTC
MBP_Rv	TGTCCTTCTCTCACCTCCTAAA
Actin_Fw	ACCCCATCGAGCACGGCATCG
Actin_Rv	GTCACCGGAGTCCATCACGATG
MEN1_Fw	TCCAGTCCCTCTTCAGCTTC
MEN1_Rv	ACCACAGCAAAGGCCACAC

Primer sequences for ChIP-PCR

Name	Sequence
MEN1_TSS_Fw	GCCCCCTCTCTACGACTGTG
MEN1_TSS_Rv	AGGACTCTCCTTGGGGTTTG
MEN1_Up5k_Fw	GCTGTGTGAGGAGGCATGTA
MEN1_Up5k_Rv	CAACTCGAATTGACGGTTGA
LIN28B_TSS_Fw	GGGGGCTATTGTTTGAATTGT
LIN28B_TSS_Rv	TTAAAGTTGGGGTGGAATGG
Nkx2-2_TSS_Fw	AGGGAGGGAGGGAAAGAAAG
Nkx2-2_TSS_Rv	GCCAACCTTTGCGTTTTTAAT

REFERENCES

1. J. Schwartzentruber, A. Korshunov, X. Y. Liu, D. T. Jones, E. Pfaff, K. Jacob, D. Sturm, A. M. Fontebasso, D. A. Quang, M. Tönjes, V. Hovestadt, S. Albrecht, M. Kool, A. Nantel, C. Konermann, A. Lindroth, N. Jäger, T. Rausch, M. Ryzhova, J. O. Korbel, T. Hielscher, P. Hauser, M. Garami, A. Klekner, L. Bognar, M. Ebinger, M. U. Schuhmann, W. Scheurlen, A. Pekrun, M. C. Frühwald, W. Roggendorf, C. Kramm, M. Dürken, J. Atkinson, P. Lepage, A. Montpetit, M. Zakrzewska, K. Zakrzewski, P. P. Liberski, Z. Dong, P. Siegel, A. E. Kulozik, M. Zapatka, A. Guha, D. Malkin, J. Felsberg, G. Reifenberger, A. von Deimling, K. Ichimura, V. P. Collins, H. Witt, T. Milde, O. Witt, C. Zhang, P. Castelo-Branco, P. Lichter, D. Faury, U. Tabori, C. Plass, J. Majewski, S. M. Pfister, N. Jabado, Driver mutations in histone H3.3 and chromatin remodelling genes in paediatric glioblastoma. *Nature* **482**, 226–231 (2012). Medline doi:10.1038/nature10833

2. G. Wu, A. Broniscer, T. A. McEachron, C. Lu, B. S. Paugh, J. Becksfort, C. Qu, L. Ding, R. Huether, M. Parker, J. Zhang, A. Gajjar, M. A. Dyer, C. G. Mullighan, R. J. Gilbertson, E. R. Mardis, R. K. Wilson, J. R. Downing, D. W. Ellison, J. Zhang, S. J. Baker; St. Jude Children's Research Hospital–Washington University Pediatric Cancer Genome Project, Somatic histone H3 alterations in pediatric diffuse intrinsic pontine gliomas and non-brainstem glioblastomas. *Nat. Genet.* **44**, 251–253 (2012). Medline doi:10.1038/ng.1102

3. J. Zhang, G. Wu, C. P. Miller, R. G. Tatevossian, J. D. Dalton, B. Tang, W. Orisme, C. Punchihewa, M. Parker, I. Qaddoumi, F. A. Boop, C. Lu, C. Kandoth, L. Ding, R. Lee, R. Huether, X. Chen, E. Hedlund, P. Nagahawatte, M. Rusch, K. Boggs, J. Cheng, J. Becksfort, J. Ma, G. Song, Y. Li, L. Wei, J. Wang, S. Shurtleff, J. Easton, D. Zhao, R. S. Fulton, L. L. Fulton, D. J. Dooling, B. Vadodaria, H. L. Mulder, C. Tang, K. Ochoa, C. G. Mullighan, A. Gajjar, R. Kriwacki, D. Sheer, R. J. Gilbertson, E. R. Mardis, R. K. Wilson, J. R. Downing, S. J. Baker, D. W. Ellison; St. Jude Children's Research Hospital–Washington University Pediatric Cancer Genome Project, Whole-genome sequencing identifies genetic alterations in pediatric low-grade gliomas. *Nat. Genet.* **45**, 602–612 (2013). Medline doi:10.1038/ng.2611

4. D. Sturm, H. Witt, V. Hovestadt, D. A. Khuong-Quang, D. T. Jones, C. Konermann, E. Pfaff, M. Tönjes, M. Sill, S. Bender, M. Kool, M. Zapatka, N. Becker, M. Zucknick, T. Hielscher, X. Y. Liu, A. M. Fontebasso, M. Ryzhova, S. Albrecht, K. Jacob, M. Wolter, M. Ebinger, M. U. Schuhmann, T. van Meter, M. C. Frühwald, H. Hauch, A. Pekrun, B. Radlwimmer, T. Niehues, G. von Komorowski, M. Dürken, A. E. Kulozik, J. Madden, A. Donson, N. K. Foreman, R. Drissi, M. Fouladi, W. Scheurlen, A. von Deimling, C. Monoranu, W. Roggendorf, C. Herold-Mende, A. Unterberg, C. M. Kramm, J. Felsberg, C. Hartmann, B. Wiestler, W. Wick, T. Milde, O. Witt, A. M. Lindroth, J. Schwartzentruber, D. Faury, A. Fleming, M. Zakrzewska, P. P. Liberski, K. Zakrzewski, P. Hauser, M. Garami, A. Klekner, L. Bognar, S. Morrissy, F. Cavalli, M. D. Taylor, P. van Sluis, J. Koster, R. Versteeg, R. Volckmann, T. Mikkelsen, K. Aldape, G. Reifenberger, V. P. Collins, J. Majewski, A. Korshunov, P. Lichter, C. Plass, N. Jabado, S. M. Pfister, Hotspot mutations in H3F3A and IDH1 define distinct epigenetic and biological subgroups of glioblastoma. *Cancer Cell* **22**, 425–437 (2012). Medline doi:10.1016/j.ccr.2012.08.024

5. D.-A. Khuong-Quang, P. Buczkowicz, P. Rakopoulos, X. Y. Liu, A. M. Fontebasso, E. Bouffet, U. Bartels, S. Albrecht, J. Schwartzentruber, L. Letourneau, M. Bourgey, G. Bourque, A. Montpetit, G. Bourret, P. Lepage, A. Fleming, P. Lichter, M. Kool, A. von Deimling, D. Sturm, A. Korshunov, D. Faury, D. T. Jones, J. Majewski, S. M. Pfister, N. Jabado, C. Hawkins, K27M mutation in histone H3.3 defines clinically and biologically distinct subgroups of pediatric diffuse intrinsic pontine gliomas. *Acta Neuropathol.* **124**, 439–447 (2012). Medline doi:10.1007/s00401-012-0998-0

6. V. Tabar, L. Studer, Pluripotent stem cells in regenerative medicine: Challenges and recent progress. *Nat. Rev. Genet.* **15**, 82–92 (2014). Medline doi:10.1038/nrg3563

7. S. M. Chambers, C. A. Fasano, E. P. Papapetrou, M. Tomishima, M. Sadelain, L. Studer, Highly efficient neural conversion of human ES and iPS cells by dual inhibition of SMAD signaling. *Nat. Biotechnol.* **27**, 275–280 (2009). Medline doi:10.1038/nbt.1529

8. B. S. Paugh, X. Zhu, C. Qu, R. Endersby, A. K. Diaz, J. Zhang, D. A. Bax, D. Carvalho, R. M. Reis, A. Onar-Thomas, A. Broniscer, C. Wetmore, J. Zhang, C. Jones, D. W. Ellison, S. J. Baker, Novel oncogenic PDGFRA mutations in pediatric high-grade gliomas. *Cancer Res.* **73**, 6219–6229 (2013). Medline doi:10.1158/0008-5472.CAN-13-1491

9. P. W. Lewis, M. M. Müller, M. S. Koletsky, F. Cordero, S. Lin, L. A. Banaszynski, B. A. Garcia, T. W. Muir, O. J. Becher, C. D. Allis, Inhibition of PRC2 activity by a gain-of-function H3 mutation found in pediatric glioblastoma. *Science* **340**, 857–861 (2013). Medline doi:10.1126/science.1232245

10. K.-M. Chan, D. Fang, H. Gan, R. Hashizume, C. Yu, M. Schroeder, N. Gupta, S. Mueller, C. D. James, R. Jenkins, J. Sarkaria, Z. Zhang, The histone H3.3K27M mutation in pediatric glioma reprograms H3K27 methylation and gene expression. *Genes Dev.* **27**, 985–990 (2013). Medline doi:10.1101/gad.217778.113

11. S. Bender, Y. Tang, A. M. Lindroth, V. Hovestadt, D. T. Jones, M. Kool, M. Zapatka, P. A. Northcott, D. Sturm, W. Wang, B. Radlwimmer, J. W. Højfeldt, N. Truffaux, D. Castel, S. Schubert, M. Ryzhova, H. Seker-Cin, J. Gronych, P. D. Johann, S. Stark, J. Meyer, T. Milde, M. Schuhmann, M. Ebinger, C. M. Monoranu, A. Ponnuswami, S. Chen, C. Jones, O. Witt, V. P. Collins, A. von Deimling, N. Jabado, S. Puget, J. Grill, K. Helin, A. Korshunov, P. Lichter, M. Monje, C. Plass, Y. J. Cho, S. M. Pfister, Reduced H3K27me3 and DNA hypomethylation are major drivers of gene expression in K27M mutant pediatric high-grade gliomas. *Cancer Cell* **24**, 660–672 (2013). Medline doi:10.1016/j.ccr.2013.10.006

12. T. D. Halazonetis, V. G. Gorgoulis, J. Bartek, An oncogene-induced DNA damage model for cancer development. *Science* **319**, 1352–1355 (2008). Medline doi:10.1126/science.1140735

13. D. Hanahan, R. A. Weinberg, The hallmarks of cancer. *Cell* **100**, 57–70 (2000). Medline doi:10.1016/S0092-8674(00)81683-9

14. R. Sethi, J. Allen, B. Donahue, M. Karajannis, S. Gardner, J. Wisoff, S. Kunnakkat, J. Mathew, D. Zagzag, K. Newman, A. Narayana, Prospective neuraxis MRI surveillance reveals a high risk of leptomeningeal dissemination in diffuse intrinsic pontine glioma. *J. Neurooncol.* **102**, 121–127 (2011). Medline doi:10.1007/s11060-010-0301-y

15. Y. Elkabetz, G. Panagiotakos, G. Al Shamy, N. D. Socci, V. Tabar, L. Studer, Human ES cell-derived neural rosettes reveal a functionally distinct early neural stem cell stage. *Genes Dev.* **22**, 152–165 (2008). Medline doi:10.1101/gad.1616208

16. P. W. Lewis, C. D. Allis, Poisoning the "histone code" in pediatric gliomagenesis. *Cell Cycle* **12**, 3241–3242 (2013). Medline doi:10.4161/cc.26356

17. I. Ben-Porath, M. W. Thomson, V. J. Carey, R. Ge, G. W. Bell, A. Regev, R. A. Weinberg, An embryonic stem cell-like gene expression signature in poorly differentiated aggressive human tumors. *Nat. Genet.* **40**, 499–507 (2008). Medline doi:10.1038/ng.127

18. J. Grembecka, S. He, A. Shi, T. Purohit, A. G. Muntean, R. J. Sorenson, H. D. Showalter, M. J. Murai, A. M. Belcher, T. Hartley, J. L. Hess, T. Cierpicki, Menin-MLL inhibitors reverse oncogenic activity of MLL fusion proteins in leukemia. *Nat. Chem. Biol.* **8**, 277–284 (2012). Medline doi:10.1038/nchembio.773

19. S. Matkar, A. Thiel, X. Hua, Menin: A scaffold protein that controls gene expression and cell signaling. *Trends Biochem. Sci.* **38**, 394–402 (2013). Medline doi:10.1016/j.tibs.2013.05.005

20. A. Yokoyama, T. C. Somervaille, K. S. Smith, O. Rozenblatt-Rosen, M. Meyerson, M. L. Cleary, The menin tumor suppressor protein is an essential oncogenic cofactor for MLL-associated leukemogenesis. *Cell* **123**, 207–218 (2005). Medline doi:10.1016/j.cell.2005.09.025

21. S. R. Viswanathan, G. Q. Daley, Lin28: A microRNA regulator with a macro role. *Cell* **140**, 445–449 (2010). Medline doi:10.1016/j.cell.2010.02.007

22. Y. Hu, G. K. Smyth, ELDA: Extreme limiting dilution analysis for comparing depleted and enriched populations in stem cell and other assays. *J. Immunol. Methods* **347**, 70–78 (2009). Medline doi:10.1016/j.jim.2009.06.008

23. M. S. Bradbury, G. Panagiotakos, B. K. Chan, M. Tomishima, P. Zanzonico, J. Vider, V. Ponomarev, L. Studer, V. Tabar, Optical bioluminescence imaging of human ES cell progeny in the rodent CNS. *J. Neurochem.* **102**, 2029–2039 (2007). Medline doi:10.1111/j.1471-4159.2007.04681.x

24. R. A. Irizarry, B. Hobbs, F. Collin, Y. D. Beazer-Barclay, K. J. Antonellis, U. Scherf, T. P. Speed, Exploration, normalization, and summaries of high density oligonucleotide array probe level data. *Biostatistics* **4**, 249–264 (2003). Medline doi:10.1093/biostatistics/4.2.249

25. A. D. Goldberg, L. A. Banaszynski, K. M. Noh, P. W. Lewis, S. J. Elsaesser, S. Stadler, S. Dewell, M. Law, X. Guo, X. Li, D. Wen, A. Chapgier, R. C. DeKelver, J. C. Miller, Y. L. Lee, E. A. Boydston, M. C. Holmes, P. D. Gregory, J. M. Greally, S. Rafii, C. Yang, P. J. Scambler, D. Garrick, R. J. Gibbons, D. R. Higgs, I. M. Cristea, F. D. Urnov, D. Zheng, C. D. Allis, Distinct factors control histone variant H3.3 localization at specific genomic regions. *Cell* **140**, 678–691 (2010). Medline doi:10.1016/j.cell.2010.01.003

26. B. Langmead, C. Trapnell, M. Pop, S. L. Salzberg, Ultrafast and memory-efficient alignment of short DNA sequences to the human genome. *Genome Biol.* **10**, R25 (2009). Medline doi:10.1186/gb-2009-10-3-r25

27. Y. Zhang, T. Liu, C. A. Meyer, J. Eeckhoute, D. S. Johnson, B. E. Bernstein, C. Nusbaum, R. M. Myers, M. Brown, W. Li, X. S. Liu, Model-based analysis of ChIP-Seq (MACS). *Genome Biol.* **9**, R137 (2008). Medline doi:10.1186/gb-2008-9-9-r137

28. C. M. Johannessen, J. S. Boehm, S. Y. Kim, S. R. Thomas, L. Wardwell, L. A. Johnson, C. M. Emery, N. Stransky, A. P. Cogdill, J. Barretina, G. Caponigro, H. Hieronymus, R. R. Murray, K. Salehi-Ashtiani, D. E. Hill, M. Vidal, J. J. Zhao, X. Yang, O. Alkan, S. Kim, J. L. Harris, C. J. Wilson, V. E. Myer, P. M. Finan, D. E. Root, T. M. Roberts, T. Golub, K. T. Flaherty, R. Dummer, B. L. Weber, W. R. Sellers, R. Schlegel, J. A. Wargo, W. C. Hahn, L. A. Garraway, COT drives resistance to RAF inhibition through MAP kinase pathway reactivation. *Nature* **468**, 968–972 (2010). Medline doi:10.1038/nature09627

29. E. Campeau, V. E. Ruhl, F. Rodier, C. L. Smith, B. L. Rahmberg, J. O. Fuss, J. Campisi, P. Yaswen, P. K. Cooper, P. D. Kaufman, A versatile viral system for expression and depletion of proteins in mammalian cells. *PLOS ONE* **4**, e6529 (2009). Medline doi:10.1371/journal.pone.0006529

30. V. Tabar, G. Panagiotakos, E. D. Greenberg, B. K. Chan, M. Sadelain, P. H. Gutin, L. Studer, Migration and differentiation of neural precursors derived from human embryonic stem cells in the rat brain. *Nat. Biotechnol.* **23**, 601–606 (2005). Medline doi:10.1038/nbt1088